RECOVERY OF RARE EARTH ELEMENTS FROM COAL FLY ASH USING IONIC LIQUIDS

A Dissertation
Presented to
The Academic Faculty

by

Laura Mast Stoy

In Partial Fulfillment
of the Requirements for the Degree
Doctor of Philosophy in the
School of Civil and Environmental Engineering

Georgia Institute of Technology
December 2021

COPYRIGHT © 2021 BY LAURA STOY

RECOVERY OF RARE EARTH ELEMENTS FROM COAL FLY ASH USING IONIC LIQUIDS

Approved by:

Dr. Ching-Hua Huang, Advisor
School of Civil and Environmental Engineering
Georgia Institute of Technology

Dr. Yuanzhi Tang
School of Earth and Atmospheric Sciences
Georgia Institute of Technology

Dr. Susan Burns
School of Civil and Environmental Engineering
Georgia Institute of Technology

Dr. Sotira Yiacoumi
School of Civil and Environmental Engineering
Georgia Institute of Technology

Dr. Arthur J. Ragauskas
Department of Chemical and Biomolecular Engineering
University of Tennessee Knoxville

Date Approved: August 19, 2021

And always, he fought the temptation to choose a clear, safe course, warning 'That path leads ever down into stagnation' – Frank Herbert, Dune

To my loving husband

ACKNOWLEDGEMENTS

I have so much gratitude for the many mentors, colleagues, friends, and family who have supported me throughout my PhD and often believed in me more than I did myself.

First, I'd like to thank my advisor, Dr. Ching-Hua Huang, who was not only a mentor but also a model of competency, grace, and diligence.

Secondly, I'd like to thank my colleagues in lab, including Cong Luo, Manasa Sadhasivan, Tianqi Zhang, Juhee Kim, Wenlong Zhang, Jordan Dobson, Rong Chen, Meiquan Cai, Penghui Du, and Jay Renew. I'd also like to thank Dr. Lisa Rosenstein, who taught me how to write and without whose guidance I would certainly not be in the position I am in now. I'd like to thank Dr. Ken Ferrier for assistance with XRF, Dr. David Tavakoli for assistance with XRD, Todd Walters for assistance with SEM-EDS, and Dr. Xenia Wirth for assistance with sampling. My deepest gratitude I extend to my undergraduate student, Victoria Diaz, whose strong work ethic and sincere, earnest curiosity revitalized my passion for this work

So many groups at Georgia Tech have enriched my experience. I'm grateful to the Tech to Teaching community, specifically Dr. Kate Williams, whose dedication to excellent teaching practices inspired me to become a more thoughtful and intentional instructor. I'm grateful to the ComSciCon-Atlanta and Georgia Tech's CEISMC (specifically Dr. Roxanne Moore) and general science communication community, whose passion for sharing science in interesting and creative ways I find deeply inspiring. I'd also like to thank the folks at VentureLab, specifically Jeff Garbers, and the folks at the Georgia

Tech Technology Licensing program, specifically Dr. Terry Bray, for their help in filing a patent based on our research and efforts to determine potential pathways to commercialization.

I'd also like to thank my PhD coach, Katy Peplin, of Thrive PhD, whose gentle but firm guidance has pushed me forward and shaped my framing of my PhD journey.

I'd like to thank my friends, especially those outside of graduate school, for reminding me of the world beyond my program. I'd like to thank my family for their love and support, especially my siblings- my brother Chris, who was an excellent, supportive roommate ready with a hug on bad experiment days; my brother Nick, who was always available to listen to me talk through things, and my sister Erica, a dear friend who has been a constant encouragement. I hope I have made you proud.

Finally, I'd like to thank my dog, because even if he can't read, I've written tens of thousands of words with him by my side. Most of all, I'd like to thank my husband, who has been my biggest cheerleader, whose love and support have carried me throughout this experience. My love, the best is yet to come.

TABLE OF CONTENTS

LIST OF TABLES

LIST OF FIGURES

LIST OF SYMBOLS AND ABBREVIATIONS

REEs	rare earth elements
CFA	coal fly ash
LCD	liquid crystal display
U.S.	United States of America
USGS	United States Geological Survey
TN	Tennessee
NC	North Carolina
EPA	Environmental Protection Agency
SEM-EDS	scanning electron microscopy - energy dispersive x-ray spectroscopy
IL	ionic liquid, or task specific ionic liquid
ICP-OES	inductively coupled plasma atomic (optical) emission spectroscopy
ICP–MS	inductively coupled plasma mass spectroscopy
EDTA	ethylenediaminetetraacetic acid
NIST	National Institutes of Standards and Technology
XRD	X-ray diffraction
°C	degrees Celsius
PT	pretreatment phase
AQ	aqueous phase
IL	IL phase
M_{PT}	Mass of the analyte in the pretreatment phase
M_{AQ}	Mass of the analyte in the aqueous phase
M_{IL}	Mass of the analyte in the ionic liquid phase

M_{total}	Total mass of the analyte
D	distribution coefficient
L	leaching efficiency
POC	primary oxide content
CFA	coal fly ash
Q	quartz
M	mullite
H	hematite
L	sillimanite
S	sodium aluminum silicate hydrate
t	metric ton
AA	ascorbic acid
γ	enrichment (or depletion)
R	recovery efficiency
TEHDGA	*N,N,N′,N′*-tetrakis-2-ethylhexyldiglycolamide
DTPA	bis(ethylhexyl)amido diethylenetriaminepentaacetic acid
N/A	not available

SUMMARY

Rare earth elements (REEs), the 15 lanthanides and Sc and Y, have played an invaluable role in the progress of clean energy technology and high-tech manufacturing in past decades. Their high demand and global scarcity have led to disruptions in supply, exacerbated by the fact that there are no adequate replacements. Thus, it is crucial to develop alternative sources to secure a steady supply of REEs. Coal fly ash (CFA), a byproduct of burning coal for electricity, may be one such source. Conventional REE-CFA recovery methods are energy and material intensive and leach elements indiscriminately, generating impure mixtures of REEs and bulk constituents. Ionic liquids (ILs) may be one solution, but to date, they have not been applied to CFA.

This dissertation focuses on developing a new valorization process based on the ionic liquid (IL) betainium bis(trifluoromethylsulfonyl)imide ([Hbet][Tf_2N]) for preferential extraction of REEs from different CFAs. Efficient extraction relies on [Hbet][Tf_2N]'s thermomorphic behavior with water: upon heating, water and the IL form a single liquid phase, and REEs are leached from CFA via a proton-exchange mechanism. Upon cooling, the water and IL separate, and leached elements partition between the IL and aqueous (AQ) two phases. REEs were preferentially extracted over bulk elements from CFAs into the IL phase then recovered in a subsequent mild acid stripping step, regenerating the IL. Alkaline pretreatment significantly improved REE leaching efficiency from recalcitrant Class-F CFAs, and additional betaine improved REEs and bulk elements' separation. Weathered CFA showed slightly higher REE leaching efficiency than unweathered CFA, and Class-C CFA demonstrated higher leaching efficiency but less selective partitioning than Class-F

CFAs. Significantly, this method consistently exhibits a particularly high extraction efficiency for scandium across different CFAs.

The IL extraction process yields a mildly acidic REE-rich solution contaminated with Fe. The second study in this thesis investigates three strategies for limiting Fe coextraction into the IL phase: magnetic separation, complexing salts, and ascorbic acid reduction. Magnetic separation, intended to reduce the amount of Fe in the initial CFA, failed to deplete Fe in CFA and ultimately increased the amount of Fe in the IL phase. When NaCl was used instead of $NaNO_3$ as an alternative salt, the overall recovery (R_{Fe}) of iron did not decrease but the distribution (D_{Fe}) of iron between the IL and AQ phases decreased from ~75 to ~14, a five-fold decrease, and the leaching efficiency (L_{REEs}) and recovery (R_{REEs}) of REEs both increased. Finally, using ascorbic acid decreased D_{Fe} even further, to ~0.16, indicating a preference for the AQ phase over the IL phase and causing R_{Fe} to also drop. These optimizations should be used together in conjunction with other strategies identified in previous work with CFA-[Hbet][Tf_2N] leaching, including alkaline pretreatment and adding supplemental betaine cation, to generate an REE-rich acidic solution with very low concentrations of Fe.

The third part of this dissertation expands upon the CFA leaching behavior with [Hbet][Tf_2N]. This IL has been shown to separate REEs from bulk elements (Si, Al, Ca, and Fe), but little is known about the behavior of other elements. Eighteen additional elements were studied (29 total) and found that in the IL phase, bulk elements were found in low concentrations (<26 wt.%), trace elements were not found (<1.6 mg/kg), and of the actinides, Th was extracted into the IL phase and U was not leached at all. REEs, as previously noted, partition largely between the AQ and IL phases. The study also identified

other important optimizations, including pH (no impact observed for pH 2-7), temperature (optimal *L* observed at 85ºC of the studied 45-85ºC range), and duration of leaching (optimal *L* observed at 3 h of the 0.5-12 h range). The process is also compared to several published CFA solid extraction methods and CFA leacheate separation methods to place the recovery method developed by this dissertation in context with existing literature. Finally, a number of process sustainability improvements are recommended, including the use of microwave heating, water and IL recovery strategies, and beneficial uses of the residual solids.

Finally, two other ILs were studied along with [Hbet][Tf_2N] to investigate the effect of IL's cation functional group modifications. The two ILs possess the same anion [Tf_2N], but one with a less acidic cation having an alcohol group, choline [Chol], and one with a more acidic cation having an alkyl sulfonic acid group, trimethylammoniumethane hydrogen sulfate ([$N_{111}C_2OSO_3H$]), in comparison with [Hbet] which contains a carboxyl group. [Chol][Tf_2N] was broadly unsuccessful at leaching almost all elements from all CFA samples tested, indicating that an additional extractant may be required to achieve high extraction efficiency. [$N_{111}C_2OSO_3H$][Tf_2N] was more successful, achieving greater or comparable leaching efficiencies; however, unlike [Hbet][Tf_2N], it did not partition the REEs into the IL phase, but rather into the AQ phase, along with other bulk and trace constituents. Further optimizations should be explored to determine if better selectivity may be induced for [$N_{111}C_2OSO_3H$].

Overall, the research outcome of this dissertation filled several knowledge gaps not only in REE recovery from CFA, but from ILs. ILs are a relatively young technology, and hydrometallurgical applications for complex materials have only recently emerged. A more

comprehensive understanding of the effects of different functional groups on key IL properties, especially with respect to acidity, informs future research and applications. Fundamentally, this thesis is about resource recovery and presents a novel method for extracting REEs from CFA. In particular, this study is among the first to demonstrate direct application of an ionic liquid to CFA for efficient recovery of REEs. As such, this work unlocks a new strategy for CFA refinement for REE recovery. The recyclability of IL and mild extraction conditions offer significant advantages for environmental sustainability. Altogether, this thesis builds a foundation for new IL-based strategies for future extractions from CFA and other REE-rich wastes.

CHAPTER 1. INTRODUCTION

1.1 Background

Rare earth elements (REEs), defined as the 15 lanthanides and Sc and Y in this study, have played an invaluable role in the progress of clean energy technology and high-tech manufacturing in past decades (Figure 1). Their high demand, in conjunction with global scarcity, has led to disruptions in supply, an issue exacerbated by the fact that adequate replacements have not yet been developed. To address the REE scarcity challenge, it is crucial that alternative sources and methods are developed to secure a steady supply of pure REEs.

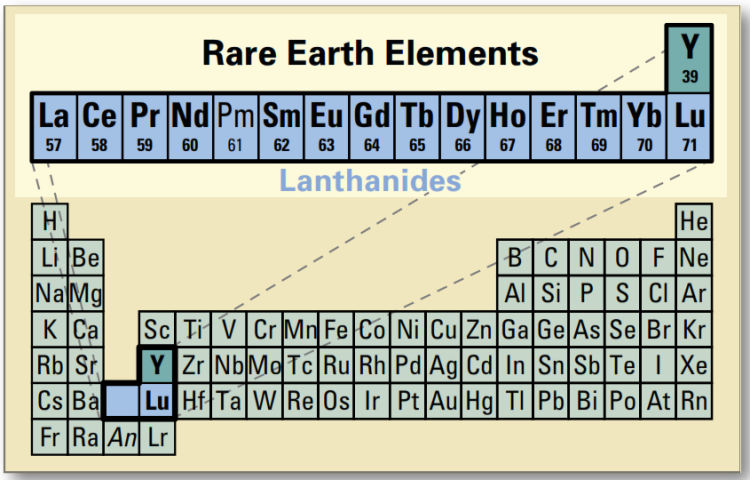

Figure 1.1 The periodic table showing rare earth elements highlighted.

One such source may be coal fly ash (CFA), a byproduct of coal combustion. Concentrations of REEs in CFA have been shown to be as high as 1500 ppm, comparable to REE levels in ore deposits.[1] Furthermore, vast quantities of coal ash are produced every year at 40-60 million t/y, and decades of burning coal for electricity have led to enormous

stockpiles, scattered in approximately 1,000 storage ponds and impoundments throughout the U.S.[2,3]

To take advantage of these widely produced waste materials, new methods must be developed to selectively extract REEs from the complex CFA matrix. Current methods are energy intensive, utilizing high heat and strong acids, and generate impure mixtures of REEs, thus presenting a significant barrier to widespread utilization.

This thesis presents an alternative based on ionic liquids (ILs). These designer solvents can be tailored by modifying the functional groups bound to the cation or anion, or by substituting either constituent entirely, with dramatic effects on IL properties.[4,5] To date, ILs have only recently been applied beyond aqueous solutions to solids, including REE-rich materials, including lamp phosphors, permanent magnets, bauxite residue, liquid crystal display (LCD) screens, and now CFA.[6-9] However, these materials present a far less compelling challenge compared to CFA due to its durable aluminosilicate structure and observed heterogeneity.

While an REE-CFA recovery process might not be economically viable now, future economic pressures may change this. Increasing government regulations around CFA disposal has made on-site storage financially unattractive, and utility companies are currently seeking to other beneficial uses as an alternative to landfilling. Additionally, China's dominance in the REE space presents a risk in terms of geopolitical instability. In 2019, China considered limiting U.S exports, a move that would devastate the economy, according to industry experts.[10] "The key questions for U.S. manufacturers are how quickly any curbs bite, whether alternative sources can be found, when, and at what cost. China's

grip over global heavy rare earths production is almost total, according to Shanghai Metals Market, and it will take a significant amount of time to build up the necessary processing capacity in other countries."[10]

CFA may provide the answer to this national security crisis, but only if efficient, selective methods are developed. In this dissertation, ILs as an effective solution were investigated.

1.1.1 Rare earth elements as critical materials

The story begins with a misnomer; rare earth elements (REEs), a set of 17 elements atomic numbers 57-71, are not by definition rare.[11,12] Indeed, some REEs are as plentiful in the Earth's crust as common metals like chromium, nickel, copper, zinc, molybdenum, tin, tungsten, or lead.[11] Even the rarest of the REEs, Tm and Lu, are 200 times more common than gold.[11] The reality is more nuanced; unlike the previously mentioned common elements, REEs are dispersed throughout the crust and are not found in concentrated (economically viable) ore deposits.[11,12]

Mining REEs has always been a challenge, environmentally and economically.[13] These issues reached a peak in the U.S. in the late 1980s and 1990s (Figure 1.2).[11] At that time, China, seeking to become a technology powerhouse, began exploiting its own REE resources.[11] China rapidly became the world's leader in REE production, producing >90% of the world's supply by the early 2000s.[11] In 2002, the United States closed its REE mining operation, ending its decades-long dominance of global production.[11] Many other countries also ended operations, unable to compete with the low prices established by China.

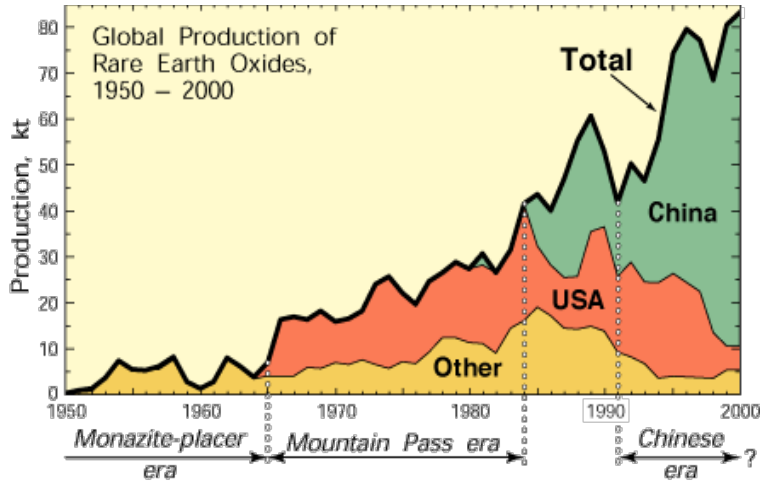

Figure 1.2. Global production of REEs from 1950 to 2000.

The transition from a largely independent and self-sufficient REE producer to nearly complete dependence on imports, from one country no less, has left a specter of unease lingering over REE supply in the United States.[11,12,14] Both the United States and the European Union have labeled REEs "critical materials."[15,16] This nomenclature is apt beyond the obvious reasons of their vulnerability to short- and long-term disruptions, which was highlighted in 2012, when China dramatically restricted REE exports.[11] (The country relaxed these restrictions following the involvement of the World Trade Organization.)[11]

Even more recently, escalating tensions between the U.S. and China have resulted in billions of dollars in tariffs from both countries across many industries, including REE processing. China provides over 80% of the U.S.'s REE needs, and experts anticipate that these critical elements could be a painful lever for the U.S.[17] In October 2018, the U.S. Geological Survey (USGS) sent scientists to Australia to investigate mining opportunities in the Outback[17]; in July 2019, President Trump ordered the Pentagon to build up U.S. capacity to produce REE-based magnets, citing them as critical for defense applications.[18]

These critical elements are not just important for permanent magnet technology; in fact, they have quietly taken on invaluable roles in a diverse variety of functions, including displays used in computer monitors and televisions, fiber-optic telecommunication cables, and cancer treatment agents.[11-13,19-21] They also contribute heavily to the global transition to a greener, low-carbon economy, through their uses as petroleum fluid cracking catalysts, automotive pollution-control catalytic converters, and magnetic refrigeration. The significance of REEs' unique chemical properties is further underscored by the fact that adequate replacements for these high-performing elements have not yet been developed.[12,19,22]

Despite their expanding roles and increased global demand, REE prices overall remain low, a fact that is both a blessing to R&D companies developing novel applications cheaply, and a curse to the same companies and countries that fear for their supply's stability and would perhaps prefer to rely on domestic producers, even with the higher price tag. Mining, however, faces serious regulations in many developed countries, and comes with its own challenges.[13,23] Furthermore, post-mining processes are required: REE-containing minerals, already somewhat rare, usually contain other elements in bulk, which must be separated to be economically viable. After extraction from solid materials, REEs are often still within impure mixtures of REEs that require further separation.[13,24] This is due to their highly similar properties (oxidation state, ionization potential, solubility, complexation behavior, boiling point, etc.). In addition to generating impure mixtures, current REE solid-extraction methods are energy and resource intensive, requiring strong mineral acids and extreme heat.[19]

Thus, to fully address the REE scarcity challenge, alternative sources and methods must be developed to secure a steady supply of pure REEs.[19]

To that end, in recent years, REE recycling has expanded to lower-value waste streams. These include bauxite residues, phosphogypsum, wastewater, slag and mine tailings; waste from other REE mining operations, which can hold significant amounts of unrecovered REEs, especially in tailings from older, less efficient operations; and post-consumer materials, including lamp phosphors, permanent magnets, batteries, and other electronics.[19] Coal has been examined briefly, and CFA is yet largely unexplored as a potential source of REEs.[25,26]

1.1.2 Coal fly ash as a potential source of REEs

Coal fly ash (CFA) is one byproduct of coal combustion for electricity generation. Unlike other combustion byproducts (which include bottom ash, boiler slag, and flue gas desulfurization brine), CFA is composed of fine particles and is generally captured by electrostatic precipitators prior to reaching the chimneys of coal-fired power plants. CFA composition is highly variable, depending on the coal's geographic source and composition, among other factors.[27,28] Major constituents include oxides of silicon, aluminum, calcium, and iron.[25,27-30] In the United States, commonly burned coals include bituminous and sub-bituminous coals, which generate Class F and Class C ashes, respectively. One notable difference is that Class C/sub-bituminous CFA has a higher lime (CaO) content than Class F/bituminous CFA (28% vs <2%), such that it is self-cementing.[30] On the other hand, the bituminous coal contains higher carbon content than sub-bituminous coal and is considered higher quality for electricity generation.[30]

Common minor constituents in CFA include a variety of elements present at trace levels (up to hundreds ppm), including arsenic, cadmium, chromium, lead, mercury, and selenium.[30-33] While these concentrations may appear negligible, the vast quantities of CFA produced annually have led to concerns about potential environmental contamination following several catastrophic ash spills.[34] Recent high-profile cases include the 2008 Kingston Tennessee coal ash spill, occurred on December 23, 2008. [35,36] Over one billion gallons of ash spilled into the adjacent Emory river, covering ~ 300 acres with an ash slurry over six feet deep (see Figure 1.3). [35,36] This volume is equivalent to ~1,660 Olympic-sized swimming pools of waste and is 100 times bigger than the Exxon Valdez oil spill in 1989. Only a few years later, in 2014 in Eden, North Carolina, another coal ash spill sent 82,000 tons of ash spilled into the Dan River over the course of a week. While these cases were catastrophic containment failure, other problems arise less dramatically; namely, the slow seep into groundwater or surface water from unlined ash basins or otherwise improperly managed landfills.[34] As a result, coal power plant owners and operators have been facing increased scrutiny and pressure to manage and close ash ponds.

As the environmental and economic costs of storage increase, there has been a recent push to recycle greater amounts of CFA. The U.S. Environmental Protection Agency (EPA) issued a ruling in November 2019 that directed facilities to close or retrofit some existing coal byproduct surface impoundments by September 2020, and utility companies are already moving to upgrade and close basins.[34,37,38]

Figure 1.3 Aerial Image of the Kingston, TN Ash Slide 12/23/2008. Source: TVA.

Current uses for CFA include concrete, structural fills, cement/raw feed for cement clinker, road base/sub-base/pavement, snow and ice control, mineral filler in asphalt, waste stabilization, and soil modification/stabilization, to name a few.[25,39] Despite this extensive list, it is estimated by the American Coal Ash Association that approximately 40% of coal fly ash is beneficially reused annually.[39] The remainder of the 60 million tons is stored in

basins and landfills across the United States.[39] Finding other opportunities than landfill disposal of CFA should be a priority for waste management research.

One such alternative is mining valuable elements from CFA. While REE levels in coal itself resemble those of common sedimentary rock, concentrations of REEs in CFA are enriched due to combustion.[27,28] In some cases, REE levels have been shown to be as high as 1500 ppm, comparable to REE levels in ore deposits.[24,30,32,33] While these CFA samples are not particularly concentrated in the heavier REEs, the more abundant Sc, La, Ce, and Nd are all present at levels indicating that extraction could be economically viable.[1]

Current REE extraction methods for solid materials include the EPA Methods 3050B, 3051, and 3052. Each of these methods utilize strong acids and heat to digest sediments, sludges, and soils to varying degrees.[40-42] The methods increase in intensity with increasing number. The mildest method, 3050B uses heat from a block digester or hot plate, nitric and hydrochloric acids, and hydrogen peroxide, and is incapable of dissolving silicate minerals.[40] Thus, it is not a total digestion technique for many solids, and will only dissolve "environmentally available" elements.[40] Similarly, Method 3051A is an alternative to 3050B that utilizes microwave heating in addition to nitric (and sometimes hydrochloric) acids.[41] Method 3052 is the only method that performs a total digestion using microwave heating, nitric acid, and hydrofluoric acid, which is capable of digesting silicate minerals.[42]

However, these EPA methods, published in the 1990s, are limited in that they are approved for analysis for specific elements; REEs are not included. The U.S. Geological Survey (USGS) published an extensive report in 2002 detailing appropriate methods for chemical analysis of geologic and other solid materials.[43] One method, like EPA Method

3052, utilizes hydrochloric, nitric, hydrofluoric, and perchloric acids, peroxides and a heating block to analyze 42 elements, though not including REEs; despite the intensity, this method is described by the authors as an incomplete digestion that will not dissolve "refractory or resistant minerals and some secondary minerals."[44] A second method published in the USGS report was specifically designed for the extraction of REEs from challenging geologic materials.[45] Unlike the other methods, it involves sintering samples with sodium peroxide, leaching with water, and acidifying with nitric acid to prepare for analysis by inductively coupled plasma atomic (optical) emission spectroscopy or mass spectroscopy (ICP-OES or ICP–MS).[45]

Other methods for REE digestion for solids also require strong mineral acids and extreme heat. Dai et al. used sulfuric acid and peroxides to digest coal samples in an ultraclave microwave high pressure reactor to analyze the geochemical and mineralogical composition.[46]

The need for milder methods has been recognized by many lab groups, but accurate REE quantification is still lacking. Kashiwakura et al. used dilute sulfuric acid to model REE leaching behavior and achieved recovery rates of only 10-50%.[27] Hasegawa et al. used aminopolycarboxylate chelates like ethylenediaminetetraacetic acid (EDTA) and ultrasound application to extract REEs and other valuable elements from various ashes with minor success.[47] Kim et al. conducted long-term leaching studies on fly ash using a mild acid (acetic acid), a strong caustic agent (sodium bicarbonate) and a strong acid (sulfuric acid) to mimic common fluids, and found low solubilities for almost all cations, but especially under mildly acidic conditions.[48] Tan et al. used a variety of chelates, including aminopolycarboylates, phosphonic acids, phosphoric acids, and oxalic acids, in addition to

mechanical grinding, heat, and mildly acidic conditions to extract REEs from waste phosphors.[49] Their many-step sequential leaching process achieved the separation of Y and Eu from La, Ce, and Tb; however, separating each REE requires further calcination processes.[49]

Thus, these processes face several significant challenges, and do not meet green chemistry goals. They often require highly acidic or corrosive solutions, and they are hazardous, energy-intensive, multi-stage, and complex, rendering them impractical at industrial scales. Most importantly, such leaching methods are indiscriminative and generate impure mixtures of REEs, necessitating further separation processes. A more environmentally sustainable method desires low concentration of acid, mild operational conditions, and high selectivity in extracting REEs.

One further challenge faced by this desired method is the variability across CFA samples. CFA composition is dependent on the coal burned itself, but the specific combustion conditions at individual power plants also have a significant impact on CFA.[27,28] These factors include grinding mill efficiency (how consistently and how finely coal is ground prior to burning); the combustion environment (temperature and oxygen supply); boiler configuration; and the rate of particle cooling.[27,28] CFA particles solidify in flue gas following combustion, and the rate of cooling impacts particle size and shape (generally spherical) and mineralogy.[27,28] Cooling occurs so rapidly that few minerals may crystallize; furthermore, crystalline phases present in CFA particles are often the result of incomplete melting of refractory phases.[27,28] Thus, CFA particles tend to be heterogeneous mixtures, dominated by amorphous glass but also containing quartz, mullite, corundum, gypsum, and various iron mineral phases.[24,27]

Understanding the REE partitioning between these various mineral phases is important for the efficient extraction of REEs from CFA. Unfortunately, partitioning behavior seems to vary between CFA samples. While Hower et al. observed that REEs tend to be associated with the glass phases, either as a constituent of the glass or within fine, discrete minerals within the glass, Dai et al. observed broader REE mineral associations.[24,50] Using scanning electron microscopy - energy dispersive x-ray spectroscopy (SEM-EDS), Dai et al. detected Y, La, Ce, Pr, and Nd in REE-bearing calcite and parasite $Ca(Ce,La)_2(CO_3)_3F_2$ in fly ash particles.[24]

Thus, the challenge to selectively extract REEs becomes more complex. Unlike leaching from REE ores or other REE-containing materials like NdFeB magnets or lamp phosphors, REEs are found within various mineral and amorphous phases in CFA. REE extraction methods must not be hindered by amorphous phases, or selectively dissolve mineral phases over glass phases.

1.1.3 Task-Specific ionic liquids (ILs)

Task-specific ionic liquids (ILs) have been hailed as an exciting development in solvent chemistry in recent decades.[51,52] ILs simply contain a cation and anion, but unlike most common salts, they tend to have freezing points at less than 100°C, due to the bulkiness and asymmetry of their cation components.[51,53] They exhibit a wide variety of other desirable properties that present a significant advantage over traditional solvents: negligible vapor pressure, low flammability, high thermal stability, broad electrochemical window, and high liquidus range.[51,53-55] They also demonstrate high tuneability as a chemical class, with nearly infinite combinations of cations and anions possible; for

example, over 30,000 imidazolium salts, a group of commons cations for ILs, may be found in the Chemical Abstracts Service database.[54] Theoretically, given suitable choices of each, an ionic liquid with specific properties for specific applications can be produced.[4,54,55] These ILs can be further customized with the incorporation of specific metal-coordinating groups into their structures.[4] These ILs, called functionalized ionic liquids have been used in a wide variety of applications.[4,5]

These applications include serving as solvents and catalysts for organic synthesis, batteries, carbon-capture technologies, natural gas separations, in pharmaceuticals, and more. ILs have also been investigated in hydrometallurgical applications. ILs, and their sister compounds, deep eutectic solvents, have been widely shown to be good solvents for metal oxides.[53,56-58] For example, phosphonium-based ILs separated cobalt from nickel, magnesium and calcium efficiently in a chloride medium without the addition of any organic solvents.[52] Alkyl sulfuric acid ILs were demonstrated to extract transition metal cations even from highly acidic (pH < 0) solutions.[59] It is this research that has led to the investigation of ILs for extraction of REEs.

1.1.4 REE Extraction using ILs

ILs have already been applied to REE extraction, from both mineral sources and non-mineral sources. Alkylnitrate-based ILs were demonstrated to successfully separate REEs from a hydrated Ca-nitrate melt containing a mixture of transition metals including nickel, cobalt, and zinc.[60] A phosphine oxide based IL mixed with other ILs, including imidazolium based ILs, was employed to extract lanthanide and actinide cations from mildly acidic aqueous solutions.[53] One common ionic liquid cation, amide-based

imidazolium, has been used in many ionic liquids to successfully extract REEs from bastnäsite-type solids and aqueous solutions.[61-63] Yang et al. reported that an imidazolium IL could be used in conjunction with an amic acid extraction agent, to recover REEs from acidic leach solutions of phosphor powders containing Fe, Al, and Zn.[64]

One exceptionally promising IL is betainium bis(trifluoromethylsulfonyl)imide, commonly referred to as [Hbet][Tf_2N], first published in 2006 by the Binnemans research group in Belgian, which has largely led the field in ionic liquid development for critical metal extraction from various non-mineral sources (Figure 1.3).[5] Their investigation and others following found that [Hbet][Tf_2N] cannot efficiently dissolve inert oxides of iron, aluminum, silicon, and cobalt.[5,6,55,65-75] The proposed mechanism relies on the acidity of the carboxylic acid group in the cation; upon deprotonation, zwitterions form, which coordinate to the metal cations effectively.[5,59,65,73] Alkyl sulfuric and sulfonic acid ILs behave similarly. Dupont et al. found that [Hbet][Tf_2N] could successfully leach Y and Eu cations from lamp phosphors without leaching the other constituents of the waste powder (other phosphors, glass particles and alumina).[6] In a separate report, Dupont et al. found that sulfonic acid functionalized ionic liquids also containing the [Tf_2N] anion demonstrated high affinity for REEs as well.[73]

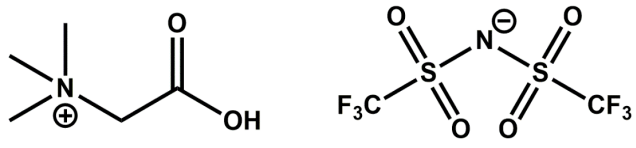

Figure 1.4 Betainium bis(trifluoromethylsulfonyl)imide, or [Hbet][Tf_2N].

1.1.5 Choosing an effective IL

Given the high customization capacity for ILs, several choices must be made: overall desired IL properties, cationic core and functionalization, and anion choice. Common cationic cores such as imidazolium, pyridinium, and pyrrolidinium, can be functionalized with alkyl groups of varying lengths and branching as well as with different functional groups. Both the cation and the anion affect properties of the ionic liquid, including viscosity, hydrophobicity, water solubility, and stability. Commonly used cations and anions are presented below.

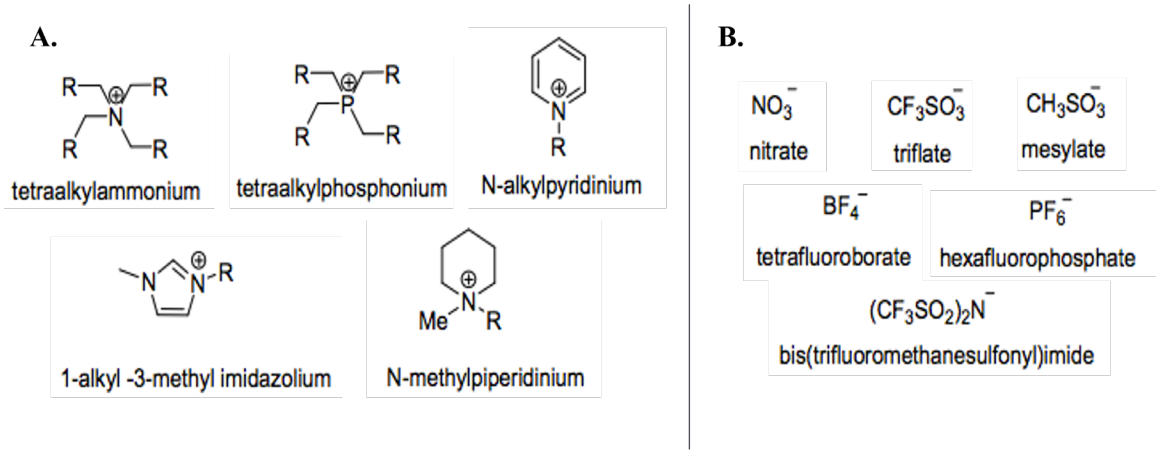

Figure 1.5 Commonly used cations (A) and anions (B).

For the purposes of extraction, ILs must be immiscible with water. This approaches a careful line; too hydrophobic, and the IL mixture becomes too viscous for efficient mass transfer.[69] Increased viscosity can be mitigated with physical methods like intensive mixing, sharking, and heating, or by mixing ILs with water or other solvents in varying proportions. Thermomorphic behavior, meaning that ILs become miscible with a solvent above or below a certain temperature, may also be exploited to optimize mass transfer. One such ionic liquid is [Hbet][Tf_2N], which displays thermomorphic behavior; after reaching

the upper critical solution temperature of 55°C, water-[Hbet][Tf_2N] solutions forms one phase, allowing for homogenous liquid-liquid extraction before cooling.[69]

Increased viscosity can also be allayed via anion selection. It is hypothesized that the affinity to REE cations is derived from the IL's cation, which is to say that the role of the anion is largely to contribute to the overall IL structure, rather than complex with metal cations. The bis(trifluoromethylsulfonyl)imide anion [Tf_2N] tends to form stable and low-viscosity ILs.[69]

Thus, the choice of cation core and functionalization is the most important of the modifiable factors. Research indicates that highly acidic functional groups like carboxylic acid groups, sulfonic acid groups, and alkyl sulfuric acid groups, may be promising.[59,69,73] These protic ILs can efficiently dissolve metal oxides because only water and metal cations are formed. When the IL cations are deprotonated, they form zwitterions, neutral molecules containing both positive and negative charges, that are able to solvate metal cations.[55] Without this ability to form zwitterions, strong coordinating anions would be required to complex the metal cation to achieve high solubility.[55,57] By virtue of this mechanism, metal salts, unlike metal oxides, are poorly soluble in these ILs due to the inefficient anion solvation.

Very limited research has been done on coal and coal byproducts with respect to REE extraction using ILs.[76,77] To the author's knowledge, to date, this is the first research presented on REE extraction directly from solid CFA using ILs. [Hbet][Tf_2N] was chosen as it appeared to be the most promising candidate given its ability to selectively solvate

metal oxides: REE oxides are soluble, and Al_2O_3 and SiO_2 are not. Chapter 2 is focused on the development of an efficient, selective [Hbet][Tf_2N] extraction process for CFA.

1.1.6 CFA Pretreatment for optimal IL extraction

[Hbet][Tf_2N]'s selectivity in solubilizing metal oxides is a critical feature, as the oxides that make up the bulk of CFA are insoluble. However, this benefit also poses a potential challenge, as current research shows that REEs are mostly dispersed throughout aluminosilicate glass phases. If this glassy phase remains unperturbed by IL extraction, pretreatments would likely be required to improve leaching efficiency. Pretreatment steps may include roasting, addition of alkaline agents, of acidic agents, of chelating agents, and/or combinations of these treatments.[78,79] Chapter 2 includes evaluation of acidic and alkaline pretreatments.

1.1.7 Green Chemistry and ILs

It should be noted that researchers have begun investigating whether ILs truly live up to their green chemistry claims. A review published by Pang et al. in 2015 found that IL toxicity was largely dependent on the structure (cation family, chain length, and anion moiety) and had varying negative effects on the different model organisms studied.[80] ILs sorption behavior onto dissolved organic matter, metal oxides, and clays also impacted the fate and toxicity of co-existing pollutants.[80] A green method should avoid toxic cations and anions when possible.[59,80] While to date there is limited data on the (eco)toxicity and biodegradability of the ILs investigated in this dissertation, they are considered to have low toxicity, as the cations are or are derived from biomolecules.

1.1.8 Regulatory and Economic Environment

Each year, the United States generates 130 million tons with ~60% beneficially reused.[2,39] The remaining ~50 million tons is landfilled or stored in ponds, representing ~27,000 tons of REE metals and ~$7.2b USD as a back-of-the-envelope calculation. [2,39] There are over 1,000 ash ponds in the United States today.[34,38,39] Decades of burning coal has led to the accumulation of ~1.5 billion tons in ponds, representing ~708,000 tons of REE metals or $208b USD. This totals to ~100 years of US need for REEs, though need is projected to increase especially with the rise in electric cars.

Following initiatives begun by Presidents Barack Obama and Donald Trump, current President Joe Biden issued several executive orders relating to establishing domestic sources of REEs, and specifically mentioned CFA as a potential source.[81,82] The most important of these is Executive Order (E.O.) 14017 "America's Supply Chains", , issued in February 24, 2021, which calls for supply chain reviews across strategically significant economic sectors: semiconductors, pharmaceuticals, high-capacity batteries, and critical minerals, including REEs.[82] It is hoped that this effort will produce guidelines (and funding) to support domestic abilities to produce and refine REEs. Currently, the Mountain Pass mine in California is operational, but produced REEs must be sent to China for processing as the U.S. does not have refinement facilities.[81]

Recovering REEs from CFA may prove to be an appropriate solution, and this opportunity appears at an important time given the increased pressure on coal power plant owners and operators. New CFA management policies are already taking effect: in January 2020, one major owner-operator in the Southeast, Duke Energy, agreed to a plan to

permanently close the company's remaining nine coal ash basins in the state, primarily by excavation with ash moved to lined landfills.[83]

This thesis, squarely placed at the nexus of REE scarcity and CFA management, offers a timely contribution to a larger body of work in support of U.S. economic prosperity and military-industrial capabilities.

1.2 Research Objectives

The overall objective of this study was to develop and optimize ILs to leach REEs from CFA selectively, with the ability of reusing the ILs over multiple cycles. The research objective was achieved by pursuing the following four specific research aims:

I. To quantitatively evaluate REE recovery using [Hbet][Tf_2N] directly from three representative CFAs in both single cycle and multiple cycles. The selected CFAs represent common characteristic types (Class C vs. Class F, unweathered vs. weathered). The comparison of single vs. multiple cycles provides an initial assessment of the recyclability of [Hbet][Tf_2N].

II. Based on the results from Aim I, to identify and investigate strategies to mitigate iron impurities in the IL phase. These include exploiting both physical properties of the CFA (magnetism) and chemical properties of the IL extraction process (complexing salts and reductants).

III. To investigate further relevant optimizations for the [Hbet][Tf_2N] extraction process and perform comparative analyses with other CFA-REE recovery extraction methods. The accomplishment of Aims I-III provides best

recommended practices for CFA-REE recovery using [Hbet][Tf_2N] as well as places it firmly in the larger context of such methods.

IV. To evaluate CFA-REE recovery using similar ILs. The selected ILs have the same anion (Tf_2N), display similar thermomorphic behavior with water, and rely on the same proton-exchange mechanism utilized by [Hbet][Tf_2N], but bear different functional groups on their cations (an alcohol and an alkyl sulfuric acid, respectively).

1.3 Organization of the Dissertation

This dissertation begins with an introduction of REEs and CFA, noting that CFA has been shown to be a promising source for REEs, and descriptions of current CFA-REE extraction methods. It then introduces ILs and describes recent studies on ILs for precious metal recovery applications before making a case for CFA-REE extraction using ILs.

Chapter 2 contains an evaluation of [Hbet][Tf_2N]'s performance extracting REEs from CFA solids. Alkaline pretreatment was required for the more recalcitrant Class-F CFAs to achieve high rates of leaching efficiency. Adding extra betaine improved extraction by dramatically increasing REE distribution into the IL phase. A recycling study further confirmed that the IL can be reused for at least three times with no loss in leaching efficiency. While not fully optimized, this process was successful as a proof-of-concept study that [Hbet][Tf_2N] can be used to successfully extract REEs from CFA. This chapter lays the foundation for chapters 3 and 4.

Chapter 3 addresses an important weakness in the [Hbet][Tf_2N] extraction process: the co-extraction of iron. Three strategies were evaluated for limiting the quantity of Fe in the IL phase: magnetic separation, salt complexation and reduction using ascorbic acid.

Magnetic separation was proven to be ineffective, but salt complexation and ascorbic acid reduced Fe dramatically and are recommended for successful separation.

Chapter 4 seeks to further optimize [Hbet][Tf_2N] extraction from CFA by investigating important process variables, including temperature, pH, and time. This is presented alongside a comparison to existing REE-CFA extraction methods and places the [Hbet][Tf_2N] recovery method in context.

In Chapter 5, two other ILs are investigated: one more acidic, and one less acidic than [Hbet][Tf_2N]. Their performance is compared to that of [Hbet][Tf_2N].

Lastly, Chapter 6 summarizes the main findings of the dissertation and offers perspectives on the future research directions.

1.4 Originality and Merit of Research

To date, this body of work is the first direct application of an IL to CFA for the successful extraction of REEs, setting it decidedly apart from most common REE-CFA separation methods which require total or near-total digestion of CFA to generate CFA leacheate. This direct application not only reduces the overall processing required for production of REE oxides and metals, but also reduces chemical and energy consumption. Furthermore, the IL has low vapor pressure and high thermal stability and is nontoxic and recyclable: all important characteristics for an industrial scale process.

Speaking more generally, ILs are a relatively young technology, and applications for complex materials have only recently emerged. The study of the impacts of modification on IL properties has trailed behind these applications, leaving a knowledge gap. A more comprehensive understanding of the effects of different functional groups on key IL properties informs future research and applications.

This research holds great significance for the field of environmental engineering and the public at large. Better REE recovery methods for CFA will provide an alternative supply of REEs, thus increasing U.S. economic competitiveness and national security. This process also reduces the potential environmental and monetary impact of CFA by reducing disposal.

Furthermore, these methods are likely to be applicable to other potentially REE-rich wastes, such as ores, acid mine drainage fluids and sludges, municipal waste incineration ashes, industrial and municipal wastewater sludges, and produced waters from oil and gas exploration sites. Post-consumer products like electronics may also be suitable for REE recovery using ILs. Further work will be needed to assess whether the methods generated herein will be appropriate.

CHAPTER 2. PREFERENTIAL RECOVERY OF RARE EARTH ELEMENTS FROM COAL FLY ASH USING A RECYCLABLE IONIC LIQUID

2.1 Abstract

Recent global geopolitical tensions have exacerbated the scarcity of rare earth elements (REEs), which are critical across many industries. REE-rich coal fly ash (CFA), a coal combustion residual, has been proposed as a potential source. Conventional REE-CFA recovery methods are energy and material intensive and leach elements indiscriminately. This study has developed a new valorization process based on the ionic liquid (IL) betainium bis(trifluoromethylsulfonyl)imide ([Hbet][Tf_2N]) for preferential extraction of REEs from different CFAs. Efficient extraction relies on [Hbet][Tf_2N]'s thermomorphic behavior with water: upon heating, water and the IL form a single liquid phase, and REEs are leached from CFA via a proton-exchange mechanism. Upon cooling, the water and IL separate, and leached elements partition between the two phases. REEs were preferentially extracted over bulk elements from CFAs into the IL phase then recovered in a subsequent mild acid stripping step, regenerating the IL. Alkaline pretreatment significantly improved REE leaching efficiency from recalcitrant Class-F CFAs, and additional betaine improved REEs and bulk elements' separation. Weathered CFA showed slightly higher REE leaching efficiency than unweathered CFA, and Class-C CFA demonstrated higher leaching efficiency but less selective partitioning than Class-F CFAs. Significantly, this method consistently exhibits a particularly high extraction efficiency for scandium across different CFAs.

2.2 Introduction

While not technically "rare," rare earth elements (REEs), defined herein as the 15 lanthanides and yttrium and scandium, play invaluable roles in a diverse variety of technologies, ranging from consumer products to defense applications.[11-13,19-21,84] These technologies depend heavily on REEs' unique chemical properties, and to date, no adequate replacements for these high-performing elements have been developed.[12,19,22,84] Recognizing this, both the United States and the European Union have labeled REEs as "critical materials", and exploration of REE-rich wastes has been prioritized.[15,16,19] These wastes include bauxite residue, wastewater, slag and mine tailings, waste from REE mining operations, and post-consumer materials.[19,84-90] More recently, coal combustion residuals, including coal fly ash (CFA), have been investigated.[25,26,89-92] The U.S. produces over 100 million metric tons (t) of coal combustion residuals annually, including 45 million t CFA; 60% of this cannot be beneficially reused and is landfilled.[1,2,93] Decades of coal combustion have led to massive CFA accumulation in exposed storage ponds.

Coal is not particularly concentrated in REEs, but CFA is enriched in REEs as a result of combustion.[2,24,25,27,28,30,32,33] Some CFAs show REE concentrations comparable to REE ores.[2,24,25,27,28,30,32,33] The total annual value of REEs from CFA was estimated to be $4.3 billion based on 2013 prices.[1,93] Thus, REE recovery may represent a valuable and sustainable alternative use for excess CFA waste.

The central obstacle in REE recovery from CFA is a sustainable, scalable, and selective method. Because CFA is composed of durable aluminosilicates, existing methods require highly corrosive solutions, and are hazardous, energy-intensive, multi-stage, and complex.

Most importantly, such leaching methods are indiscriminative and generate impure mixtures of REEs and bulk elements, necessitating further separation processes. Dai et al. used H_2SO_4 and concentrated H_2O_2 to completely digest coal samples in an ultraclave microwave high-pressure reactor for REE extraction.[46] Taggart et al. found that sintering with NaOH at 450°C followed by strong acid leaching extracted ~100% REEs from most CFAs.[78] King et al. demonstrated high REE recoveries (~100%) for the Powder River Basin ashes (Class-C ashes) using strong acids, but other ash types (e.g., Appalachian and Illinois basin ashes, (Class-F ashes)) only achieved middling recoveries (<50%) with strong acids and only slightly better with strong bases (~70%).[79] Attempts to use milder conditions have been made, but to date they fail to achieve high efficiency. Kashiwakura et al. applied dilute H_2SO_4 to CFA and achieved REE recovery rates of 10-50%.[27] All described methods co-leach bulk elements and consume large amounts of chemicals. Downstream separation techniques for REE-containing aqueous solutions have been developed including liquid membranes, passive columns, and biosorption.[91,94-96]

Highly tunable ionic liquids (ILs) present another REE separation strategy, having emerged in recent decades as a green solution due to its low flammability and negligible vapor pressure for many industrial processes and applications.[51,53] Betainium bis(trifluoromethylsulfonyl)imide, commonly referred to as [Hbet][Tf_2N] (Figure 1.3), first published by Nockemann and co-workers, is one such IL.[5,69,97] [Hbet][Tf_2N] is unique among ILs because it demonstrates thermomorphic solubility with water: at room temperature, it is slightly hygroscopic and absorbs approximately 13% water by mass; but as temperatures increase, its water solubility increases, and above 55ºC, becomes fully miscible with water and forms one phase.[69,97] This behavior makes it effective for

partitioning metals from aqueous solutions as well as directly from solids: aqueous-IL mixtures or aqueous-IL-solid mixtures are heated to form one liquid phase, and then cooled to form two liquid phases, with leached elements partitioning between the liquid phases.[6,7,69,97] Elements in the IL phase can be stripped using mildly acidic solutions, making them recyclable and thus limiting chemical consumption and waste generation.[6-8]

Subsequent research found that [Hbet][Tf_2N] could selectively solvate solid metal oxides. In particular, REE oxides are highly soluble by [Hbet][Tf_2N], but oxides of iron, aluminum, silicon, or uranium are not.[5,6,65,68,69] Leaching occurs via a proton-exchange mechanism (Equation 1):[5,65,68,69]

$$REE_2O_3 + 6\,[Hbet][Tf_2N] \leftrightarrow 2[REE(bet)_3][(Tf_2N)_3] + 3\,H_2O \quad (1)$$

Previous studies have found that [Hbet][Tf_2N] could successfully leach Y and Eu cations from lamp phosphors, Nd from NdFeB magnets, and Sc from bauxite residue.[6-8]

Importantly, CFA presents significantly different challenges than REE-containing solutions or previously studied REE-rich wastes. In CFA, REEs are partitioned into both mineral and amorphous phases.[24,50,93,98] Previous research reported REEs occurring as discrete particles or particles encapsulated in glassy phases in CFA.[64] Particles were composed of minerals like apatite and zircon as well as REE oxides, REE phosphates, and REE-Fe oxides.[64] Furthermore, there is high variability across CFA based on coal origin and ash weathering condition.[24,50,93,98] Notably, most reported data describe unweathered CFAs; there is a dearth of data on REE partitioning in weathered CFAs, of which the U.S. has millions of tons available and currently serves no beneficial reuse purpose.

To date, ILs have not been applied directly to CFAs. Extensive literature search found one recent study that applied several ILs to CFA leachates, produced via digestion with strong acids (concentrated/undiluted HF, HCl, and HNO_3), and achieved low REE recovery (37.4%).[99] Similar to King et al., bulk elements (Al, Ca, Si) were co-extracted.[79,99]

In this study, the application of IL directly to CFA particles for REE recovery was explored for the first time. As a proof-of-concept study, the research was aimed at addressing several specific questions: (1) Would the [Hbet][Tf_2N] IL be able to preferentially extract REEs from solid CFA materials? (2) How various CFA types might behave differently under such an extraction procedure? (3) What strategies could enhance the extraction efficiency? And (4) Could the IL be recycled for repeated use? As presented below, encouraging results were obtained that indicate the promise of this novel approach. Two strategies were explored to answer Objective (3): alkaline pretreatment and addition of supplemental betaine.

2.3 Materials and Methods

2.3.1 Chemicals and Materials.

Betaine hydrochloride (99%) was obtained from Acros Organics. Lithium bis(trifluoromethane)sulfonimide (99.95% purity) was obtained from Sigma Aldrich and Iolitec. Sodium nitrate (99.0%) was obtained from Alfa Aesar. Concentrated hydrochloric acid (37 wt.%, 99.999% trace metals basis) and concentrated nitric acid (70 wt.%, 99.999% trace metals basis) were obtained from Sigma Aldrich. All chemicals were obtained at the highest purity and used without further purification. Deionized water (≥18 mΩ-cm) was produced from a Milli-Q water purification system (Millipore, Billerica, MA, USA).

This study examined three representative CFAs (Figure S1): one unweathered Class-F (CFA-F1), one weathered Class-F (CFA-F2) and one unweathered Class-C (CFA-C1) (Table 2.1). The unweathered CFAs were produced recently and had not been subjected to weathering, while weathered CFA was produced years ago and obtained from an ash storage pond. Specifically, CFA-F1 is the NIST SRM 1633c ash, obtained from Sigma Aldrich. The other two CFA samples were obtained from industry partners. CFA-F2 was obtained from an ash pond at a power plant in Georgia that is no longer active. From 1980 to 2015, the pond received both fly ash and bottom ash, another coal combustion residual. After coal combustion, the residual bottom ash and fly ash were hydraulically sluiced to the pond separately then combined at the pond inlet. Samples were taken at depths between 0.15 and 1.5 m (0.5–5 ft) below ground surface in the pond and are likely less than 10 years old based on estimates from ash pond personnel. CFA-C1 was obtained from a power plant in Georgia that is still active and was collected shortly after combustion and stored dry.

2.3.2 [Hbet][Tf_2N] Synthesis.

[Hbet][Tf_2N] was synthesized in a one-step method following previous studies.[5,65] Briefly, aqueous solutions of betaine chloride (HbetCl) and lithium bis(trifluoromethylsulfonyl)imide ($LiTf_2N$) were prepared to achieve an equimolar ratio of Hbet:Tf_2N and combined at room temperature while stirring. After one hour, the aqueous phase was separated from the IL phase. The IL phase was then washed with small aliquots of cold deionized water to remove chloride impurities. Washing was deemed complete when no chloride impurities were detected using the silver nitrate test. Dry IL was obtained by drying using a vacuum centrifuge at 70°C. [Hbet][Tf_2N] is hygroscopic and absorbs 13% water by mass.[6,7,68,69] To achieve a resultant mixture water content of 13% by mass,

deionized water was added. IL samples were stored as water saturated samples (13% by mass) sealed at room temperature.

Table 2.1 CFA Characteristics

	CFA-F1			CFA-F2	CFA-C1
Origin	NIST			Power Plant 1	Power Plant 2
CFA type	Class F			Class F	Class C
Condition	Unweathered			Weathered	Unweathered
Source*	NIST			Ash Pond	Fresh
Major Oxide Composition (wt. %)					
SiO_2	45.6			52.4	38.4
Al_2O_3	25.1			30.5	11.9
Fe_2O_3	15			8.6	5.2
POC	85.7			91.5	55.5
CaO	1.9			1.6	25.2
REE Composition (mg/kg)					
Sc	37.6			39.7	20.6
Y	105.2			91.4	43.7
La	87			86.5	53.3
Ce	180			169.1	89.8
Nd	87			95.5	55.5
Eu	4.7			3	2
Dy	18.7			14.3	7.3
Σ REEs	520.2			499.4	272.2
Mineralogy of CFA (wt. %)					
	a	b	c	a	a
Quartz (Q)	7.5	7.2	0.3	6.5	7.7
Mullite (M)	16.4	16.9	38.9	15.0	13.8
Amorphous	73.9	61.8	58.2	68.2	64.4
Sillimanite (L)	1.3	-	0.8	5.7	-
Hematite (H)	0.8	5.4	1.8	-	-
Magnetite	-	-	-	-	7.7
Berlinite	-	-	-	4.6	-
Chlorocalcite	-	-	-	-	6.4
Sodium aluminum silicate hydrate (S)	-	8.8	-	-	-

Notes: *More information on source can be found in Text S1. Major oxide composition and REE composition are for untreated CFAs. CFA-F1 data can be found in the NIST SRM 1633c report. Data for CFA-F2 and CFA-C1 are from complete digestion analysis. Conditions: a. Untreated; b. after 5.0 M NaOH pretreatment; c. after IL leaching.

2.3.3 CFA Characterization.

Major oxide composition was determined by X-ray fluorescence (XRF) spectrometry using a Bruker Tracer III and analyzed using SP1XRF software. Mineral composition was determined using powder x-ray diffraction using a Cu-K alpha radiation source (Panalytical XPert PRO Alpha-1 XRD). Rutile was used as an internal standard for phase quantification. Phase quantification was performed using an automatic Rietveld analysis in the HighScore XRD analysis software by Malvern Panalytical. A scanning electron microscope with electron-dispersive spectroscopy (SEM-EDS) (Zeiss Ultra60 FE-SEM) was used to image and map elemental composition of discrete CFA particles.

For trace element composition, including REE composition, CFA samples were digested following a modified EPA Method 3052.[42] Briefly, CFA samples were digested for 18 h at ~90°C in a 1:1 (v/v) mixture of HF and concentrated HNO_3. The liquid phase was then evaporated on a hot plate in a fumed hood. Concentrated H_2O_2, concentrated HNO_3, and DI water were then added to digest any remaining material. The liquid mixture was digested for another 18 h at ~90°C. The samples were then diluted with 5% HNO_3 and analyzed by inductively coupled plasma-optical emission spectrometry (ICP-OES) (PerkinElmer Optima 8000). Accuracy was checked against digestion of a NIST standard CFA sample (SRM 1633c). The complete digestions of CFA-F1 (i.e., the NIST standard) yielded composition results within 2% of difference compared to those in the NIST report, indicating good precision. The detection limit for REEs and Fe was around 1.0 μg/L; the detection limit for Al, Ca, and Si was 10 μg/L.

Most CFAs are fine-grained powders ranging from tan to dark gray in color (Figure 2.1). Class-F CFAs tend to be darker due to their higher iron content.[100-104]

Figure 2.1 Color photograph of CFA samples.

Note: CFA-F1 (left), CFA-C1 (center), CFA-F2 (right).

Regardless of class, unweathered CFA is composed of glass aluminosilicate spheres and unburnt carbon particles (Figure 2.2 - Figure 2.3).[100-104]

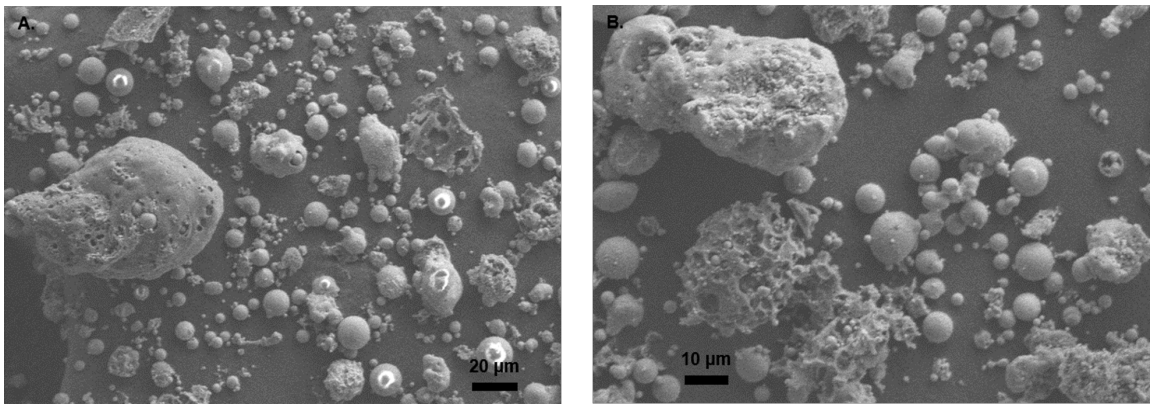

Figure 2.2 SEM images of CFA-F1.

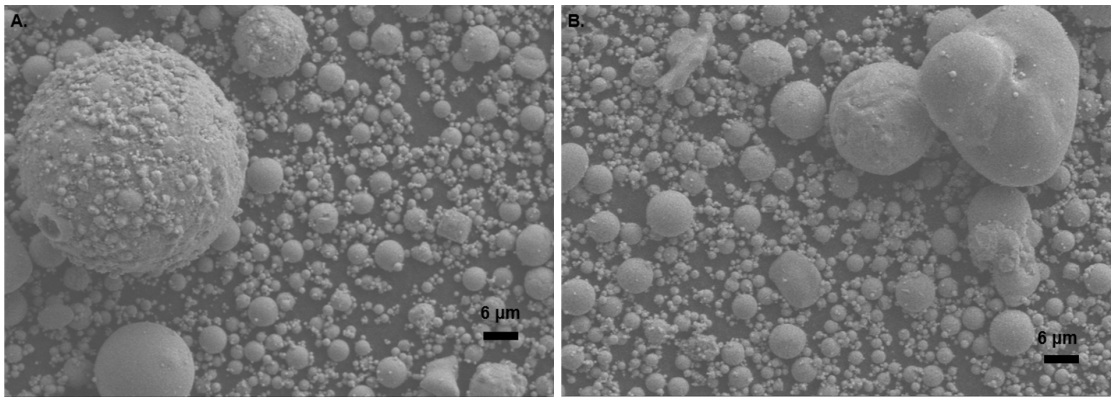

Figure 2.3 SEM images of CFA-C1.

In contrast, weathered CFAs like CFA-F2 have more heavily encrusted aluminosilicate spheres as well as agglomerations of smaller spheres (Figure 2.4), as the result of weathering and precipitation in ash ponds.[100-102]

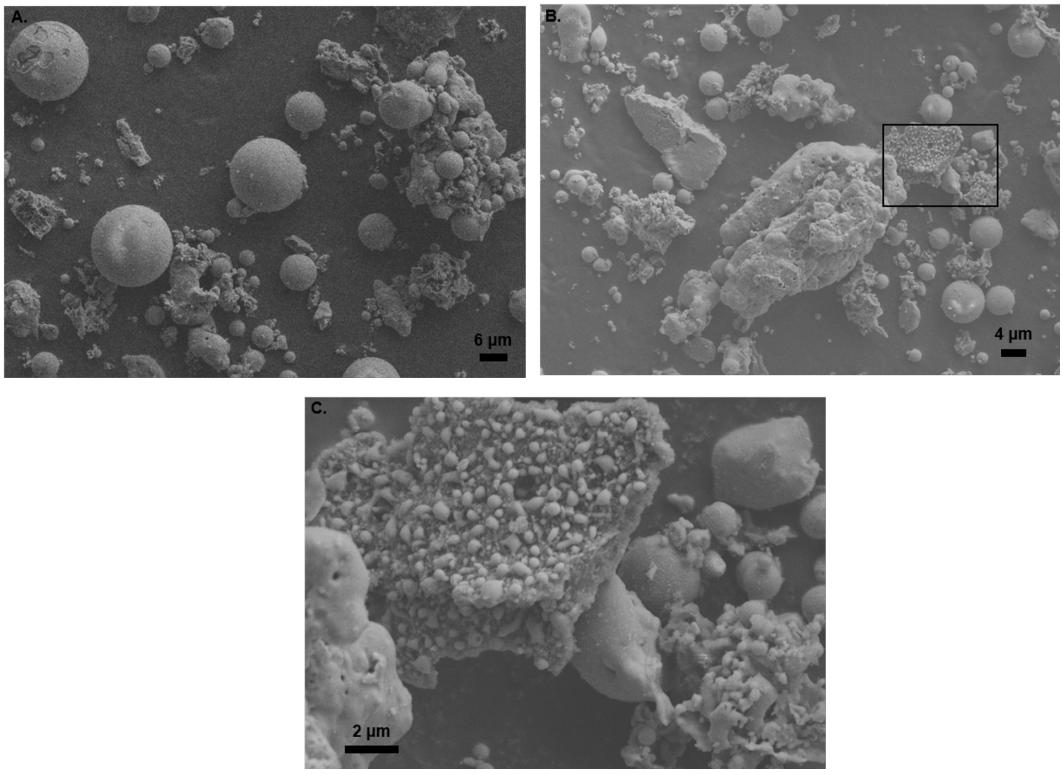

Figure 2.4 SEM images of CFA-F2.

Note: Image C is the inset in the box in Image B.

2.3.4 *CFA Pretreatment.*

Small glass vials were filled with 50 mg of CFA and a fixed amount of pretreatment solution (HNO_3 or NaOH). A small magnetic stir bar was added to each vial, and the ash-solution mixtures were stirred in an oil bath heated to 85°C for five hours. After cooling, the vials were centrifuged for 30 minutes, and the supernatant was removed. The supernatant was diluted with 5% HNO_3 and analyzed by inductively coupled plasma-optical emission spectrometry (ICP-OES). The remaining ash particles were washed using small amounts of deionized water, filtered using a Buchner funnel with 0.22-µm Whatman filter paper, and dried in a low temperature oven (~80°C) prior to analysis.

2.3.5 *Leaching and Stripping Experiments.*

Pretreatment, leaching, and stripping followed the scheme below (Figure 2.5).

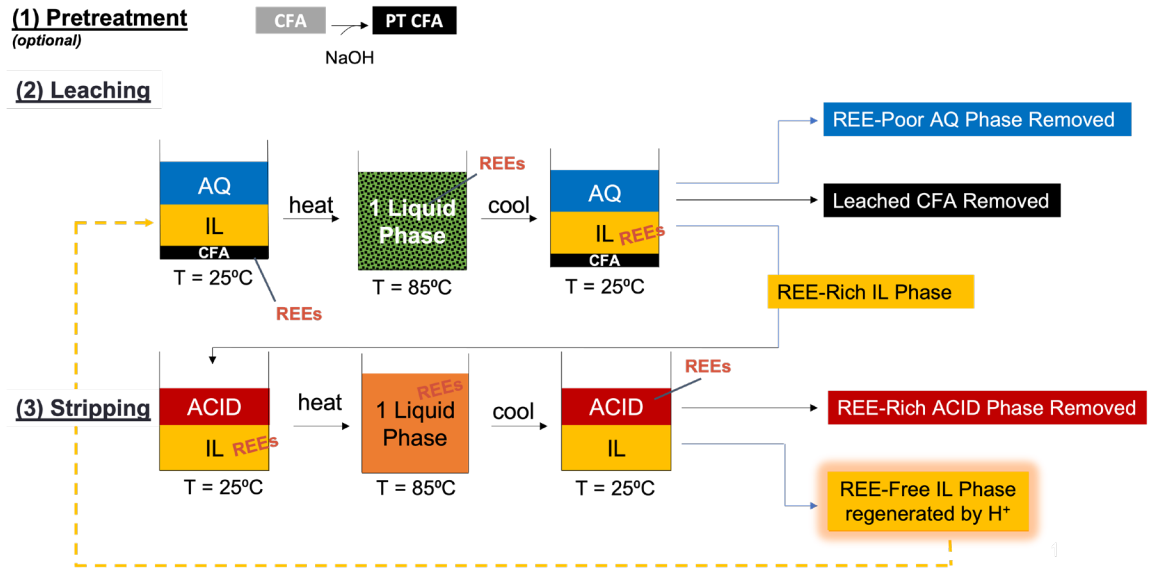

Figure 2.5 IL leaching and stripping scheme.

2.3.5.1 Leaching.

Small glass vials were filled with 50 mg of CFA, 2.3 g water-saturated IL, and 1.7 g aqueous solution of 1.0 M $NaNO_3$, achieving an IL: water ratio of 1:1 by mass. $NaNO_3$ salt was added to promote separation and minimize the mutual solubilities of water and [Hbet][Tf_2N].[6,7,68,69] The aqueous solution was adjusted with small amounts of HNO_3 and NaOH to reach pH 3.50 ± 0.05 prior to mixing with IL.[6,7,69] A small magnetic stir bar was added to each vial, then the vial was shaken vigorously before being placed in an oil bath heated to 85°C for three hours where the sample was gently stirred continuously by the magnetic stir bar. Upon heating, [Hbet][Tf_2N] formed one phase with water. After three hours, the vial was removed from the oil bath and allowed to cool to room temperature before being stored at 4°C overnight. The phases separated upon cooling.

The aqueous phase was removed and diluted with 5% HNO_3 before ICP-OES analysis. The IL phase was transferred to a new vial for stripping. CFA was washed using small amounts of deionized water, collected by filtration using a Buchner funnel with 0.22-µm Whatman filter paper, and dried in a low temperature oven (~75°C) prior to analysis.

2.3.5.2 Stripping.

A small magnetic stir bar was added to a new vial containing the IL layer from the leaching experiments. 1.5 M HCl was added as a stripping phase to achieve a 1:1 mass ratio with the IL phase. The vial was shaken vigorously before being placed in an oil bath heated to 85°C for 1.5 hours, where the sample was gently stirred continuously by the

magnetic stir bar. Then, the vial was removed and allowed to cool to room temperature before being stored at 4°C overnight. The stripping phase was then diluted with 5% HNO_3 before ICP-OES analysis.

2.3.6 Recycling.

After stripping, the IL was reused in another leaching-stripping cycle with a new amount of CFA and aqueous solution, as detailed above, and it was used for a total of three leaching-stripping cycles. Between each cycle, the IL phase was contacted with two aliquots of cold deionized water, shaken vigorously, and then allowed to separate. The water phases were removed and dilute with 5% HNO_3 for ICP-OES analysis. This step removed excess acids from the IL phase before reuse.

2.3.7 Quantification of Extraction and Separation.

Elements may be leached from the CFA by the pretreatment (M_{PT}) step, and by the IL/water extraction into the aqueous phase (M_{AQ}) and the IL phase (M_{IL}), respectively, where M represents mass. The mass in the IL phase was determined by that measured in the stripping phase. Previous studies have demonstrated that all elements are completely stripped by the stripping phase from the IL using HCl at concentrations ≥ 1.0 M.[68,69]

To quantify the extraction and separation of elements from CFA, leaching efficiency (*L*) and distribution coefficient (*D*) were calculated. *L* represents how much an element is extracted by the procedures compared to its total amount (M_{total}) in the CFA (Equation 2). The total mass of each element in the CFA was determined by total digestion analysis performed in this study or from reported data.

$$L\ (in\ \%) = \frac{M_{PT}\ +\ M_{AQ}\ +.M_{IL}}{M_{Total}} \quad (2)$$

D is the ratio between the element's final mass in the IL phase and its mass in the aqueous phase (AQ) (Equation 3):

$$D = \frac{M_{IL}}{M_{AQ}} \quad (3)$$

All leaching and stripping tests were performed in duplicate. *L* and *D* were calculated for elements in each experimental trial and the averages were reported.

Preferential extraction of REEs over bulk elements can be illustrated in two ways. The first is by higher leaching efficiencies for REEs relative to bulk elements. REEs comprise approximately 0.5 wt.% of CFA, while bulk oxides compose over 80% wt. (Table 2.1). The second is by REEs achieving higher distribution values than bulk elements. High values of *D* indicate an element's preference to partition into the IL phase; low values of *D* indicate a preference for the aqueous phase.

2.4 Results and Discussion

2.4.1 Characterization of CFAs.

The classification of CFAs is based on primary oxide content (POC) – the sum of Si, Al, and Fe oxides – and Ca content.[105] Class-F ashes tend to have low Ca content (< 15%) and POC ≥ 70%, whereas Class-C ashes tend to have high Ca content (15-30%) and POC

≥ 50%.[25,106] It has been reported that Class-C ashes tend to have lower REE content compared to Class-F ashes, which is reflected in this study (Table 2.1).[1,25] All CFA samples displayed expected physical and morphological properties.[104]

Notably, weathered ashes like CFA-F2 show mineralogical differences. Following combustion, CFA may be mixed with water to form a slurry that can be pumped to a storage pond, where the CFA is weathered by water from above and below.[106] This hydration has two major effects: (1) new mineral phases develop, including carbonates, and amorphous clays (from glass hydrolysis); and (2) alkaline metals are leached.[106] Thus, weathered CFA may contain lower quantities of potentially interfering elements and present higher REEs concentrations in more accessible mineral forms.[106] In this study, the REE content of CFA-F2 was slightly less than that of CFA-F1.

Mineralogy also differed between Class-C and Class-F CFAs (Table 2.1). Class-F ashes usually contain nonreactive crystalline phases of mullite, sillimanite, and quartz. While Class-C ashes usually contain approximately the same proportion of quartz, they also are composed of reactive crystalline calcium phases like free lime, anhydrite, tricalcium aluminate, and calcium sulfoaluminate.[106,107] Ca minerals are often soluble in acidic solutions. Taggart et al. hypothesized that leaching from high Ca-CFAs demonstrated higher REE recovery with acid-based leaching because Ca dissolution exposed additional surface area of CFA particles, providing greater access to REEs.[1,78,79] Hence, it is anticipated that leaching efficiency and distribution will be higher for CFA-C1 compared to the Class-F CFA-F1 and CFA-F2.

2.4.2 IL Extraction from CFAs without Pre-treatment.

Owing to [Hbet][Tf_2N]'s thermomorphic behavior, leaching and stripping can be performed by contacting the IL with aqueous solutions and applying heat. In addition to its role in partitioning, water also reduces the viscosity of the mixture, which increases mass transfer. $NaNO_3$ was added to the aqueous phase to promote separation between the aqueous and IL phases.[7,68,69] The results for all CFA samples are shown in Figure 2.6.

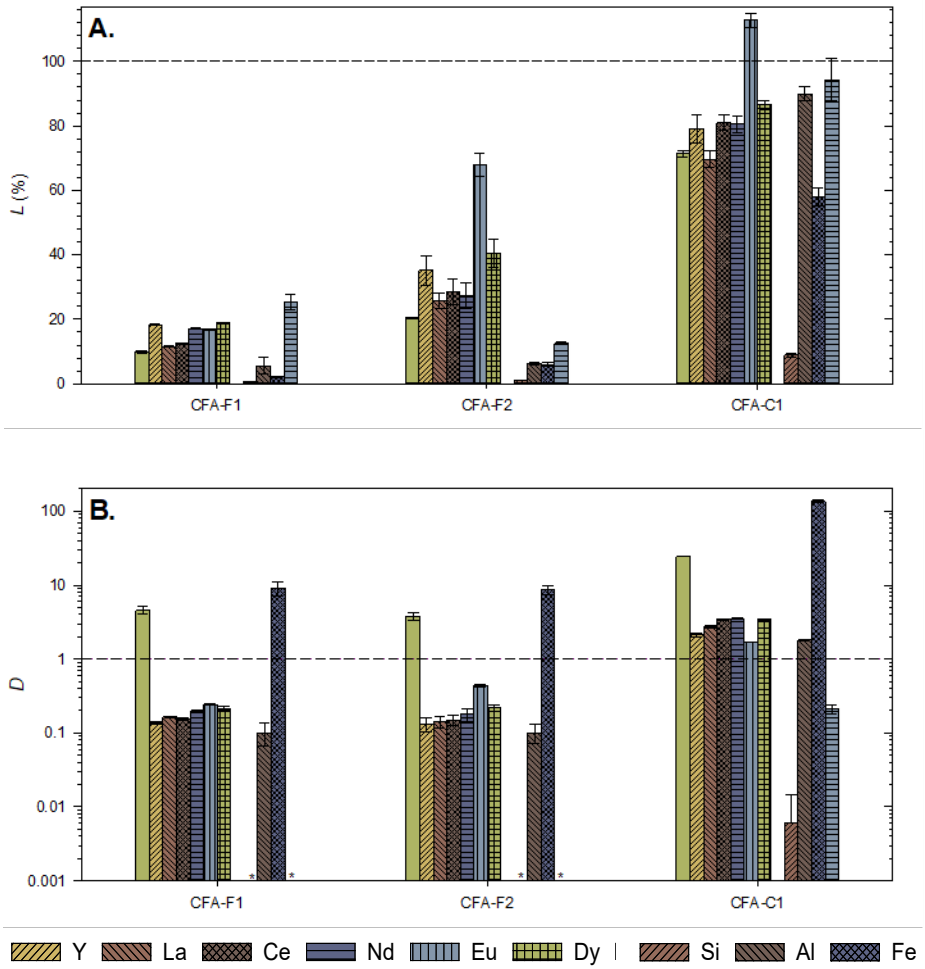

Figure 2.6 Average leaching efficiency *L* (A) and average distribution *D* (B) after IL extraction process for all CFAs without pretreatments.

*Note 1: Error bars indicate standard deviation of duplicate samples. Note 2: In **(B)**, columns marked with an * indicate zero, i.e., elements (Ca and Si) were not found in the IL phase. Note 3:*

Extraction efficiencies >100% may be the result of low initial concentration in the solid (Eu) or potential enrichment in the CFA as the results of alkaline pretreatment.

2.4.2.1 Class-F Ashes.

Class-F ashes demonstrated low leaching efficiencies for all REEs (L_{REEs} <~20% and <~40% for CFA-F1 and CFA-F2, respectively), as well as for bulk elements (L_{Bulk} < 7%) (Figure 2.6). Considering that about 71-83% of CFA composition is Al_2O_3 and SiO_2, and the leaching efficiency was only ~6% for Al and negligible for Si for both ashes, it can be concluded that the CFA particles were largely unaffected by the IL process. L_{Ca} was higher for CFA-F1 vs. CFA-F2.

The distribution between IL and AQ phase, D_{REEs}, was similar for both CFAs, and low values were observed for most REEs ($D_{REEs} \leq 0.21$ for CFA-F1, $D_{REEs} \leq 0.44$ for CFA-F2) with the exception of Sc (D_{Sc} = 4.6 for CFA-F1, 3.8 for CFA-F2). Interestingly, while Sc displayed the highest *D*, it had the lowest leaching efficiency of all REEs. Bulk elements largely demonstrated low distributions ($D_{Al,\ Ca,\ Si} < 0.10$ for CFA-F1; $D_{Al,\ Ca,\ Si} < 0.65$ for CFA-F2) with the exception of Fe (D_{Fe} = 9.2 for CFA-F1, 8.8 for CFA-F2).

It is expected that weathered ashes like CFA-F2 lack major cations and contain more amorphous content compared to unweathered ash as a result of exposure to standing water.[106] Theoretically this would result in considerably higher D_{REEs} and L_{REEs} in weathered versus unweathered CFA. The weathered CFA-F2 analyzed in this study did not contain a higher proportion of amorphous phases compared to CFA-F1 according to the XRD analysis (Table 2.1), and *L* was only slightly higher for REEs and negligibly different for bulk elements. These results support literature indicating that weathering induces morphological changes in the CFA that, rather than resulting in more accessible REEs,

entraps them in secondary (or tertiary) mineral formation.[106] It also may be that the CFA-F2 sample only demonstrates minor weathering damage compared to other CFAs.

2.4.2.2 Class-C Ash.

The Class-C CFA-C1 demonstrated high $L_{REE,avg}$ (~83%), with Sc displaying a slightly lower value (average L_{Sc} = 71.4%) (Figure 2.6). Unlike with the Class-F CFAs, leaching efficiencies were high for Al, Ca, and Fe, while L_{Si} remained low for CFA-C1.

Class-C ashes are widely known to be less recalcitrant than Class-F ashes. Taggart et al. noted that Powder River Basin CFAs (Ca-rich Class-C CFAs) have lower total REE concentrations but demonstrated superior recovery by nitric acid (pKa = -1.4) extraction.[78,79] They hypothesized that CaO dissolved under the acidic condition, exposing additional CFA particle surface area and releasing REEs.[31,32] In this study, the equilibrium pH of the IL leaching process is around 1.3 and [Hbet][Tf_2N] has pKa around 1.82.[68,69] Furthermore, King et al. surmised that acid leaching of CFA may generate a Si-rich gel layer over the ash, which may be destabilized by Ca.[78,79,108-110] Thus, it is expected that Ca-rich Class-C CFAs leach more significantly under acidic conditions than Class-F CFAs.

CFA-C1 also showed higher D for all elements compared to CFA-F1 and CFA-F2, indicating that, not only is more material leached from this CFA, but more distributes into the IL phase (Figure 2.6). Notably, for all REEs, $D_{REEs} > 1$. Scandium showed distribution (D_{Sc} = 24.2) an order of magnitude higher than D_{Sc} for CFA-F1 and CFA-F2. The high D_{REEs} may be the result of greater accessibility of the REEs promoted by CaO dissolution during leaching. While D_{Ca} is higher for CFA-C1 than other ashes, the value remains low

(D_{Ca} = 0.21), indicating that even for Ca-rich ashes, calcium does not partition strongly into the IL phase.

2.4.2.3 IL-AQ Partitioning Mechanism.

Across all CFAs, Sc and Fe both consistently showed a strong preference for the IL phase ($D > 1$). This behavior is consistent with previous literature on [Hbet][Tf_2N]. Under acidic conditions, carboxylic acid-based extractants tend to form strong complexes with ions with high charge density and high electronegativity. Trivalent REEs have high charge density, but Fe^{3+} and Sc^{3+} display higher charge density as a result of their smaller ionic radii.[7,8,111,112] Thus, Fe- and Sc-betaine complexes tend to be more stable than other REE-betaine complexes, leading to more efficient extraction into the IL phase.[7,8,111] As for the other bulk elements, Si showed no potential to partition into the IL phase likely because silica is poorly soluble due to its formation of oxyanions, which are sterically hindered from complexing with betaine. The partitioning mechanism for Al and Ca is not known, but other studies on this IL in simple aqueous systems surmised that partitioning depends on a number of factors beyond steric geometry, including ionic radius, charge density, basicity, and electronegativity.[111] Free Al may precipitate as an aluminosilicate or form other complexes with anions leached from the CFA, which Matusiewicz et al. identified as F^-, Cl^-, CO_3^{2-}, NO_3^-, and SO_4^{2-}, as well as oxyanions of heavy metals.[113]

2.4.3 Evaluation of Pretreatment of CFA.

The extraction results from CFA-F1 and CFA-F2 indicate that the CFA particles remained mostly intact in the IL leaching/stripping procedure. Given the low L_{Al} and L_{Si} values and the understanding that REEs are likely dispersed throughout the aluminosilicate

glass phases, pretreatments of CFAs were evaluated to improve REE extraction. An effective pretreatment should minimize REE loss during pretreatment, increase leaching efficiency for REEs, and promote phase separation for REEs and bulk elements (high D_{REEs} and low D_{Bulk}). Pretreatment should also minimize the production of additional wastes.

Aluminosilicate materials can be attacked by either acidic or alkaline treatments.[32,78,79,107,114] Varying concentrations of acidic and alkaline solutions (1.0-10.0 M NaOH; 1.0-5.0 M HNO_3) were tested on CFA-F1 at different solid/liquid ratios (1:10, 1:25, and 1:50 (g ash)/(mL solution). The results are summarized in Table 2.2.

Table 2.2 Elements leached from CFA-F1 using acidic and alkaline pretreatments (wt. % lost relative to total mass reported in NIST certificate)

Treatment	ACIDIC						ALKALINE								
	5.0 M HNO_3			10.0 M HNO_3			1.0 M NaOH			5.0 M NaOH			10.0 M NaOH		
S/L ratio (g/mL)	1:10	1:25	1:50	1:10	1:25	1:50	1:10	1:25	1:50	1:10	1:25	1:50	1:10	1:25	1:50
Sc	18	14.1	8.4	15.7	12.4	6.9	-	-	-	-	-	-	-	-	-
Y	28.2	25.5	21	25.4	22.6	19.9	-	-	-	-	-	-	-	-	-
La	21.5	21.7	22.5	19.3	20.7	21.2	-	-	-	-	-	-	-	-	-
Ce	24.4	25.2	29.5	21.6	24.9	24.7	-	-	-	-	-	-	-	-	-
Nd	38.4	45.7	62.6	35.7	48.6	68.6	-	-	17.8	4.3	14.3	25.3	3.9	13	40.9
Eu	-	-	-	-	-	-	-	-	-	-	-	-	-	-	-
Dy	27.2	-	-	24.8	-	-	-	-	-	-	-	-	-	-	-
Si	-	-	-	-	-	-	7.1	11.9	1.2	50.6	40.4	66.8	10.6	38.4	90.8
Al	10.2	36	8.7	7.8	3.5	35.9	0.8	3.4	9.2	7	4.4	0.7	5.6	3.3	1.6
Fe	12.9	12.3	10	12.4	12.5	11.5	-	0.4	0.2	0.4	0.9	2.2	0.4	1.9	2.8
Ca	10.4	11.5	13.8	9.7	10.8	13.7	1.1	2.7	5.2	1.1	2.6	5.2	1	2.6	5.3
Mg	19.5	18.3	17.6	17.2	16.4	16.8	0.3	0.6	0.8	0.3	0.3	0.6	0.3	-	-
Mn	31.3	27.6	22.8	27.7	26.4	22.8	-	-	-	-	-	-	-	9.6	16.2
Ti	7.8	8	8.3	6.1	6.5	6.7	-	-	-	0.1	0.1	0.2	0.1	0.2	0.4

Note: A "-" indicates that the element was not detected.

Overall, acidic pretreatments leached 20-70% of certain REEs while alkaline pretreatments leached undetectable levels of REEs at all tested solid/liquid ratios for CFA-F1, with the exception of Nd. More Nd leached as the solid/liquid ratio and NaOH concentration increased.

Acidic pretreatments leached relatively small amounts of Al, Ca, and Fe at all solid/liquid ratios, while Si was not detected in the leachate solution. Minor constituents (Mg, Ti, and Mn) leached consistently across all acidic treatments. In contrast, alkaline pretreatments generally leached small amounts (< 10 wt. %) of all elements with the exception of Si, with Si loss increasing as alkaline content (concentration and solid/liquid ratio) increased. Under alkaline conditions, Si demonstrated significant leaching above 5.0 M NaOH, ranging from 27-67%. NaOH is widely known to be a desilication agent.[1,78,79]

The ideal pretreatment should damage the aluminosilicate structure but not to dissolve it completely. Alkaline pretreatments were deemed to be more promising as they minimized REE loss but leached Si significantly. The alkaline pretreatments at 1:50 g/mL were eliminated due to high bulk element leaching and the desire to minimize additional waste. Thus, alkaline pretreatments of CFAs at solid/liquid ratios of 1:10 and 1:25 g/mL were adopted and followed by the IL leaching/stripping to determine the optimal strategy to increase REE extraction efficiency.

2.4.4 IL Extraction of CFA-F1 with Alkaline Pretreatment.

Overall, alkaline pretreatment increased REE leaching efficiency (Figure 2.7). For pretreatments by 1.0 M NaOH, solid/liquid ratios of 1:10 and 1:25 approximately doubled L_{REEs} from that of untreated CFA. Pretreatments with 5.0 and 10.0 M NaOH increased L_{REEs} to above 50%, averaging above 75%. The best pretreatment achieving acceptable L_{REEs} was determined to be 5.0 M NaOH at 1:10 solid/liquid ratio for moderate alkaline liquid concentration and volume. Alkaline pretreatment also increased L_{Bulk} (Figure 2.7) but appeared to have a maximum for Al (~40%) and Fe (~20%).

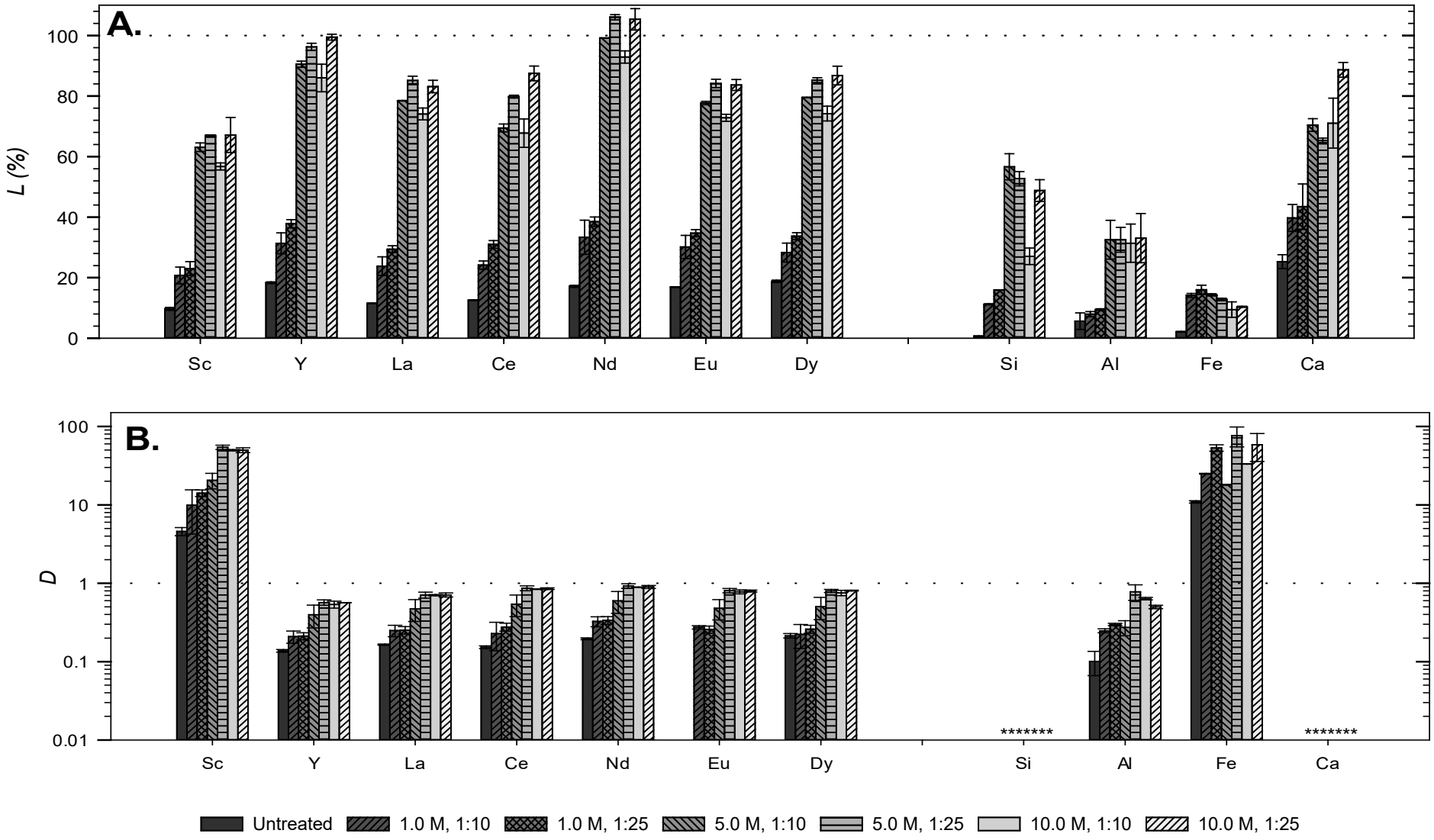

Figure 2.7 Average leaching efficiency L (A) and average distribution D (B) after IL extraction process for CFA-F1 with all pretreatments.

*Note: Pretreatments include 1.0 M, 5.0 M, and 10.0 M NaOH at a solid/liquid ratio of 1:10 or 1:25 g/mL. Error bars indicate standard deviation of duplicate samples. In (B), columns marked with an * indicate zero, meaning that these elements (Ca and Si) were not found in the IL phase.*

Interestingly, alkaline pretreatment also increased REE distribution coefficients (Figure 2.7. The highest D_{REEs} were observed for pretreatments by 5.0 and 10.0 M NaOH at solid/liquid ratios 1:10 and 1:25, with no significant difference among these four pretreatments. Unfortunately, these D_{REEs} values (approaching 1) indicate no strong IL phase preference, which ultimately confounds attempts to streamline separation. Of the four bulk elements, only D_{Al} and D_{Fe} were impacted by alkaline pretreatment, as Si and Ca did not partition into the IL phase (Figure 2.7). Under all conditions, Fe exhibited a strong preference for the IL phase (D_{Fe} >>1). Al only showed a response under strong conditions.

Considering the desire to limit waste production, the solid/liquid ratio of 1:10 g/mL was chosen for further testing on other CFAs. Loss from CFA-F2 and CFA-C1 are shown below (Table 2.3 and Table 2.4, respectively).

Table 2.3 Elements leached from CFA-F2 using alkaline pretreatments at solid/liquid ratio (g/mL) of 1:10 (wt. % lost relative to total mass as determined by total digestion)

Element/Treatment	ALKALINE		
	1.0 M NaOH	5.0 M NaOH	10.0 M NaOH
Sc	0.33	0.47	1.28
Y	0.12	0.16	0.16
La	0.12	0.05	0.12
Ce	0.08	0	0
Nd	0.14	0.08	0.17
Eu	4.72	0.98	3.84
Dy	0.79	0.83	0.56
Si	7.8	50.7	41.1
Al	3.2	1.8	2.8
Fe	2.5	4.1	6.7
Ca	25.4	22.7	21.6

Table 2.4 Elements leached from CFA-C1 using alkaline pretreatments at solid/liquid ratio (g/mL) of 1:10 (wt. % lost relative to total mass as determined by total digestion)

Element/Treatment	ALKALINE		
	1.0 M NaOH	5.0 M NaOH	10.0 M NaOH
Sc	0.13	0.13	0.14
Y	0.11	0.11	0.11
La	0.15	0.08	0.07
Ce	0.27	0	0
Nd	0.18	0	0
Eu	0.18	0.14	0.09
Dy	0.1	0.09	0.07
Si	1.9	12.9	18.7
Al	23.9	7.5	9.1
Fe	3.2	3.9	4.6
Ca	13	11.9	13

2.4.5 IL Extraction of all CFAs with Alkaline Pretreatment at 1:10 g/mL.

Three alkaline pretreatments (1.0 M, 5.0 M, and 10.0 M NaOH at a 1:10 g/mL solid/liquid ratio) were further evaluated to be coupled with IL leaching on three CFA samples. The solid/liquid ratio of 1:10 g/mL was chosen based on the desire to limit waste production. Pretreatment by 5.0 M NaOH was found to be the most efficient (Figure 2.8, and Figure 2.9).

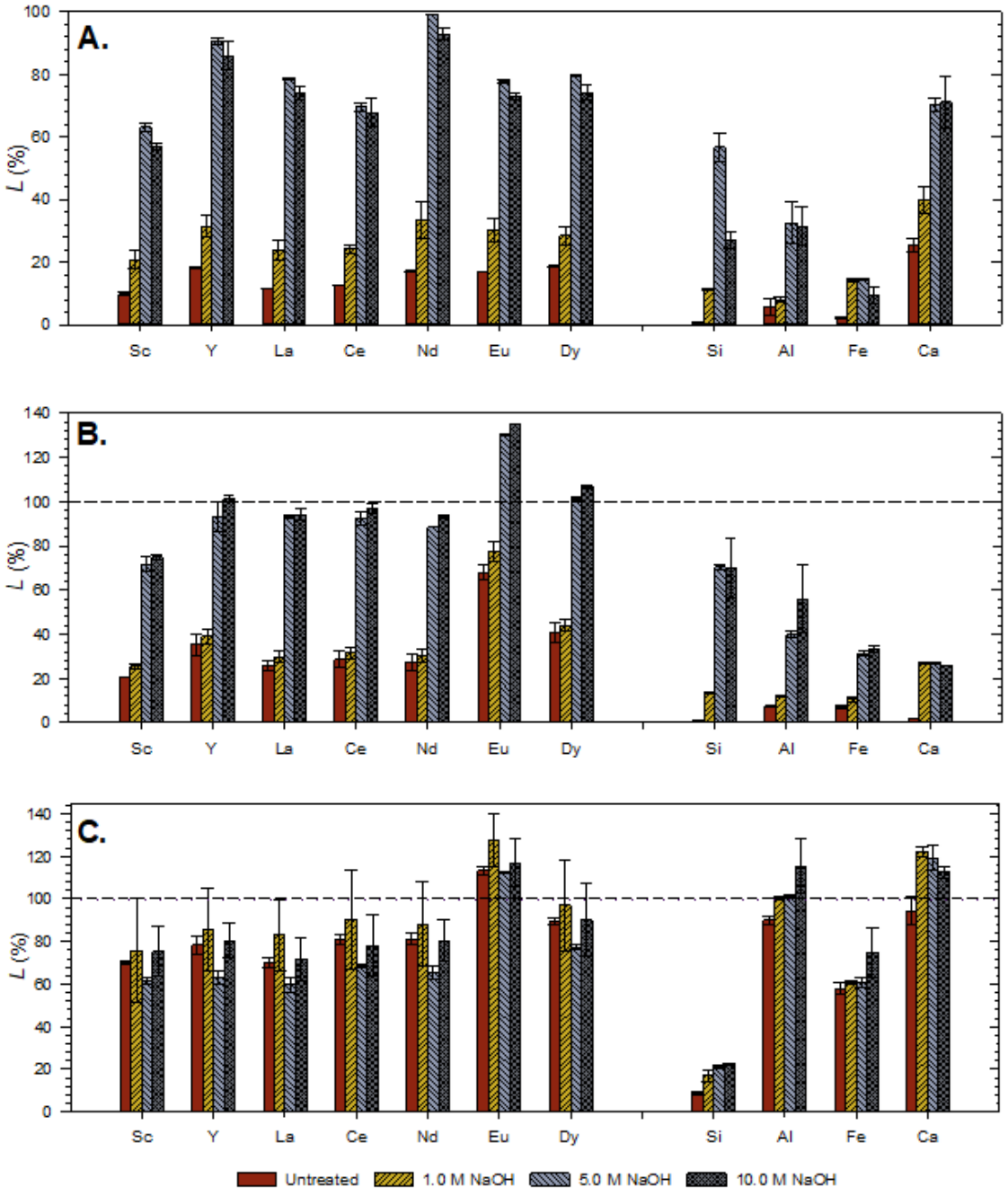

Figure 2.8 Average leaching efficiency *L* for alkaline pretreated CFA-F1 (A), CFA-F2 (B), and CFA-C1 (C) after IL extraction.

Note: CFAs pretreated with 1.0, 5.0, and 10.0 M NaOH at a solid/liquid ratio of 1 g/10 mL. Error bars indicate standard deviation of duplicate samples. Extraction efficiencies >100% may be the result of low initial concentration in the solid (Eu) or potential enrichment in the CFA as the results of alkaline pretreatment.

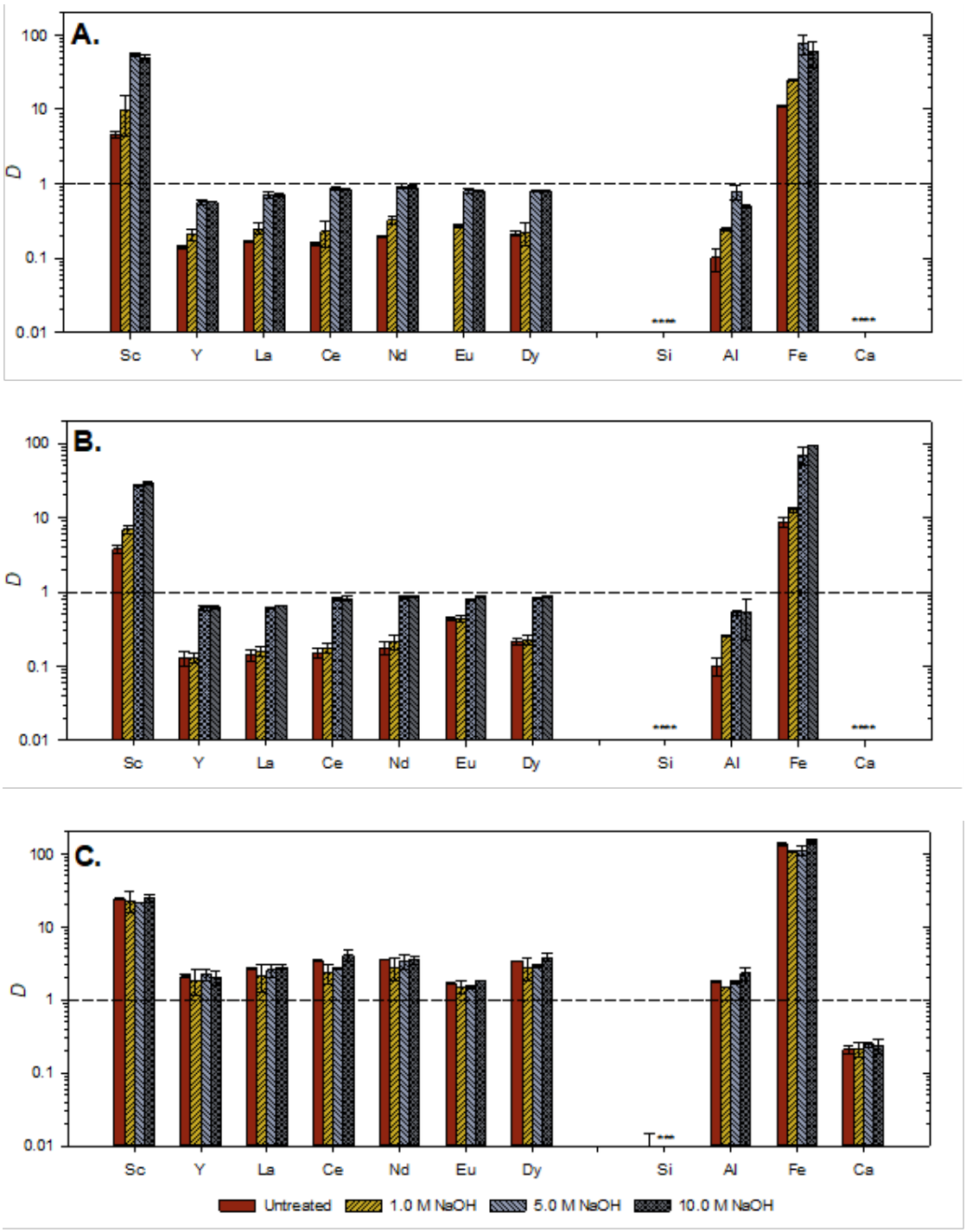

Figure 2.9 Average distribution *D* for CFA-F1 (A), CFA-F2 (B), and CFA-C1 (C), after IL extraction.

*Note: CFAs pretreated with 1.0, 5.0, and 10.0 M NaOH at a solid/liquid ratio of 1 g/10 mL. Error bars indicate standard deviation of duplicate samples. Columns marked with an * indicate zero, meaning that these elements (Ca and Si) were not found in the IL phase.*

For ease of comparison, IL *L* and *D* by CFA type at the optimal alkaline pretreatment conditions, 5.0 M NaOH at 1:10 g/mL ratio are shown below (Figure 2.10).

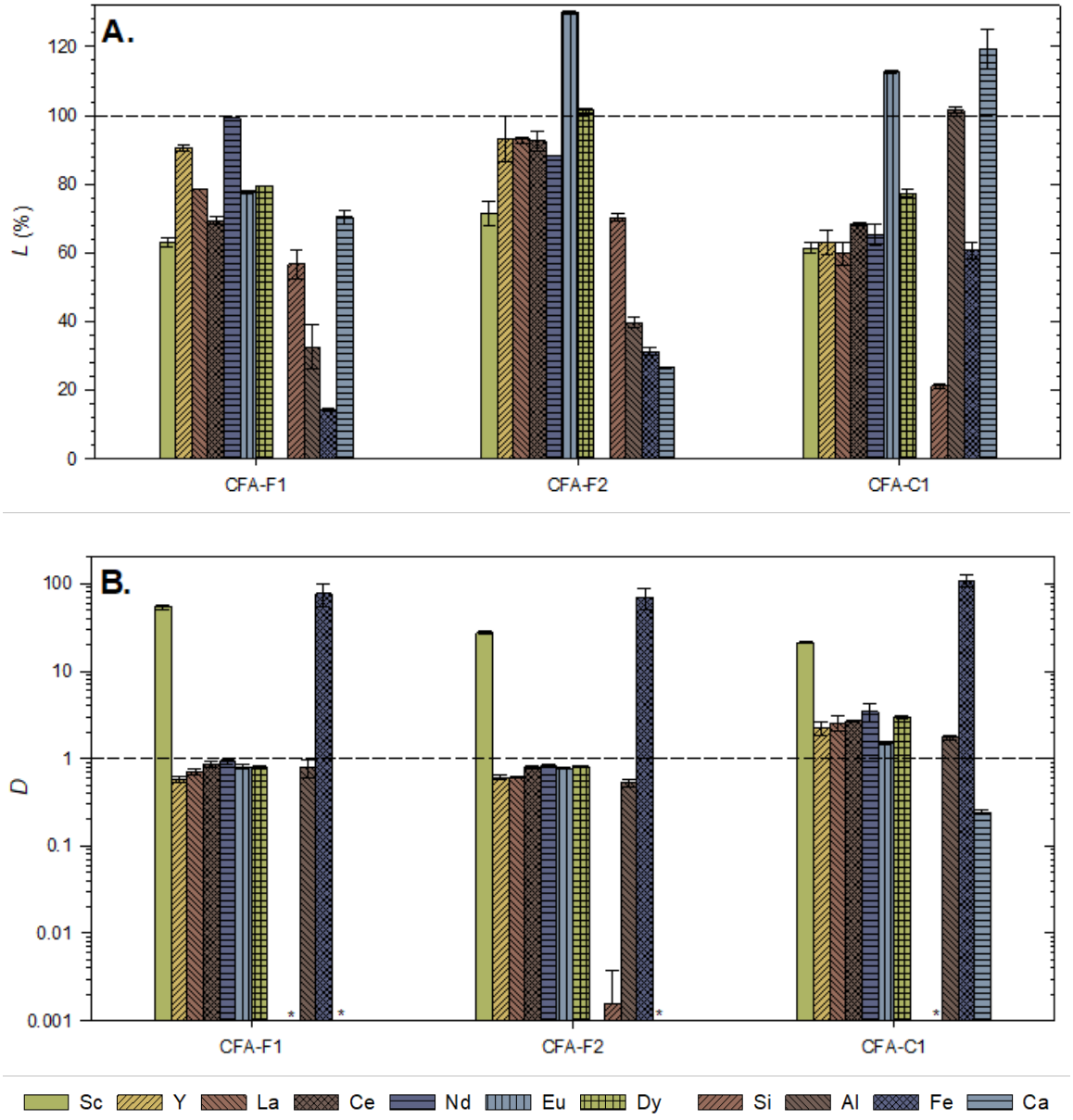

Figure 2.10 Average leaching efficiency *L* (A) and average distribution D (B) after IL extraction process for all CFAs pretreated with 5.0 M NaOH at 1:10 g/mL ratio.

*Note: Error bars indicate standard deviation of duplicate samples. In **(B)**, columns marked with an * indicate zero, meaning that these elements (Ca and/or Si) were not found in the IL phase for CFA F-1 and F-2. Extraction efficiencies >100% may be the result of low initial concentration in the solid (Eu) or potential enrichment in the CFA as the results of alkaline pretreatment.*

2.4.5.1 Unweathered vs. Weathered Class-F Ashes.

For both CFA-F1 and CFA-F2, alkaline pretreatment resulted in <~5 wt. % loss for REEs, Al, and Fe (Table 2.2 and Table 2.3). Si loss was approximately the same for both ashes, with the highest losses reported for 5.0 M NaOH. Interestingly, CFA-F2 demonstrated significantly higher losses in Ca (~23 wt.% vs. 1 wt.%) and Fe (~4 wt.% vs. 0.4 wt.%).

Alkaline pretreatment of CFA-F1 and CFA-F2 increased leaching efficiencies for all elements (Figure 2.8 and Figure 2.10). Pretreatments by 5.0 and 10.0 M NaOH showed dramatic improvements, without significant difference between the two conditions. Notably, L_{REEs} was higher for the weathered ash CFA-F2 than the unweathered CFA-F1 (97% and 77%, respectively). Similar to *L*, distribution *D* for all elements increased sharply with either 5.0 M or 10.0 M NaOH pretreatments (Figure 2.9 and Figure 2.10).

2.4.5.2 Class-C vs. Class-F Ash.

Similar to the Class-F CFAs, alkaline pretreatments resulted in negligible losses of REEs (<0.5 wt.% loss) but demonstrated higher losses for Al, Ca, and Fe (Table 2.4). Surprisingly, Si loss was low (<20 wt.%) even at high alkaline concentrations. L_{REEs} was already high for CFA-C1 ($L_{REE,avg}$ = 83.0%) without pretreatment. Alkaline pretreatments did not improve L_{REEs} (Figure 2.10 and Figure 2.8); in fact, they either had negligible impact or decreased L_{REEs}. L_{Bulk} was largely unaffected, with small increases observed for Al and Ca. There was no observed impact on *D* for any element by the pretreatment (Figure

2.10 and Figure 2.9). This may be the result of low Si leaching. For Class-C ashes, alkaline pretreatment did not improve or hinder L_{REEs} and D_{REEs}, and thus was deemed unnecessary.

2.4.5.3 XRD/SEM Analysis of CFA-F1 after Pretreatments and IL Extraction

CFA-F1 was analyzed by XRD and SEM for mineralogical and morphological changes resulting from alkaline pretreatment and IL leaching. Pretreatment of 5.0 M NaOH at a solid/liquid ratio of 1:10 g/mL resulted in loss (~10%) of amorphous content and the formation of hematite and sodium aluminum silicate hydrate, while quartz showed minor loss and mullite was unaffected (Table 2.1 and Figure 2.11).

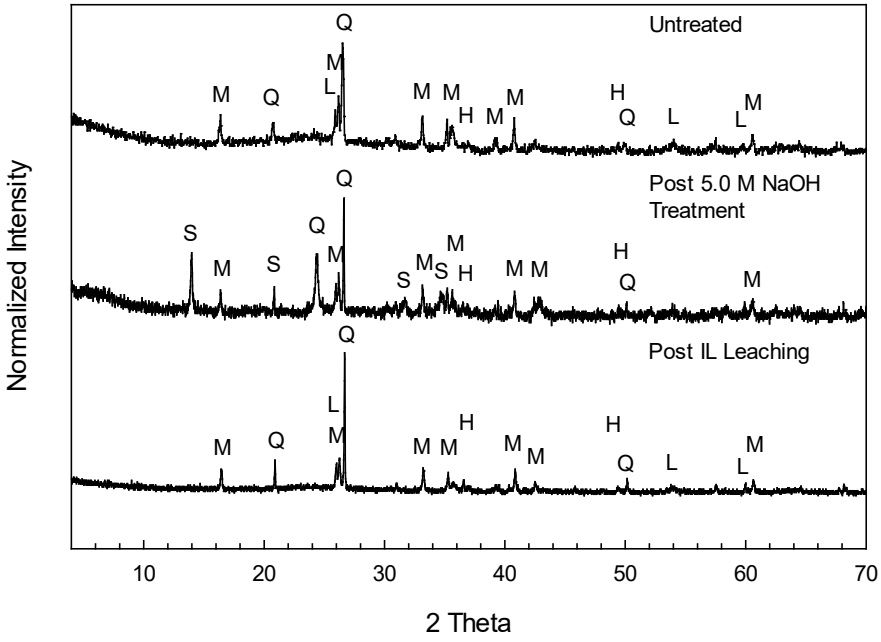

Figure 2.11 Normalized XRD patterns for CFA-F1 that was untreated, pretreated by 5.0 M NaOH at solid/liquid ratio of 1:10 g/mL, and finally by IL leaching.

Note: Q = quartz; M = mullite; H = hematite; L = sillimanite; S = sodium aluminum silicate hydrate.

SEM imaging (Figure 2.12) revealed two different surface morphologies: rosettes typical of hydrosodalite, and a ball of yarn shape typical of hydroxysodalite.[115-117] Previous research indicates that CFA responds to alkaline treatment via desilication. NaOH dissolves glass phases: hydroxide ions break apart SiO_4 tetrahedral subunits via nucleophilic attack on Si-O bonds.[1,78,79,94] Silica leaches into solution but reaches its maximum solubility and precipitates as amorphous silicates, including hydrosodalite and hydroxysodalite.[107,108,116,118] EDS analysis (Figure 2.13) confirmed the presence of $Na_2(AlSiO_3)_3$, a complex sodium silicate (often shown as $AlSiO_3(OH)_4^{3-}$) described in literature as a product of sodalite dissolution under alkaline conditions.[119-121] These silicates may act as a sink for leached metals during IL leaching.[79]

The IL leaching had minimal effect on the amorphous content but resulted in the disappearance of quartz and sodium silicates (Table 2.1 and Figure 2.11), which were likely dissolved by the acidic IL (pKa = 1.82).[115-117] No sodium appeared in the EDS analysis of the post IL leaching CFA, indicating dissolution into the aqueous phase during IL leaching (Figure 2.14). Increases in the weight percentage of mineral phases is likely the result of the persistence of those phases despite loss of material, which was supported by previous research.[122]

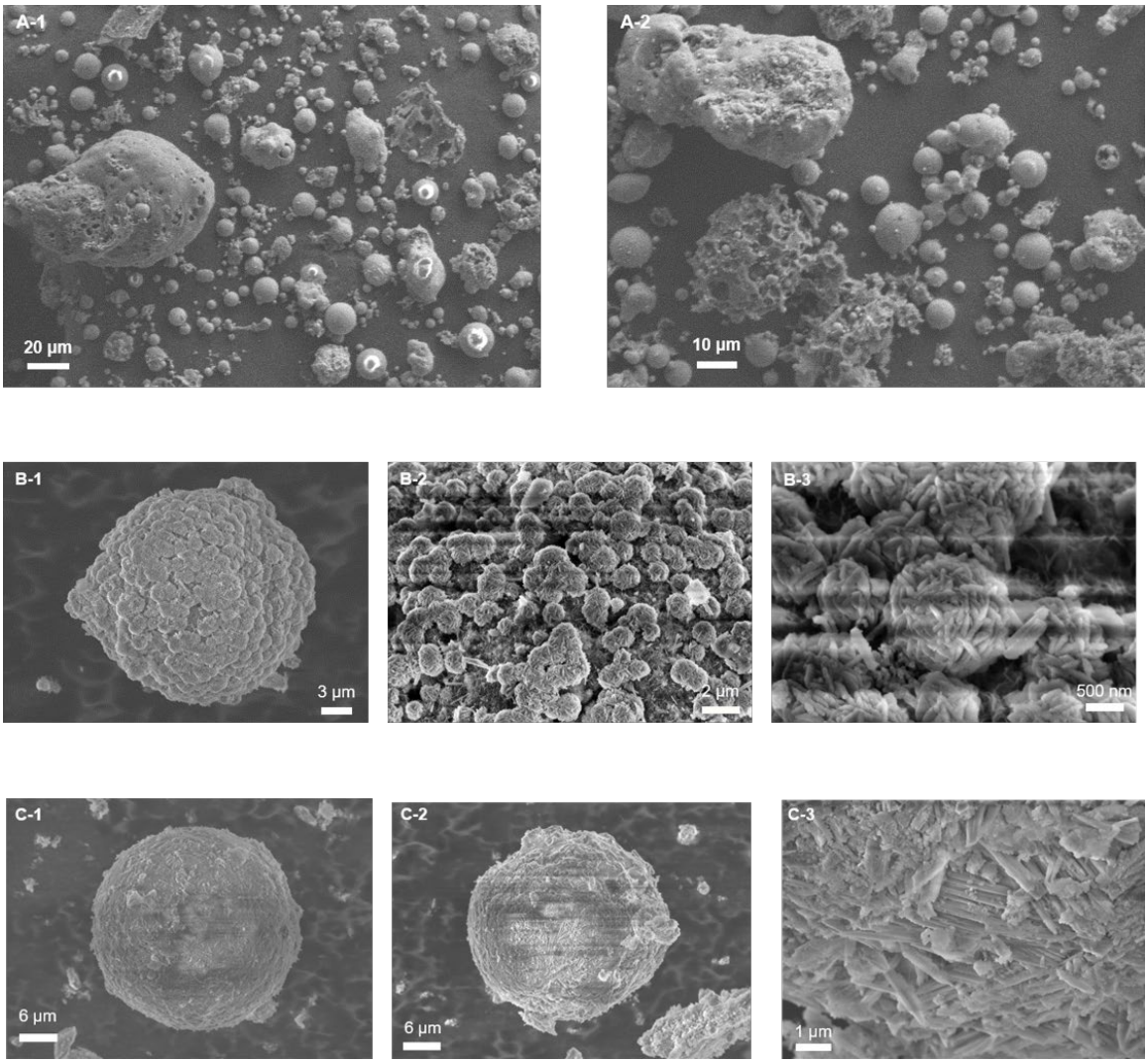

Figure 2.12 SEM images for CFA-F1 that was untreated (A), following 5.0 M NaOH pretreatment at solid/liquid ratio of 1:10 g/mL (B), and following final IL leaching (C).

*Note: The images in **B** show the same spot under increasing magnification. Image **C-3** is a magnification of the center of image **C-2.***

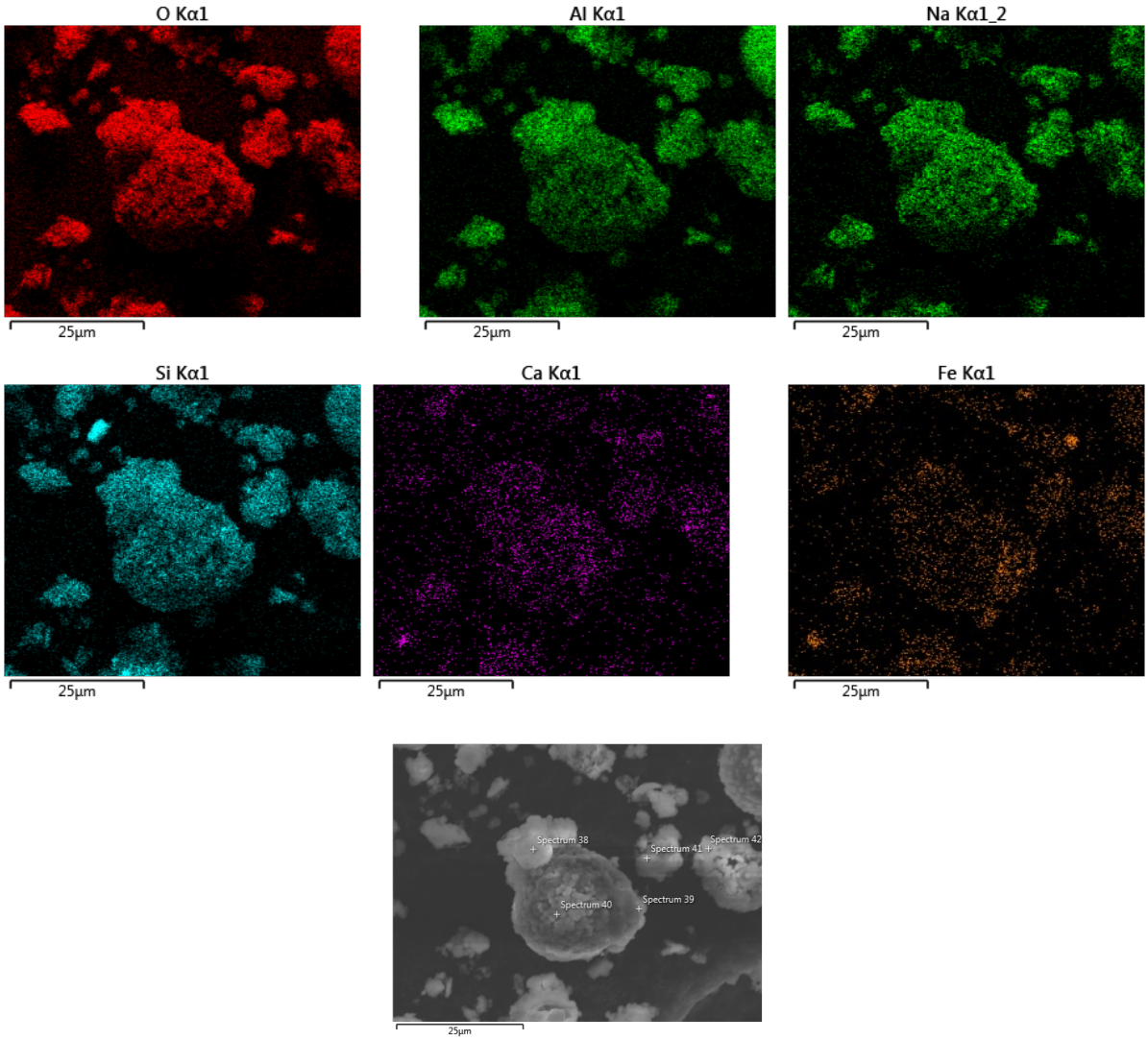

Figure 2.13 EDS mapping of CFA-F1 following pretreatment with 5.0 M NaOH at solid/liquid ratio of 1:10 g/mL.

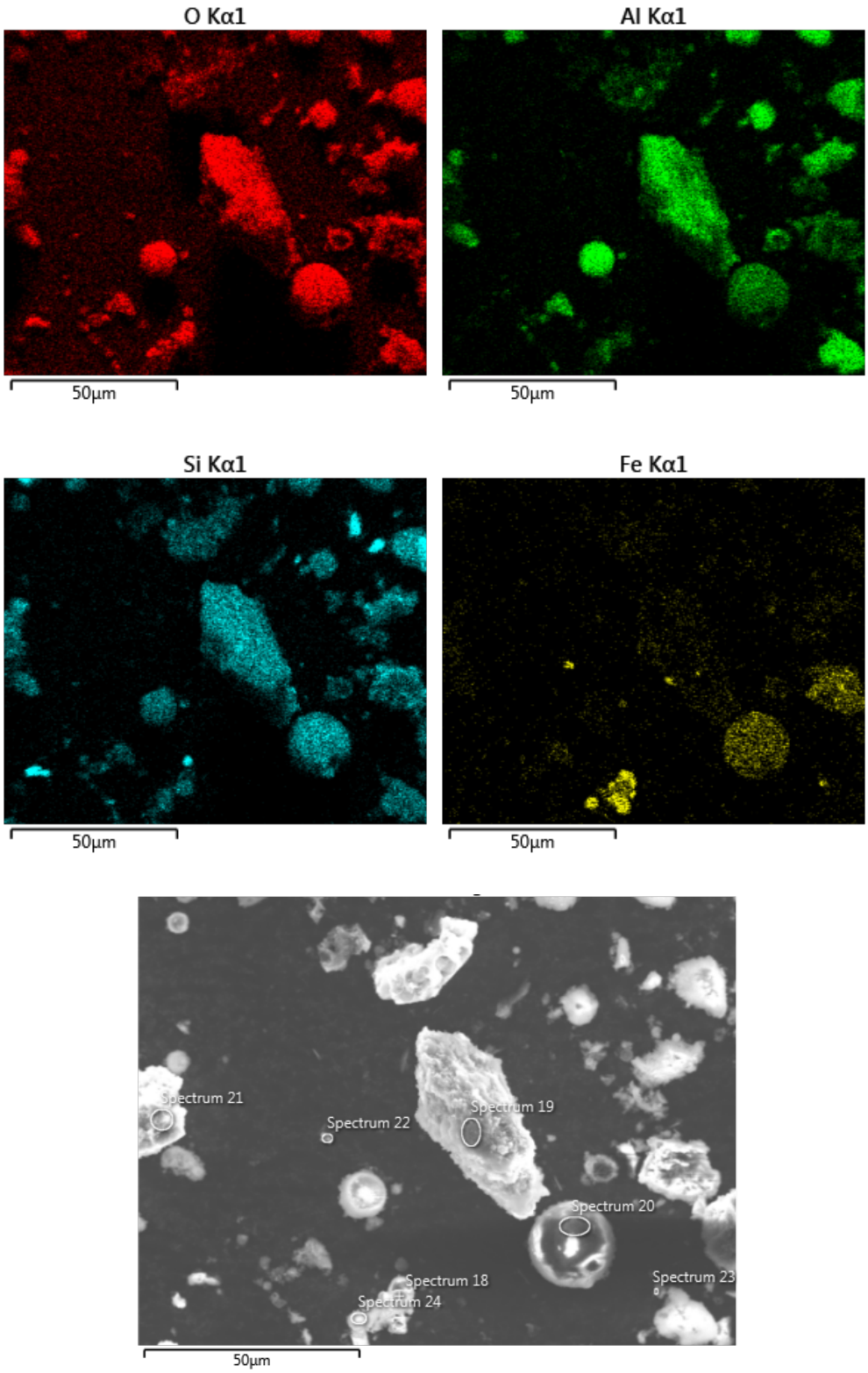

Figure 2.14 EDS mapping of CFA-F1 following pretreatment with 5.0 M NaOH and IL leaching.

2.4.5.4 CFA Leaching Mechanism.

Alkaline pretreatment can dissolve the glass phases of CFA: hydroxide ions break apart SiO_4 tetrahedral subunits via nucleophilic attack on Si-O bonds.[1,78,79,94,123-127] Silica leaches into solution but precipitates as sodium aluminum silicates upon reaching maximum solubility.[108,123,124] This was confirmed via XRD and SEM analysis on CFA-F1 following alkaline pretreatment (Figure 2.11-Figure 2.14). Minor losses of quartz, sillimanite, and amorphous content, and no effect on mullite were observed (Table 2.1 and Figure 2.11).

The newly formed sodium silicates and quartz were mostly dissolved by acidic IL leaching as confirmed by XRD and SEM analysis (Table 2.1, Figure 2.11-Figure 2.14). Furthermore, it is well known that under acidic conditions, glass phases leach alkali metals through diffusion, substituting these elements for H^+ or H_3O^+.[79,123,124] This phenomenon would expose additional CFA surfaces for dissolution.[79]

Previous research shows CFA desilication via alkaline pretreatment weakened the aluminosilicate matrix by converting more stable quartz and amorphous phases to acid-susceptible zeolites and unstable amorphous silica precipitates.[79,124,128] It is hypothesized that the combination of alkaline pretreatment and acidic IL leaching made REEs in CFA more accessible for extraction.

Notably, weathered Class-F CFA showed higher L_{REEs} compared to unweathered Class-F CFA. One cause may be physical damage from weathering, including fractures of aluminosilicate glass spheres. Weathering likely exposes additional surface area to both alkaline pretreatment and IL leaching.[1,106] Another cause may be Ca. Ca mineralogy is known to differ between weathered and unweathered CFAs, and CFA-F2, the weathered

Class-F CFA, lost more Ca in alkaline pretreatment than CFA-F1, despite having approximately the same amount of Ca (1.75 wt. %).[106] Ca leaching from CFA in sequential alkaline-acidic treatments is not well understood mechanistically. Under acidic conditions, many Ca minerals dissolve, and dissolved Ca can destabilize the Si-rich gel layer that forms over CFA particle surfaces, which likely promotes additional dissolution.[78,79,129] In contrast, under alkaline conditions, dissolved Ca can form Ca-silicates, which may act as a REE sink or prevent leaching.[79,130] It is hypothesized that for the weathered Class-F CFA, both the physical damage as well as the dissolution of Ca exposed additional surfaces for IL leaching, leading to higher L_{REEs} from CFA-F2. For Class-C CFAs, Ca is easily leached without pretreatment; with alkaline pretreatment, dissolved Ca forms Ca-silicates that entrap REEs.[79] This phenomenon may explain the decrease in L_{REEs} for Class-C CFAs following alkaline pretreatment in this study.

2.4.6 Improving Distribution of REEs in IL.

Alkaline pretreatment demonstrated that L_{REEs} could be successfully increased while keeping L_{Bulk} low. To further improve this process, separation between REEs and bulk elements must be increased, by increasing D_{REEs} and decreasing D_{Bulk}.

2.4.6.1 Enhancement by Betaine.

Vander Hoogerstraete et al. found that adding betaine in large excess (>100x) to REEs would achieve higher distribution ratios.[68,69] They postulated that excess betaine shifted Eq. 1 towards the formation of $[REE(bet)_3][Tf_2N]$ complexes, which prefer the IL phase.[68,69] They were able to increase D_{Nd} from < 1 to over 100.[68,69] Hence, solid betaine chloride was dissolved into to the aqueous phase solution (1.0 M $NaNO_3$) to achieve

concentrations of 1, 5, 10, 50, 100, and 200 mg betaine/g aqueous solution. The pH was modified with small amounts of NaOH and HNO_3 as needed. The same IL leaching/stripping protocol was followed as described in *2.5.1*.

D_{REEs} increased with increasing betaine for all REEs with the exception of Sc, indicating that REEs increasingly partitioned into the IL phase (Figure 2.7). Overall, D_{REEs} increased to 1.0 at betaine concentration of 1 mg/g and peaked at the highest betaine concentration of 200 mg/g ($D_{Ce,\ Dy,\ La,\ Y} > 4.0$). D_{Sc} remained high but decreased some with increasing betaine concentration.

D_{Al} followed a similar, nearly linear increase with increasing betaine and did not exceed 1.0 until 50 mg/g betaine was added (Figure 2.7). Betaine addition did not influence Ca or Si partitioning (D_{Ca} and D_{Si} remained at near zero). D_{Fe} increased at all levels of additional betaine and approached infinity above 50 mg/g betaine due to negligible amounts of Fe in the aqueous phase and high amounts of Fe in the IL phase (see Eq. 3).

Adding betaine also influenced leaching efficiency (Figure 2.7). At betaine concentrations of 1, 5, and 10 mg/g, L_{REEs} was > 90%. Though L_{REEs} exceeded 90%, D_{REEs} remained ~1 under these conditions, indicating that the majority of REEs leached out of the CFA and partitioned approximately equally into the IL and liquid phases. At above 10 mg/g betaine concentration, however, L_{REEs} fell below the levels achieved by the 5.0 M NaOH pretreatment alone (< 60%).

Leaching efficiency for Al, Ca, and Fe were largely unaffected by increasing betaine (Figure 2.7). While D_{Al} and D_{Fe} increased with increasing betaine, L_{Al} and L_{Fe} were largely unchanged. L_{Si} increased at intermediate levels of betaine addition.

2.4.6.2 Mechanisms.

There could be several possible explanations for the decrease in L_{REEs} while D_{REEs} increased with increasing betaine. Si may be responsible for this phenomenon. As betaine was added, D_{Si} remained near zero, indicating Si does not complex with betaine, as is consistent with previous literature.[5,7,65,68,69] However, L_{Si} followed a pattern similar to that of REEs, first increasing with small additions of betaine and then decreasing at higher betaine levels. It was observed during experimentation that the betaine chloride solutions added acidity, and experiments occurring days apart required additional alkaline input to correct pH. (Noted the pH of the aqueous phase was always checked and corrected to pH = 3.50±0.05 if necessary immediately prior to extraction experiments.) Lower than expected L_{Si} values in concert with negligible D_{Si} indicate that Si leached into solution only to precipitate as secondary silicates; in fact, under acidic conditions, Si forms orthosilicic acid (SiO_4^-), which self-polymerizes to form gels. As previously stated, King et al. found that acid leaching of CFA may generate a Si-rich gel layer.[79,108] If this gel coated CFA particle surfaces, it might preclude access to the REEs, resulting in lower L_{REEs} values but not necessarily lower D_{REEs}. REEs able to escape the Si-gel would strongly partition into the IL phase in the presence of additional betaine.

Another potential explanation for the decreased L_{REEs} at high levels of extra betaine is that other metal cations not measured in this study may complex with betaine in competition with REEs, as is indicated by the linear relationship emerges between log distribution D and log additional betaine concentration for many of the REEs, with the exception of Sc (Figure 2.15, Table 2.5).

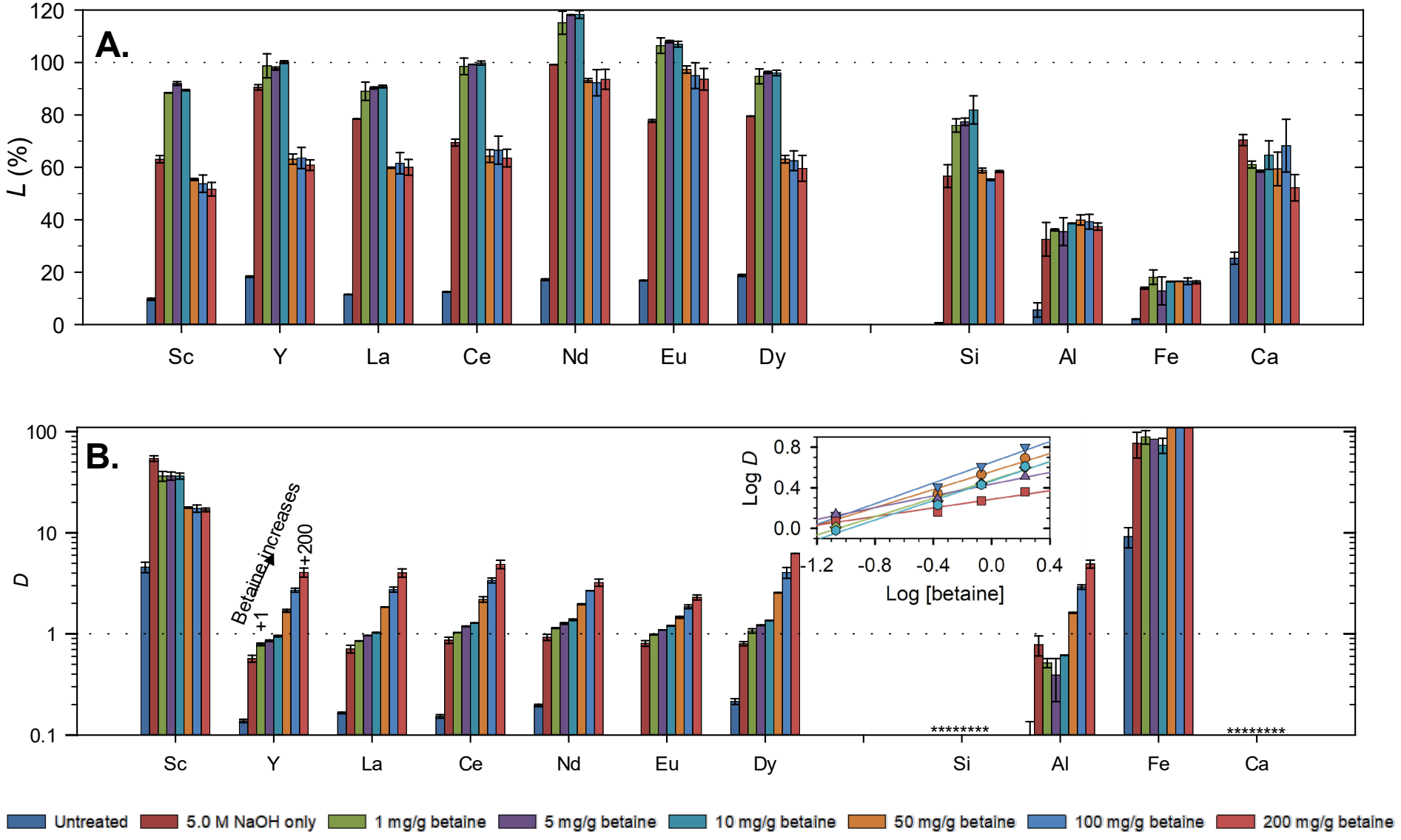

Figure 2.15 Effects of extra betaine: leaching efficiency L (A) and distribution D (B) after IL extraction for pre-treated CFA-F1, and with additional betaine (ranging 0 mg/g – 200 mg/g).

*Notes: "Untreated" = CFA-F1 without alkaline pretreatment or extra betaine. "5.0 M NaOH Only" = alkaline pretreated CFA-F1 (solid/liquid ratio of 1 g/10 mL) without additional betaine. Error bars indicate standard deviation of duplicate samples. In **(B)**, columns marked with an † indicate an extremely large value of D. In **(B)**, columns marked with an * indicate zero, meaning that these elements (Ca and Si) were not found in the IL phase. Inset in (**B**) is the linear relationship between log D and log betaine (mol betaine/kg aqueous solution). Extraction efficiencies >100% may be the result of low initial concentration in the solid (Eu) or potential enrichment in the CFA as the results of alkaline pretreatment.*

Table 2.5 Linear regression analysis of log distribution D versus log betaine (mol/kg) for REEs

Element	Slope	R^2
Sc	-15.58	0.8338
Y	0.4813	0.9764
La	0.4509	0.9856
Ce	0.4437	0.9772
Nd	0.2872	0.9789
Eu	0.2131	0.9325
Dy	0.5045	0.9819

Using the similar approach to that in the study by Vander Hoogerstraete et al. in which the authors extracted Nd^{3+} ions from $Nd(Tf_2N)_3$-containing aqueous solution using [Hbet][Tf_2N] and extra betaine added to the aqueous phase, the following equation could describe the reaction[69]:

$$REE^{3+}{}_{aq} + n * (bet)_{aq} + y(Tf_2N^-)_{aq} + x * H_2O \rightarrow [REE(bet)_n(H_2O)_x][(Tf_2N)]_y$$

$$Define: \quad [REE(bet)_n(H_2O)_x][(Tf_2N)]_y = [REE^{3+}]_{IL}$$

$$K_{eq} = \frac{[REE^{3+}]_{IL}}{[REE^{3+}]_{aq}[bet]^n{}_{aq}[Tf_2N^-]^y{}_{aq}}$$

$$Recall: \quad D = \frac{[REE^{3+}]_{IL}}{[REE^{3+}]_{aq}}$$

$$K_{eq} = \frac{D}{[bet]^n{}_{aq}[Tf_2N^-]^y{}_{aq}}$$

$$D = K_{eq} * [bet]^n{}_{aq} * [Tf_2N^-]^y{}_{aq}$$

$$\log_{10} D = \log_{10} K_{eq} + n * \log_{10}[bet]_{aq} + y * \log_{10}[Tf_2N^-]_{aq}$$

Research done by Vander Hoogerstraete indicates that the concentration of bistriflimide in the aqueous phase remains constant when betaine chloride is added in different amounts.[69] Thus, the K_{eq} and bistriflimide terms can be combined as a single constant, B, as in the following equation:

$$\log_{10} D = n * \log_{10}[bet]_{aq} + B$$

Log D vs log [betaine] can then be plotted (Figure 2.15).

The slope of the log D vs log [bet] represents the number of betaine ligands per metal cation of interest. Previous research using concentrated, single-cation feedstock solutions of $NdTf_2N$ without pH adjustments determined this value to be ~1.5 betaine ligands per Nd atom, indicating the formation of $[Nd_2(bet)_3(H_2O)_y]^{3+}$.[68,69] In the solid state, Nd and other REEs form bidentate complexes with eight betaine ligands.[65,68,69] In this study, the ratio was found to be considerably lower at 0.2 to 0.5 (Table 2.5), and no obvious trend among the elements (e.g., charge density, atomic radius and electronegativity) could be drawn

based on the current results. Electroneutrality might be achieved using [Tf_2N^-] or other anions present (nitrate, chloride, etc.).

A major difference exists between this study and the previous work in that the alkaline-pretreated CFA is a much more complex material than single-metal solution/oxide and contains a variety of elements at trace to moderate levels that could potentially exert influence.[24,30,32,33] These other elements might compete with REEs for additional betaine. Betaine might also impact the dissolution of CFA solid during the extraction step. Overall, the enhanced effect of extra betaine is useful and further research is required to elaborate on the affected mechanisms.

2.4.7 Recycling of IL.

For this leaching/stripping extraction process to be viable, the IL phase should be reusable. Previous literature using both aqueous feedstocks and REE-rich solids found that the IL could be reused following stripping without any additional steps. Theoretically, stripping should be sufficient to regenerate the IL phase; however, previous research also found that extraction efficiency decreased following contact with low pH solutions. This observation was reasonable given the IL's proton exchange mechanism (Eq. 1).[68,69,72] In this study, after extraction of the pretreated CFA-F1, the IL was contacted with cold DI water following stripping to remove excess acids. Then, the IL was reused for leaching of new CFA-F1 sample. This process was repeated twice. Both L_{REEs} and D_{REEs} were stable over three cycles (Figure 2.7). Slight decreases were observed for D_{Al} and D_{Fe} in the 2nd and 3rd cycles. Analysis of the wash solutions showed negligible quantities of any elements.

This indicates that this IL can be used successfully over multiple cycles without significant degeneration or loss in extraction efficiency or partitioning.

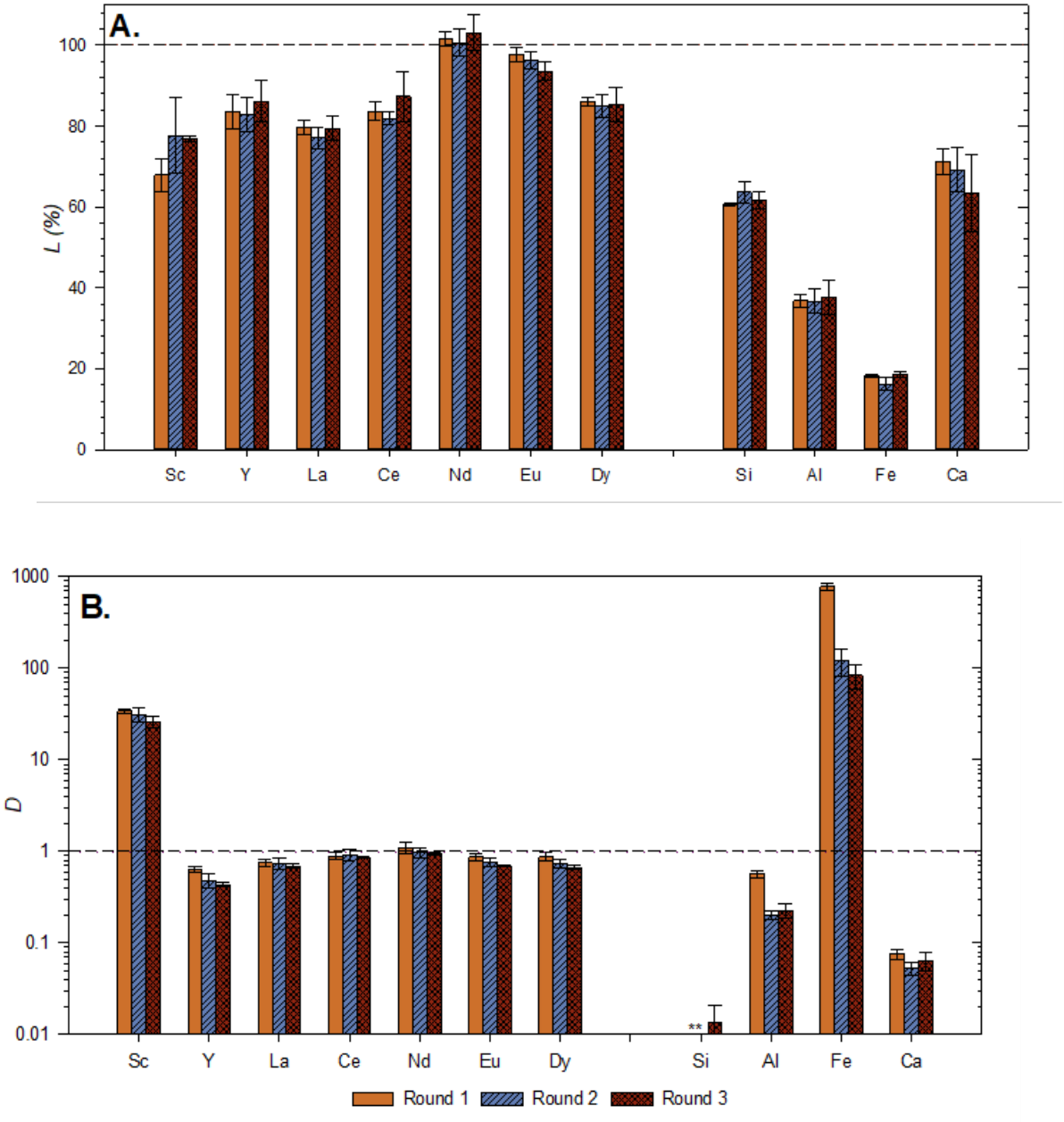

Figure 2.16 Reuse of IL experiments: leaching efficiency L (A) and average distribution D (B) after IL extraction for alkaline pretreated CFA-F1.

Notes: CFA was pretreated with 5.0M NaOH at a solid/liquid ratio of 1 g/10 mL. The same IL aliquot was reused in 2nd and 3rd rounds of extraction. Error bars indicate standard

*deviation of triplicate samples. In (B), columns marked with an * indicate zero, meaning that these elements (Si) were not found in the IL phase*.

2.5 Environmental Significance.

CFA contains many elements present at trace levels (up to hundreds mg/kg), including arsenic, cadmium, chromium, lead, mercury, selenium, uranium, and thorium.[30,32,33] While the concentrations of these metals are low in CFA, the toxin levels may become significant over million tons of CFA, and recent incidents of spills from CFA-holding ponds have provoked justifiable concerns about potential environmental contamination, which have prompted governmental regulation and ash pond closures.[34,37] As the environmental and economic costs of storage increase, there has been a push to recycle CFA, including decades' worth of weathered CFA.

Utilizing CFA as a source of REEs presents itself as an attractive solution to not only this problem but also the REE scarcity crisis. With global demand for REEs steadily increasing, the surface mining operations have expanded, leading to pollution. In China, for example, poorly regulated heap and in-situ leaching ponds have contaminated surface water, groundwater and soils in surrounding communities.[131-134]

Mining operations do not only face challenges in waste generation and management, but also in chemical consumption. Thus, the IL described herein presents a major advantage due to its regenerative ability. Meanwhile, the potential risk of ILs themselves should not be neglected. A recent review by Pang et al. found that toxicity of ILs was largely dependent on the structure (cation family, chain length, and anion moiety) and had varying negative effects on the different model organisms studied.[80] While there is limited toxicity

data on the IL described in this paper, its cation, betaine is a nontoxic biomolecule derived from choline. A recent study found that a similar IL, 1-ethyl-3-methylimidazolium bis(trifluoromethylsulfonyl)imide (emim [Tf_2N]), is "practically harmless" based on its EC_{50} value.[135,136]

The novel method reported in this study combines the extraction of REEs from CFA and separation of REEs from bulk elements in one IL leaching step, finally yielding an acidic solution relatively rich in REEs and poor in CFA's bulk elements. This study is among the first to demonstrate direct application of an ionic liquid to CFA for efficient recovery of REEs. While downstream REE separation, through methods like electrodeposition, calcination, and precipitation, will still be required to achieve single element concentrates, this work unlocks a new strategy for CFA refinement for REE recovery. The recyclability of IL and mild extraction conditions offer advantages for environmental sustainability. This preferential, low-waste approach effectively extracts REEs from both weathered and unweathered CFAs and thus warrants deeper inquiry. Further work will improve the efficacy and lower the costs associated with this process.

This chapter has been published in the journal: Environmental Science and Technology.

CHAPTER 3. MINIMIZING IRON CO-EXTRACTION IN RECOVERY OF RARE EARTH ELEMENTS FROM COAL FLY ASH USING A RECYCLABLE IONIC LIQUID

3.1 Abstract

Rare earth elements (REEs) are essential for modern technologies and the United States currently lacks a secure domestic supply as well as a supply chain. Coal combustion residuals, specifically coal fly ash (CFA), has been investigated as a potential source. Previous work found that REEs could be preferentially extracted using a recyclable acidic ionic liquid, (IL) betainium bis(trifluoromethylsulfonyl)imide ([Hbet][Tf_2N]). The IL extraction process yields a mildly acidic REE-rich solution contaminated with Fe. This study investigates three strategies for limiting Fe coextraction into the IL phase: magnetic separation, complexing salts, and ascorbic acid reduction. Magnetic separation, intended to reduce the amount of Fe in the initial CFA, failed to deplete Fe in CFA and ultimately increased the amount of Fe in the IL phase. When NaCl was used instead of $NaNO_3$ as an alternative salt, R_{Fe} did not decrease but D_{Fe} decreased from ~75 to ~14, a five-fold decrease, and L_{REEs} and R_{REEs} both increased. Finally, using ascorbic acid decreased *DFe* even further, to ~0.16, indicating a preference for the AQ phase over the IL phase and causing R_{Fe} to also drop. These optimizations should be used together in conjunction with other strategies identified in previous work with CFA-[Hbet][Tf_2N] leaching, including alkaline pretreatment and adding supplemental betaine cation, to generate an REE-rich acidic solution with very low concentrations of Fe.

3.2 Introduction

Rare earth elements (REEs) play critical roles in many high-tech applications.[11-13,19-21,84] To date, there are no adequate replacements for these 15 lanthanides and yttrium and scandium, and due to their unique susceptibility to supply chain disruption, REEs have been labeled by both the United States and the European Union as "critical materials".[15,16,19] Exploration into recovery from alternative sources has investigated bauxite residue, wastewater, slag and mine tailings, waste from REE mining operations, post-consumer materials, and more recently, coal combustion residuals.[19,25,26,84-92] These residuals, specifically coal fly ash (CFA), have REE concentrations ranging from 300-1500 ppm, 4-8 times higher than the parent coal. While about 40% of CFAs are beneficially reused, the remainder (~70 million metric tons) is landfilled. Decades of coal combustion have filled storage ponds across the U.S., where they pose significant risks to the environment and public health due to trace levels of toxins like arsenic, mercury, and lead, among other elements. Recovery of REEs from CFA is an attractive alternative to storage.

Current REE recovery methods require highly corrosive solutions and high pressures and temperatures to extract the elements from the recalcitrant CFA matrix, composed of durable aluminosilicates. As a result, the processes are hazardous, chemically consumptive, and energy intensive. They are furthermore indiscriminate, generating impure mixtures of REEs and bulk elements, necessitating additional separation steps. A green and industrially viable solution should both extract REEs and separate them from the bulk material, limiting downstream processing.

Chapter 2 investigates a preferential method utilizing a recyclable agent, the ionic liquid (IL) betainium bis(trifluoromethylsulfonyl)imide, commonly referred to as [Hbet][Tf_2N] (Figure 1.3).[137] [Hbet][Tf_2N] features a built-in extraction mechanism through its thermomorphic solubility with water. When cool, it is mostly immiscible with water, absorbing approximately 13% water by mass; above 55ºC, it becomes fully miscible with water and forms one phase.[6,7,69,97] This behavior can be exploited to partition metals from an aqueous solution (or solid) into the IL phase.[6,7,69,97] The IL phase can subsequently be stripped using mildly acidic solutions.[6-8] [Hbet][Tf_2N] can successfully partition REEs from aqueous solutions, from REE oxides, and from REE-rich solids including lamp phosphors, permanent magnets, and bauxite residue.[6-8] Importantly, REE oxides are soluble in this IL, but aluminum, silicon, or uranium oxides are not.[5,6,55,65-75,138,139] This makes this IL an especially strong choice for extraction, as CFA is largely composed of aluminosilicates (50-80 wt.%, Table 2.1).

In Chapter 2, [Hbet][Tf_2N] was applied to three representative types of CFA and achieved high leaching efficiencies for REEs (approaching 100%) for all CFAs.[137] Pretreatment with an alkaline solution was required for the more recalcitrant Class-F CFAs, but not for the less resistant, Ca-rich Class-C CFAs. Importantly, alkaline pretreatment did not cause loss of REEs, unlike the acidic pretreatments investigated. Furthermore, adding additional betainium promoted high REE partitioning into the IL phase over the aqueous (AQ) phase. It was also demonstrated that the IL could be used over multiple leaching-stripping cycles, offering an opportunity to reduce chemical consumption in REE extraction. The process yields a mildly acidic REE-rich solution, with minimal concentrations of most bulk elements. While downstream REE separation, through

methods like electrodeposition, calcination, and precipitation, will still be required to achieve single element concentrates, this work unlocks a new strategy for CFA refinement for REE recovery.

One key optimization required for industrial viability is addressing iron (Fe) co-extraction, which was found to be a significant and persistent limitation in the IL-REE-CFA extraction method.[137] Fe(III) strongly binds with the carboxylic acid on the betainium cation due to its high charge density (a property it shares with trivalent REEs) and thus partitions strongly favorably into the IL phase. In complexation, six protons are exchanged for a trivalent metal, here shown as REE (Equation 1):[5,65,68,69]

$$REE_2O_3 + 6\,[Hbet][Tf_2N] \leftrightarrow 2[REE(bet)_3][(Tf_2N)_3] + 3\,H_2O \qquad (2)$$

Chapter 2 showed that IL extraction caused low Fe leaching from Class-F CFAs: <10% for untreated CFA, ~15-30% for alkaline-pretreated CFAs. Moderate leaching was observed for Class-C CFAs (60% with or without alkaline pretreatment).[137] However, for all types of CFA, Fe partitioned completely into the IL phase, leading to a mixture of Fe and REEs in the IL phase.

Fe occurs in CFA both as discrete minerals, commonly magnetite and hematite, and dispersed throughout the glassy aluminosilicate matrix.[30,140] These metal oxides are sparingly water soluble, and spinel minerals like magnetite are highly stable.[140] As such, literature has shown that Fe does not leach from CFA easily. Under neutral and alkaline conditions, negligible amounts of Fe are leached.[32,33,48,140-143] Fe becomes soluble in strongly acidic solutions (pH < 1.5), but even under aggressive conditions, less than 1% of

Fe is leached.[140] In the IL extraction method, the pKa of [Hbet][Tf_2N] is around 1.82,[68,69] which appears to provide sufficient acidity (along with other mechanisms) for low to moderate Fe leaching from CFA.[137]

In this chapter, three strategies for limiting Fe coextraction in the recovery of REEs from CFA using [Hbet][Tf_2N] are investigated. The three strategies were selected based on potential effectiveness and referred to as: (1) magnetic separation, (2) alternative salt anions, and (3) ascorbic acid reduction (Figure 3.1, Figure 3.2, and Figure 3.3), respectively). The first is a physical separation process on the CFA solids, while the latter two are chemical modifications to the IL extraction process.

The magnetic fraction of CFA is likely rich with iron and can be successfully separated by magnetic separation.[30,144-148] Literature further indicates that REE concentrations are lower in the magnetic fraction compared to total CFA.[30,147,149] Thus, magnetic separation may further concentrate REEs as well as decrease Fe available for leaching.

During leaching of CFA by IL/AQ mixture, a metal salt (e.g., $NaNO_3$) is added to the AQ phase to facilitate phase separation of IL and AQ. Complexing salts with anions that form Fe complexes may facilitate Fe partitioning into the AQ phase.[6,7,68,69] For example, previous research showed improved Fe transfer to the AQ phase in the presence of chloride or oxalate anions in [Hbet][Tf_2N]-water systems in recovery from NdFeB magnets.[7]

Finally, adding ascorbic acid to induce iron reduction may be promising because betaine complexes much more favorably with Fe(III) than Fe(II). Onghena et al. reported that Fe extraction into the IL phase was decreased following applying Fe reduction with ascorbic acid to bauxite residues.[8]

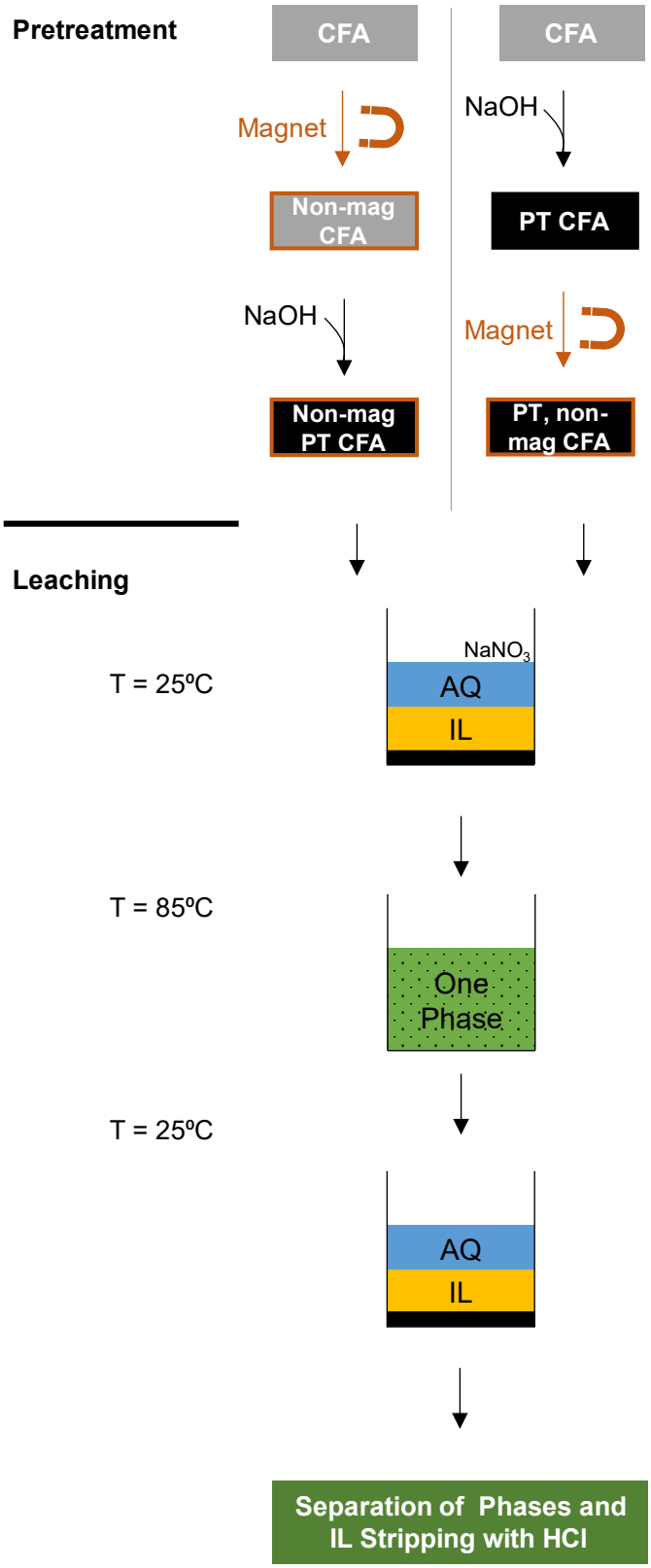

Figure 3.1 Scheme depicting the magnetic separation IL extraction optimizations.

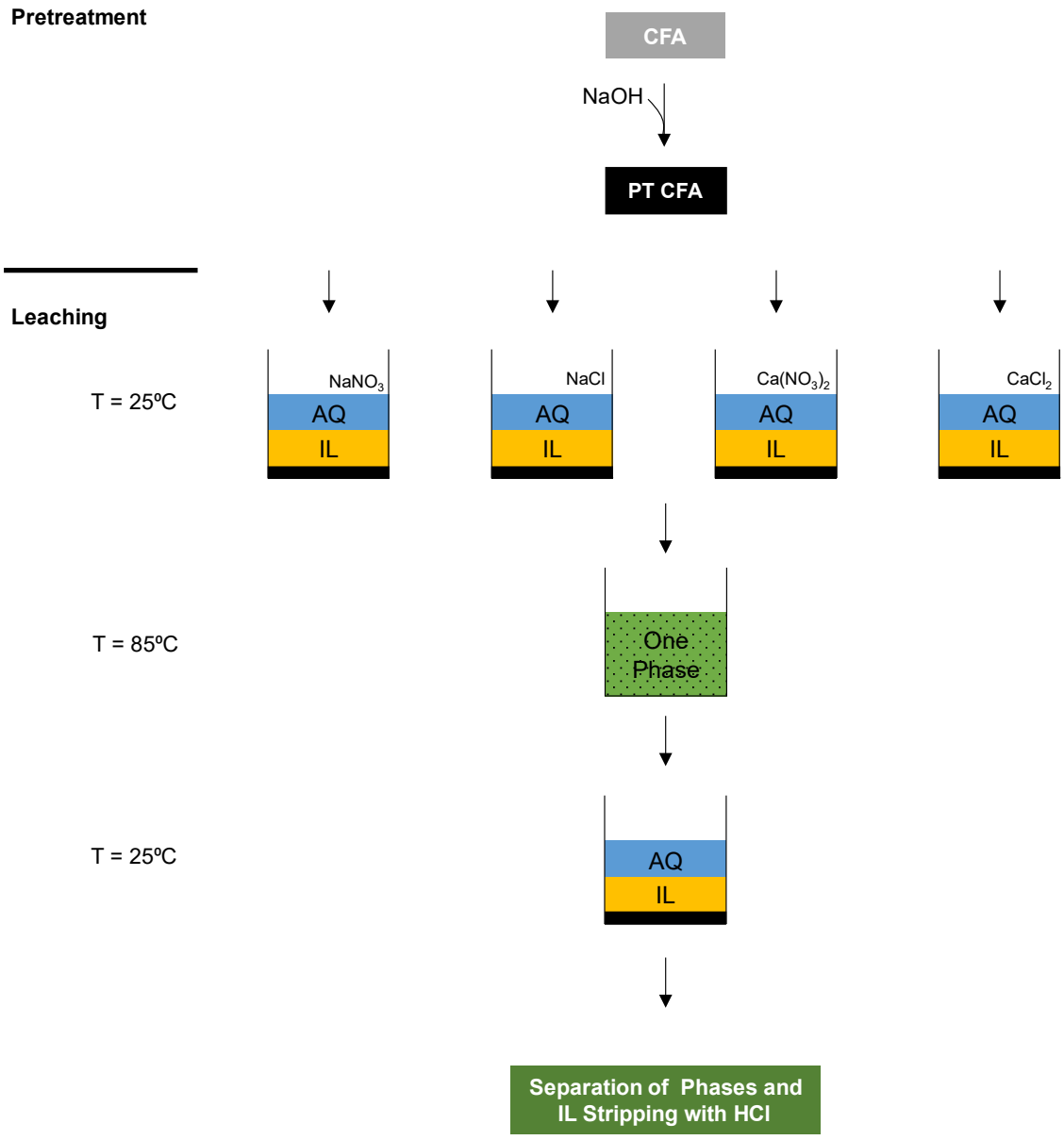

Figure 3.2 Scheme depicting the complexing salts used in the IL extraction optimizations.

Note: The different salts were added in the AQ phase.

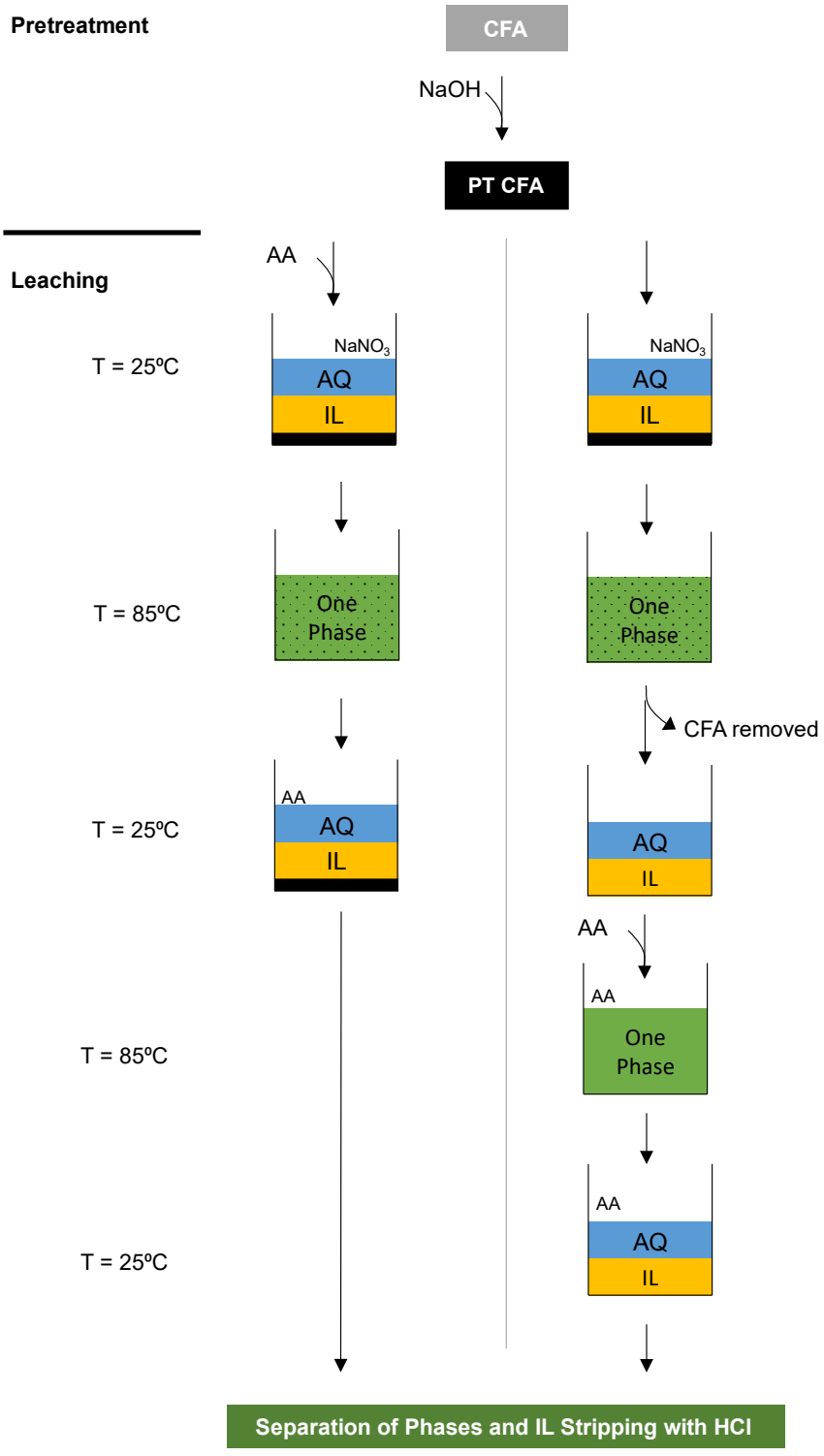

Figure 3.3 Scheme depicting the utilization of AA in IL extraction optimizations

Note: Direct addition of AA is shown at left; AA addition following CFA removal is shown at right.

3.3 Materials and Methods

3.3.1 Chemicals and Characterization.

Most chemicals used can be found in Chapter 2 (see *Section 2.3.1*). Additionally, ascorbic acid (AA), ammonium acetate, ammonium hydroxide, $FeSO_4$, ferrozine, $CaCl_2$, and NaCl were obtained from Sigma Aldrich. All chemicals including CFAs were used without further purification. The strong magnet (catalogue number BX0X08-N52) was obtained from K&J Magnetics.

Two unweathered CFAs (one Class-C, CFA-C1, and one Class-F, CFA-F1) and one weathered CFA (Class-F, CFA-F2) were comprehensively characterized previously (Table 2.1).[137] Characterization included major oxide and trace element composition analysis, and mineral composition quantification. A full description is in Chapter 2 (see *Section 2.3.3*).

3.3.2 [Hbet][Tf_2N] Synthesis.

IL synthesis was performed as described previously in Chapter 2 (see *Section 2.3.2*).[5,65]

3.3.3 CFA Alkaline Pretreatment.

Alkaline pretreatment was performed as described in a previous study.[137] Briefly, CFA was mixed with 5.0 M NaOH solution in a ratio of 1:10 g/mL and heated with a stir bar at 85°C for five hours. After cooling, the supernatant was removed for elemental analysis by inductively coupled plasma-optical emission spectrometry (ICP-OES) to quantify loss from pretreatment. The CFA was washed with DI water, filtered, and dried at ~80°C prior to leaching and stripping with the IL.

3.3.4 Magnetic Separation of CFA.

Large plastic vials were filled with 1.5 g CFA and 15 mL DI water. A strong Grade N52 Nd magnet (4933 Gauss) was placed in a plastic bag then submerged in the solution. The vials were placed on a platform shaker for 5 min at 120 rpm. The magnet-in-bag with magnetic fraction of CFA attached was then gently removed. The CFA remaining in the vial was the non-magnetic fraction. The remaining CFA solids were collected by filtering through a Buchner funnel with 0.22-μm Whatman filter paper and dried in an oven (~80°C). Only wet separation was performed, as dry separation has been reported to cause particle agglomeration.[148]

As shown in Figure 3.1, magnetic separations were performed on both untreated and alkaline-pretreated CFA. Following magnetic separation, the untreated nonmagnetic fraction underwent alkaline pretreatment. These nonmagnetic, alkaline-treated CFA fractions were subjected to IL leaching and stripping. Total digestion was also performed on these CFA samples to determine composition (see Chapter 2, section 2.3.3).

Enrichment (gamma, γ) of the target elements in the nonmagnetic fraction was calculated by Equation 4:

$$\gamma = \frac{C_{nonmagnetic}}{\chi_{nonmagnetic} \times C_{Total}} \tag{4}$$

$\gamma > 1$: enrichment, $\gamma < 1$: depletion

where $C_{nonmagnetic}$ was the element's concentration in the nonmagnetic fraction, $\chi_{nonmagnetic}$ is the nonmagnetic fraction of the CFA by mass, and C_{Total} was the element's concentration in the original untreated CFA.[137]

3.3.5 Leaching and Stripping Experiments.

The leaching and stripping process was described in Chapter 2 (see *Section 2.3.5)*.[137]

3.3.5.1 Leaching.

Briefly, dry alkaline pre-treated CFA, water-saturated IL, and 1.0 M $NaNO_3$ aqueous solution were added to a small vial to achieve a liquid-liquid (IL:AQ) mass ratio of 1:1 and solid-liquid ratio of 12.5:1 (mg:g). $NaNO_3$ was added to promote IL:AQ phase separation.[6,7,60,68,69] The pH of the $NaNO_3$ solution was adjusted to 3.50±0.05 with HNO_3 and NaOH prior to mixing.[6,7,69] The vial was heated to 85°C in an oil bath with a stir bar for three hours. Then, the vial was cooled to room temperature, then stored at 4°C overnight. The AQ phase was removed and prepared for analysis by ICP-OES. The IL phase was transferred to a new vial for stripping. The CFA was filtered and washed with DI water, then dried at ~80°C.

3.3.5.2 Stripping.

Briefly, 1.5 M HCl was added to the new IL-containing vial to achieve a liquid-liquid (IL:HCl) mass ratio of 1:1. The vial was heated with a stir bar to 85°C for 1.5 h. The vials were cooled as before. The HCl phase was removed and prepared for analysis by ICP-OES.

3.3.6 Leaching with Complexing salts.

Other salts (NaCl, $Ca(NO_3)_2$, $CaCl_2$) were used in place of $NaNO_3$ at similar concentrations (1.0, 2.0, and 3.0 M) as described in *Section 3.3.5.1* and Figure 3.2.

3.3.7 Ascorbic Acid Addition.

The ascorbic acid (AA) solutions were prepared the same day as used and stored at 4ºC wrapped in aluminum foil between preparation and use. AA addition was tested in two ways: (i) in CFA leaching or (ii) following CFA leaching (after CFA removal) (Figure 3.3). For (i), AA was added to the $NaNO_3$ solution to achieve various concentrations, and pH was adjusted to 3.50±0.05. This solution acted as the AQ phase following leaching as described in *3.3.5.1.*

For (ii), leaching of CFA proceeded as described in *2.5.1.* Upon cooling, the AQ and IL phases were transferred into a new vial without the CFA. Concentrated AA in $NaNO_3$ at pH 3.50±0.05 was added. The new sample (IL+AQ+AA) was immediately placed in a hot oil bath following procedures in *3.3.5.1.* The solution was later stripped following procedures in *3.3.5.2.* Following stripping, the IL was washed twice with small amounts of ice-cold DI water, which were diluted and analyzed by ICP-OES, the stripping following *3.3.5.2* was performed a second time.

Fe speciation in the AQ and IL phases was evaluated by the ferrozine method after reduction of ferric to ferrous ion by hydroxylamine. A 0.01 M ferrozine solution was prepared in 0.10M ammonium acetate solution. An ammonium acetate buffer was prepared using a from 10M ammonium acetate solution adjusted to pH 9.5 with a solution of

ammonium hydroxide (28 wt.%). Standards were prepared from 1000 ug/mL Fe(II) stock using $FeSO_4$. The spectrophotometer was standardized with DI water at 562nm.

Following leaching, the AQ phase was removed and diluted for immediate ferrozine testing. Similarly, following stripping, the HCl phase was removed and diluted for immediate ferrozine testing.

3.3.8 Quantifying Extraction.

Leached elements are distributed by mass (M) between three phases: the pretreatment (M_{PT}) phase, the AQ phase (M_{AQ}), and the IL phase (M_{IL}). M_{IL} was determined by the element stripped using mild acids assuming complete stripping based on previous studies.[68,69]

To quantify the extraction and separation of elements from CFA, three parameters were identified: leaching efficiency (*L*), distribution coefficient (*D*), and recovery efficiency (*R*). Leaching efficiency, *L,* shows total extraction of each element into all phases from the starting CFA (M_{total}) (Equation 2). For experiments involving magnetic separation, M_{total} reflects the mass of an element in the nonmagnetic fraction only.

$$L\ (in\ \%) = \frac{M_{PT}\ +\ M_{AQ}\ +.M_{IL}}{M_{Total}} \tag{2}$$

Distribution coefficient, *D,* reflects an element's preference for the IL phase over the AQ phase as the ratio between the element's final mass in the IL phase and its mass in the AQ phase (Equation 3):

$$D = \frac{M_{IL}}{M_{AQ}} \quad (3)$$

Recovery efficiency, *R,* represents the combined effect of leaching efficiency and distribution. When M_{PT} is negligible, R can be computed using Equations 2 and 3, generating Equation 5:

$$R\ (\%) = \frac{M_{IL}}{M_{Total}} \cong \frac{L \cdot D}{1 + D} \quad (5)$$

M_{PT} is negligible for all REEs and low for Al, Ca, and Fe for all CFAs.[137] As with *L*, For experiments involving magnetic separation, M_{Total} reflects the mass of an element in the nonmagnetic fraction only. For REEs, high *L*, *D* and *R* are desired. For the bulk elements (Al, Si, Ca, Fe), low *L*, *D,* and *R* are desired, with a low *R* value being the most important.

All trials were performed in duplicate. All calculations were performed for each element in each trial then averaged.

3.4 Results and Discussion

3.4.1 CFA Characterization.

The three CFAs investigated in this study displayed all expected physical and morphological properties, which have been discussed in depth in a Chapter 2 (see Section 2.4.1).[104,105,137] Class-F ashes have low Ca content (<15%) and primary oxide content (POC, ΣSi+Al+Fe oxides) ≥70%, while Class-C ashes have high Ca content (15-30%) and POC ≥50%.[105,106] Class-F CFAs also tend to have slightly higher Fe and REE content.[1]

Class-F and Class-C CFAs also differ in mineralogy. Class-F ashes usually contain nonreactive crystalline phases of mullite, sillimanite, and quartz. While Class-C ashes usually contain approximately the same proportion of quartz, they also contain reactive crystalline calcium phases.[106,107]

CFA mineralogy is also impacted by weathering. Though weathered CFA is generally poorly studied, weathered CFAs have been shown to contain minerals formed as a result of hydration following water exposure and saturation in ash ponds.[106] These minerals include carbonates, portlandite (hydrated lime), amorphous clays (from glass hydrolysis), chlorides, Ca-rich minerals and amorphous iron oxides.[106] In this study, CFA-F2, a weathered Class-F CFA, also contained lower REE and Fe content.

Fe content in CFA is largely determined by the parent coal, with high-iron coals producing high-iron CFAs. Fe oxide content in the U.S.-based CFAs ranges from 3.2-25.5 wt.%, a trend that is generally reflected globally.[150] The CFAs in this study fell within this expected range (5-15%, Table 2.1).[137] Fe is found in CFA as discrete minerals of hematite (Fe_2O_3), magnetite (Fe_3O_4), and maghemite (γ-Fe_2O_3), goethite(α-FeOOH), mixed Fe(II)/Fe(III) spinels, Fe(III)-bearing mullite, and Fe(II)/Fe(III) silicates.[30,140,151] Quantitative XRD detected magnetite in the CFA-C1 (7.7 wt.%) and hematite in the CFA-F1 (0.8 wt.%) (Table 2.1).[137] No Fe-bearing minerals were detected in CFA-F2, though previous literature reports that weathered CFAs contain hematite and magnetite.[106] Crystalline Fe features have been observed on the surfaces of CFA particles in various studies; Kutchko et al. showed that Fe oxides are found both as surface condensation phenomenon and also as dispersed throughout solid particles.[29,152] They found that CFA is composed of >50% amorphous aluminosilicate spheres and, to a lesser degree, of iron-rich

spheres that are composed of mixed Fe-oxides and amorphous aluminosilicates in varying ratios.[29]

3.4.2 Magnetic Separation.

One way to decrease Fe concentration in the IL phase is to remove it from the starting CFA. Fe-bearing minerals, including magnetite, are often (but not always) magnetic, and the magnetic fraction of CFA can be successfully separated.[30,144-147,149,153] The literature broadly indicates that there is significant enrichment of Fe in magnetic phases in CFAs.[30,144-149,153] However, there is also evidence that crystalline Fe may be dispersed throughout amorphous glassy phases in CFA.[148,154] Liu et al. noted that Fe phases like hematite and magnetite may be encapsulated in the glass phase.[93] If Fe is both magnetic and dispersed throughout CFA particulates, it is unlikely that nonmagnetic fraction would be depleted in Fe. Nonmagnetic Fe would also be dispersed throughout both magnetic and nonmagnetic fractions. Thus, it is important to examine the enrichment (or depletion) of Fe in the nonmagnetic fraction prior to investigating CFA leaching with the IL.

The literature is inconclusive with respect to the relationship between REEs and magnetic phases, but it appears that REEs overall associate with nonmagnetic fractions.[30,147,149] Lin et al. found REEs enrichment in non-magnetic CFA fractions and association with non-magnetic minerals.[147] Dai et al. also found that REEs enrichment specifically in the aluminosilicate glass phases, and depletion in magnetic and mullite-corundum-quartz fractions.[30] Zhang et al. found no relationship between REEs and magnetism.[149] Using spectroscopy techniques, Liu et al. found that REE speciation in Class-F CFAs includes REE oxides (40−55%), REE-bearing hematite (20−30%), and REE

phosphates (20−25%) and apatite (a Ca-phosphate, 20−35%).[93] In contrast, Class-C CFAs contained a significant fraction of REE oxides (35−50%) and other species in varying proportions, including REE phosphates and REE-bearing hematite.[93] Other possible REE species include zircon (Zr-based silicate), and REE-bearing glass phases.[93] All identified species are nonmagnetic, indicating that nonmagnetic phases show REE enrichment.

For the purposes of this study, ideally, the nonmagnetic fractions should be depleted in Fe but enriched in REEs. The nonmagnetic fraction may consist of more recalcitrant amorphous or aluminosilicate phases, which may negatively impact *L*. Minimal impact is expected for *D*, as the same proton-exchange mechanism is still at work, and REEs likely remain in competition with other elements (including remaining Fe, potentially) for betaine complexation. If the impact on *L* is significant, *R* may also decrease.

3.4.2.1 Fe enrichment in nonmagnetic fraction.

Of the three CFAs tested, both Class-F CFAs had high magnetic content, while the Class-C sample had low magnetic content (67-92 vs. 8-19 wt.%, respectively, Table 3.1). This is unsurprising as Class-C CFAs have low Fe relative to Class-F CFAs by definition, which was also observed in this study (Table 2.1).[105] Alkaline pretreatment increased magnetic content for unweathered CFA-F1 and CFA-C1 (by 19 and 11 wt.%, respectively, Table 3.1). No statistically significant impact was observed for the weathered CFA-F2. Alkaline pretreatment is a known desilication process; removal of Si from CFA may remove non-magnetic phases from unweathered CFAs at a greater proportion than weathered CFA. Previous analysis by XRD found that hematite (a nonmagnetic Fe mineral) increased from 0.8 to 5.4 wt.% in unweathered CFA after alkaline pretreatment, and SEM-

EDS analysis found Fe-rich spheres.[137] Kutchko et al. found that some Fe-rich spherical particles are composed entirely of Fe oxides, while others are mixed (Fe-Al-Si particles).[29] In contrast, previous work did not detect any Fe minerals at all in weathered CFA samples.[137] Akinyemi et al. found that Fe demonstrated higher leachability from unweathered CFA compared to weathered CFA.[155] Unweathered CFA contained Fe in accessible acid-soluble (<5%) or oxidizable (~50%) phases, with the remaining Fe in the residual phase (~40%), while weathered CFA contained Fe almost entirely in the residual (>95%).[155] This residual phase is accessible only with aqua regia. It is hypothesized that in weathered CFA, Fe is dispersed throughout both magnetic and nonmagnetic phases.

Table 3.1 Magnetic and non-magnetic fractions of all CFA samples.

Sample	Status	Avg $\chi_{magnetic}$ (%)	Avg $\chi_{nonmagnetic}$ (%)
CFA-F1	Untreated	72.4 ± 3.3	27.6 ± 3.3
	Alkaline PT	91.5 ± 3.6	8.5 ± 3.6
CFA-F2	Untreated	73.3 ± 9.0	26.7 ± 9.0
	Alkaline PT	67.2 ± 2.1	32.8 ± 2.1
CFA-C1	Untreated	7.7 ± 1.2	92.3 ± 1.2
	Alkaline PT	19.1 ± 3.2	80.9 ± 3.2

In this study, no CFA samples showed depletion of Fe following magnetic separation, regardless of if pretreatment was the first or second step (Table 3.2, Figure 3.4). In fact, Fe was neither enriched nor depleted for most samples, indicating that Fe was not concentrated in the magnetic fraction, despite the large magnetic mass fraction composing the majority of Class-F CFA. One sample, CFA-F1, even demonstrated Fe enrichment ($(\gamma_{Fe} = 3.7)$ when alkaline pretreatment preceded magnetic separation. This is likely due to the low mass fraction of the nonmagnetic fraction ($\chi_{nonmagnetic} = 8$ wt.%, Table 3.1). This sample was also enriched in Si and Al ($\gamma_{Si} = 2.0$ $\gamma_{Al} = 13.6$, Figure 3.4). Alkaline pretreatment also likely

reduced the non-magnetic fraction as it is composed of durable aluminosilicates attacked in desilication; remaining solid is likely composed of the most recalcitrant phases.[137]

Table 3.2 Fe and total REE Enrichment in magnetic separation.

Fe (wt.%)						
	CFA-F1		**CFA-F2**		**CFA-C1**	
Initial Concentration	10.5		6.0		3.6	
First Treatment	M	PT	M	PT	M	PT
Avg $\chi_{nonmagnetic}$	0.27	0.08	0.32	0.32	0.91	0.79
Avg Conc. $_{nonmagnetic}$	2.9	3.2	2.5	2.6	3.0	3.3
Avg Expected† Conc. $_{nonmagnetic}$	2.8	0.9	1.9	1.9	3.3	2.9
Enrichment	1.0	3.7	1.3	1.4	0.9	1.1

ΣREEs (ppm)						
	CFA-F1		**CFA-F2**		**CFA-C1**	
Initial Concentration	520.0		499.0		272.0	
First Treatment	M	PT	M	PT	M	PT
Average $\chi_{nonmagnetic}$	0.3	0.1	0.3	0.3	0.9	0.8
Avg Conc. $_{nonmagnetic}$	503.3	573.0	504.9	510.1	274.5	250.7
Avg Expected† Conc. $_{nonmagnetic}$	140.4	43.0	161.6	159.1	247.6	214.7
Enrichment	3.6	13.3	3.1	3.2	1.1	1.2

Notes: M indicates magnetic treatment was first, followed by alkaline pretreatment. PT indicates that alkaline pretreatment was performed first, then magnetic separation was performed. †Expected concentration assuming no enrichment or depletion.

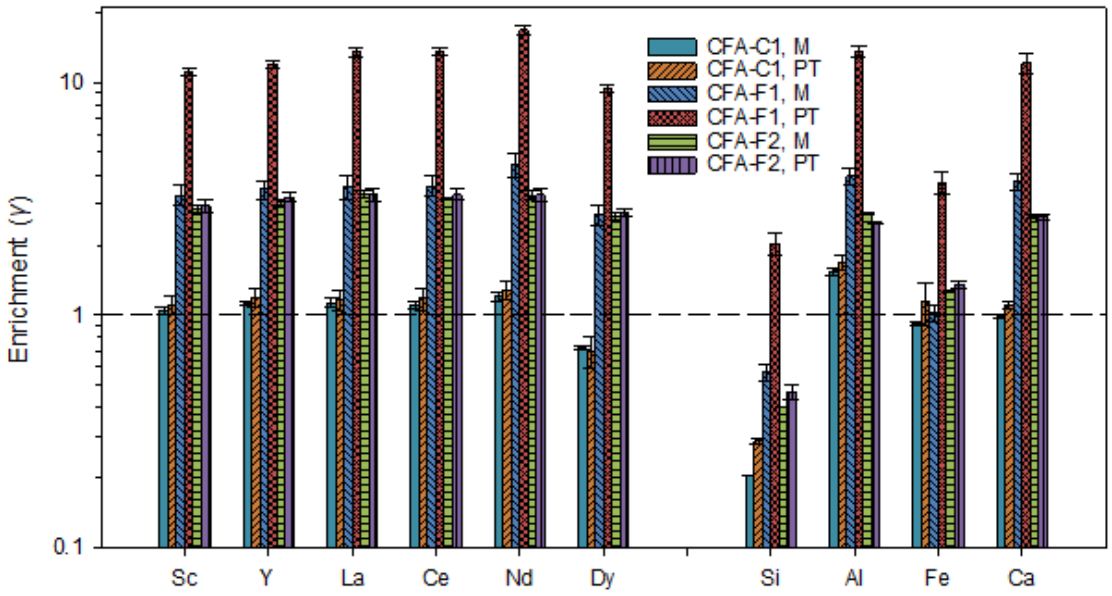

Figure 3.4 Average elemental enrichment following magnetic separation.

Notes: Eu was not detected in the enriched solids CFA and was thus excluded. Above, M indicates the magnetic separation was performed first, then alkaline pretreatment was performed on the nonmagnetic CFA fraction. PT indicates that alkaline pretreatment was performed, then magnetic separation was performed. Error bars indicate standard deviation of duplicate samples.

3.4.2.2 REE enrichment in nonmagnetic fraction.

In this study, both weathered and unweathered Class-F CFAs showed enrichment of all REEs regardless of if alkaline pretreatment was the first or second step (Table 3.2, Figure 3.4). Class-C CFA showed negligible REE enrichment. CFA-F1, the sample that demonstrated Fe, Si, and Al enrichment showed particularly strong REE enrichment when alkaline pretreatment preceded magnetic separation (γ_{REEs} = 13.3). The combinations of alkaline pretreatment and magnetic separation led to total REE concentrations at ~500-573 ppm for Class-F CFAs and ~250-275 ppm for CFA-C1 (Table 3.2).

Because magnetic separation was unsuccessful at reducing Fe concentration in CFA, it was unlikely to be successful at reducing Fe co-extraction into the IL phase. IL leaching

and stripping was still performed. Rigorous analyses and discussion are provided in Sections 3.4.2.3 and 3.4.2.4, and a summary is available in *Section 3.4.3.5*.

3.4.2.3 Impact of magnetic separation on IL extraction for Fe and other bulk elements

Leaching efficiency increased for Fe, as well as the other bulk elements (Figure 3.4). This may indicate that in the nonmagnetic CFA fraction, Fe is found in more accessible or acid-susceptible phases. Interestingly, L_{Fe} increased for both Class-F CFAs when magnetic separation was performed prior to alkaline treatment, indicating that the pretreatment affects nonmagnetic and magnetic phases differently.

In contrast, for Class-C CFA, L_{Fe} was not impacted by magnetic separation (Figure 3.4). Given that there was no depletion for Fe, this likely indicates that there are negligible mineralogical differences between the nonmagnetic and magnetic fractions. This is not surprising given that CFA-C1 is largely not magnetic ($\chi_{nonmagnetic}$=92.3%, Table 3.1). Decreases in L were also observed for Al and Ca, indicating that the non-magnetic fraction of CFA-C1 is slightly more recalcitrant.

Interestingly, for all types of CFAs, the overall amount of Fe did not vary significantly with magnetic separation (Figure 3.5). This in indicates that Fe leaches from accessible phases from the nonmagnetic fraction, not from the magnetic fraction. Further, depletion indicates that Fe is likely to be dispersed throughout the aluminosilicate phase in nonmagnetic forms (like the nonmagnetic Fe mineral hematite), rather than in magnetic minerals.

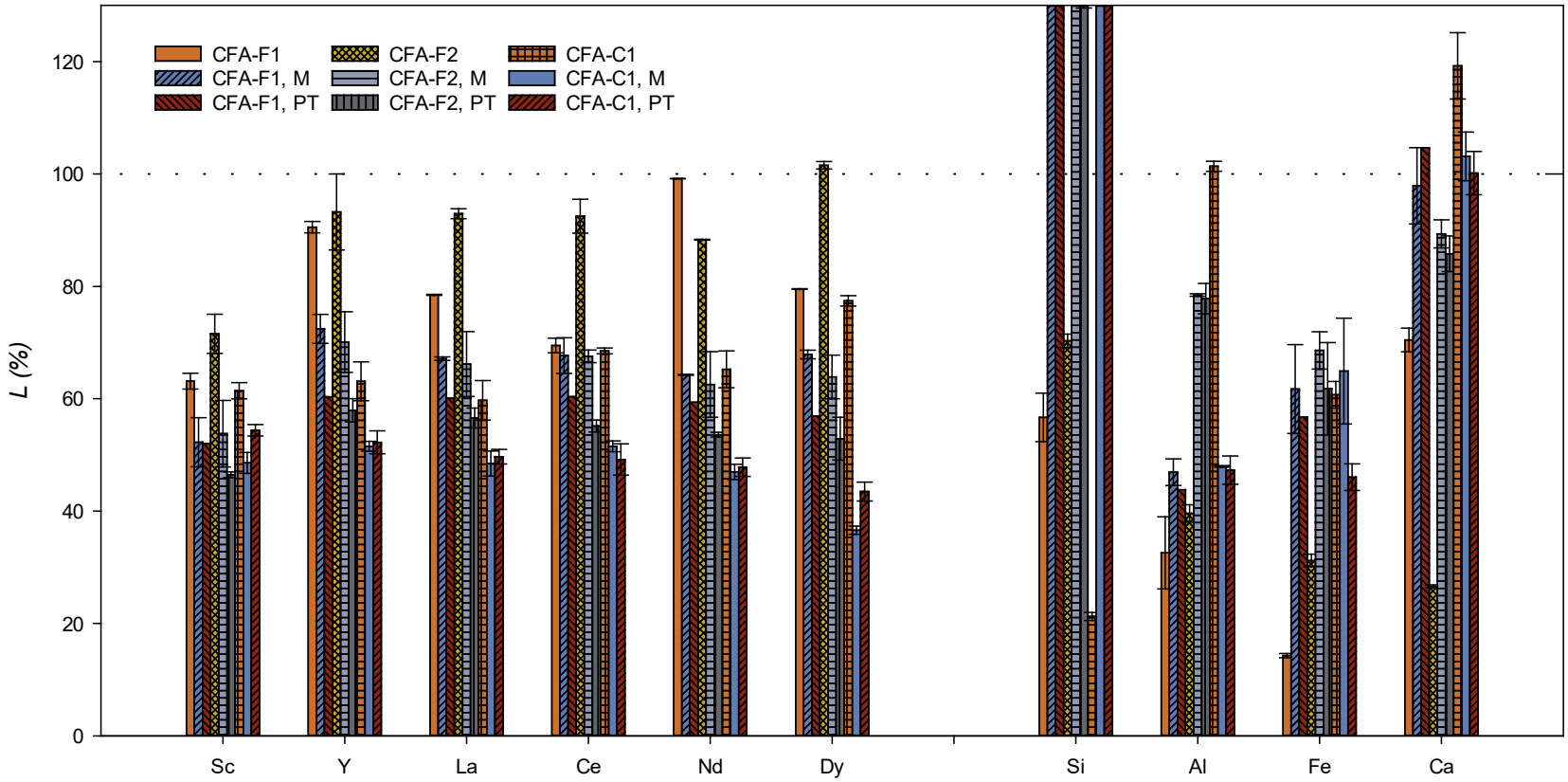

Figure 3.5 Average leaching efficiency L of CFA-F1, CFA-F2, and CFA-C1 after IL extraction process with magnetic separation.

Note: Above, M indicates the magnetic separation was performed first, then alkaline pretreatment was performed on the nonmagnetic CFA fraction. PT indicates that alkaline pretreatment was performed, then magnetic separation was performed. Error bars indicate standard deviation of duplicate samples. L is calculated relative to the CFA solid produced following alkaline pretreatment and magnetic separation, which is why several extraction efficiencies >100% are present (notably for Si).

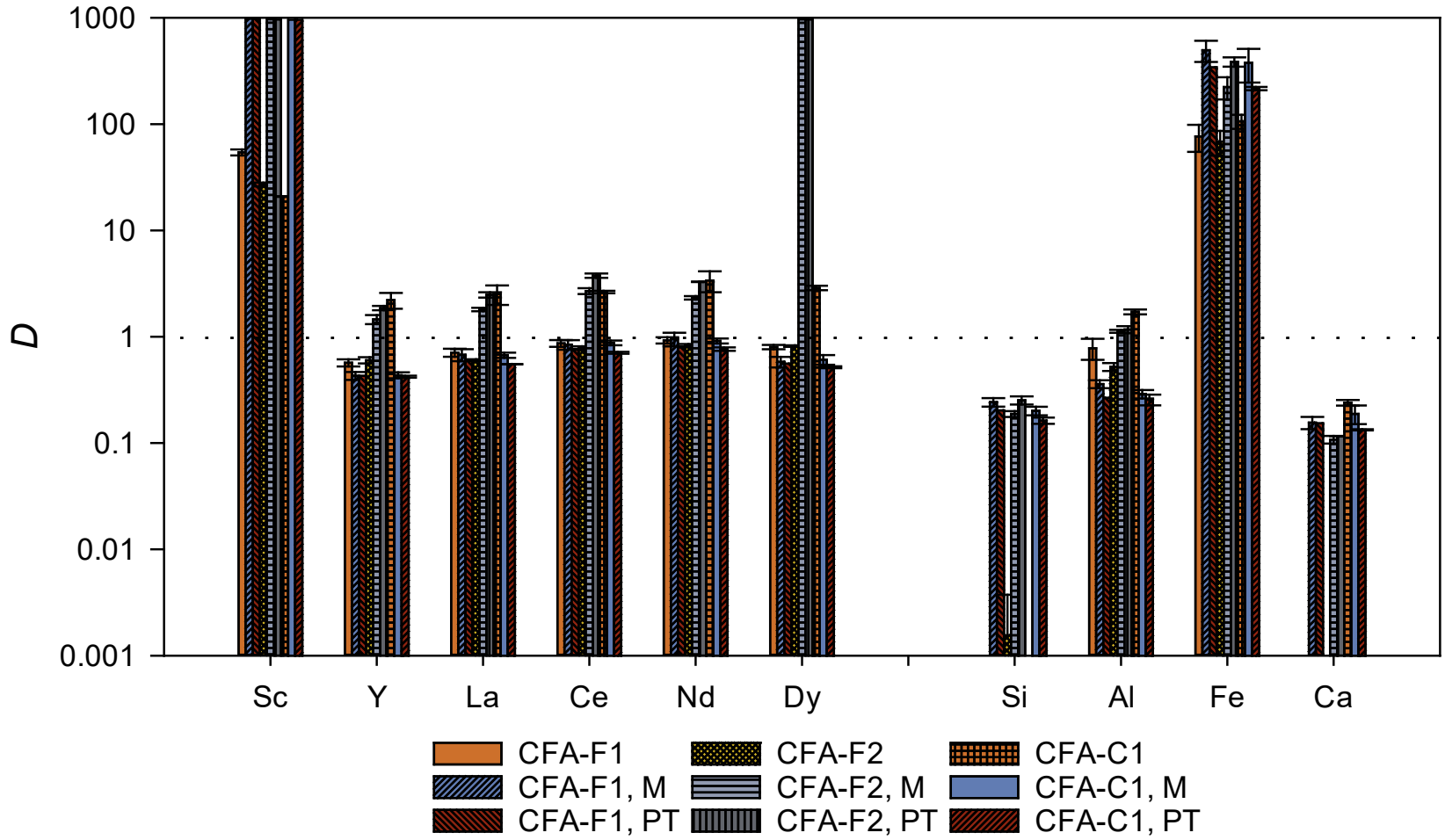

Figure 3.6 Average distribution, D, for CFA-F1, CFA-F2, and CFA-C1 after IL extraction process with magnetic separation

Notes: Above, M indicates the magnetic separation was performed first, then alkaline pretreatment was performed on the nonmagnetic CFA fraction. PT indicates that alkaline pretreatment was performed, then magnetic separation was performed. Error bars indicate standard deviation of duplicate samples.

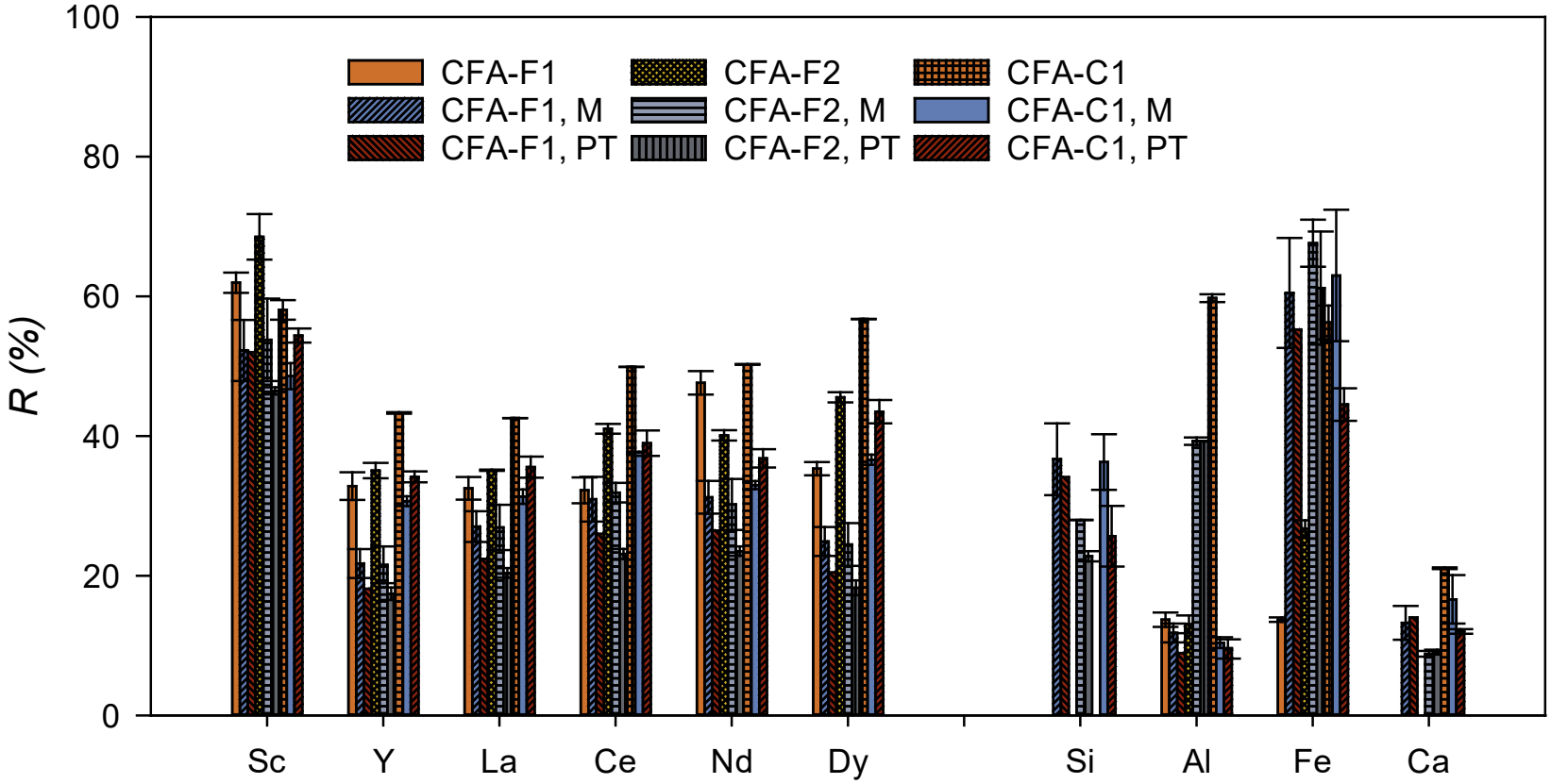

Figure 3.7 Average recovery R of alkaline pretreated CFA-F1, CFA-F2, and CFA-C1 after IL extraction process.

Notes: Above, M indicates the magnetic separation was performed first, then alkaline pretreatment was performed on the nonmagnetic CFA fraction. PT indicates that alkaline pretreatment was performed, then magnetic separation was performed. Error bars indicate standard deviation of duplicate samples. R is calculated relative to the CFA solid produced following alkaline pretreatment and magnetic separation.

D_{Fe} did increase with magnetic separation for all CFAs, but because D is a ratio of IL to AQ phases, these increases are negligible (representing an increase from >95.5% to >99% Fe in the IL phase, for example, Figure 3.5). For all CFAs D_{Al} decreased (though not to zero), and D_{Si} increased from 0 but remained low (D<0.2, Figure 3.5). D_{Ca} increased for Class-F CFAs but decreased to nearly zero for Class-C CFA. Overall, these increases represent impurities in the IL phase.

Impurities in the IL phase can be evaluated using recovery efficiency, R (Figure 3.6). For unweathered CFA, magnetic separation decreases R_{Fe} but increases R_{Ca} and R_{Si} (R_{Al} is unchanged). For weathered CFA, magnetic separation increases all R values, including R_{Fe}. Increases are likely the result of enrichment (Table 3.2). The difference in R_{Fe} is likely the result of different mineralogical structures of the nonmagnetic phases of the unweathered and weathered CFAs as described above.

3.4.2.4 Impact of magnetic separation on IL extraction for REEs.

Despite REE enrichment in the Class-F CFAs, leaching efficiency L_{REEs} decreased for Class-F CFAs (Figure 3.4). The unweathered Class-F CFA that demonstrated very high enrichment when alkaline pretreatment preceded magnetic separation had negligible or worse L_{REEs} relative to CFA without magnetic separation. It is likely that REEs not associated with the magnetic phase are found in more recalcitrant minerals or glassy phases. It is also possible that the REEs became entrained in Si flocs during acidic IL leaching: under low pH conditions, zeolites decompose to Si flocs that can polymerize and form larger particles.[108]

Class-C CFA also had decreased L_{REEs}. Class-C CFAS tend to leach REEs more readily under acidic conditions compared to Class-F CFAs due to their higher Ca content; previous work found that alkaline pretreatment was not necessary to achieve high L_{REEs} for Class-C CFA and in fact decreased L_{REEs}.[137]

As expected, magnetic separation did not have a significant impact on D_{REEs} (Figure 3.5). Like D_{Fe} , D_{Sc} increased for all CFA samples, and Class-C CFA demonstrated increased D_{Dy}. Both while likely increased as a result of [Hbet][Tf_2N]'s well-documented preference for complexation with ions with high charge densities. For Class-F CFAs, Sc's increase may be due to enrichment (Figure 3.4). D_{Dy} likely increased due to its low concentration (<5mg/kg alkaline-pretreated, magnetically separated CFA-C1).

All REEs show decreased R with magnetic separation, regardless of whether alkaline pretreatment preceded or followed the separation (Figure 3.6). This proved true for all CFA types, regardless of enrichment. This indicates that the nonmagnetic fraction is much more recalcitrant than the magnetic fraction or CFA whole.

3.4.2.5 Summary of impact of magnetic separation on IL extraction (L, D, & R) for Fe and REEs.

Magnetic separation was significantly less successful than expected. Magnetic separation did not deplete Fe in the CFA samples as desired, and furthermore, R_{Fe} increased for both Class-F CFA samples. REEs did show enrichment in the Class-F CFAs, but R_{REEs} also decreased. The decrease in R_{REEs} can be attributed to decreased L_{REEs}, since there were only moderate to negligible changes in D_{REEs}, indicating that the nonmagnetic phase is more recalcitrant than the bulk CFA solid. It is likely that nonmagnetic CFA phases contain

more recalcitrant CFA phases like mullite, quartz, and amorphous phases, as well dispersed, nonmagnetic Fe as oxides or minerals.

Within this study, magnetic separation is determined to be poorly effective due to decreased R_{REEs}. Future research should explore other CFAs as well as whether high L_{REEs} (and thereby high R_{REEs}) can be improved for the nonmagnetic fraction.[137]

3.4.3 Complexing Salts.

As explained in *Section 3.3.5.1*, 1.0 M $NaNO_3$ is added to the AQ phase of IL leaching experiments to promote separation between the IL and AQ phases. $NaNO_3$ was chosen because: (i) it only has a minor salting-out effect (IL in the water phase = 13 wt.%, versus 14 wt.% in pure water);[7] (ii) Na does not complex with oxalate (a potential REE precipitation/IL stripping agent not used in this study but used in similar applications);[6,7] (iii) neither Na^+ or NO_3^- is extracted as impurities into the IL phase;[7] and (iv) $NaNO_3$ is an economic choice of salts. Other salts, however, have been investigated to optimize [Hbet][Tf_2N] for different applications. Several salts ($NaNO_3$, NaCl, $Ca(NO_3)_2$, and $CaCl_2$) and concentrations (1-3 M) were tested on CFA-F1 in this study.

3.4.3.1 Impact of complexing salts on IL extraction (L,D,R) for Fe and other bulk elements.

Leaching efficiency increased for Fe, Al, and Si with all other salts examined (NaCl, $Ca(NO_3)_2$, and $CaCl_2$) compared to the standard $NaNO_3$ (Figure 3.4). L_{Ca} increased with NaCl but decreased with the Ca salts (Figure 3.4). Distribution increased for both Ca and Si with all salts, while Al decreased with all salts (Figure 3.4). $Ca(NO_3)_2$ had no impact on

D_{Fe}, but both chloride salts caused a dramatic decrease in D_{Fe} (~80% decrease). Recovery analysis indicates that differences between the different salts are minor for all bulk elements, including Fe (Figure 3.4). Despite the decrease in D_{Fe}, D_{Fe}, is still sufficiently high to result in high extraction into the IL phase (when D_{Fe}=14, IL phase=~93.5%).

NaCl resulted in higher L_{bulk} than $NaNO_3$; a similar trend was not observed for $Ca(NO_3)_2$ vs. $CaCl_2$. Further, D_{Ca} and D_{Si} were higher for NaCl, while D_{Al} and D_{Fe} were higher for $NaNO_3$. For the Ca-salts, no changes were observed for Al and Si, but D_{Ca} was higher with $CaCl_2$ and D_{Ca} was higher with $CaNO_3$.

Previous studies found that chloride salts could be used to influence Fe partitioning in [Hbet][Tf_2N] systems, specifically causing it to shift its distribution into the AQ phase from the IL phase.[7] In their system, adding a 1.0 M KCl caused Fe to distribute preferentially into the AQ phase (D_{Fe}=~0.33).[7] Other target elements (Nd, Dy, and Co) showed negligible differences between KCl and KNO_3.[7] In the CFA-IL-AQ system, D_{Fe} did decrease, but not to the point of switching phase preference. This is likely because Fe is in competition with other transition metals for chloride complexation, as CFA contains many metals (e.g., Ti, Mn, Cu, Co, Zn, Ni, Cr, and V).[33,150,156] Interestingly, no difference was observed between NaCl and $CaCl_2$, the latter of which contains twice as much Cl^-, indicating there might be a threshold effect.

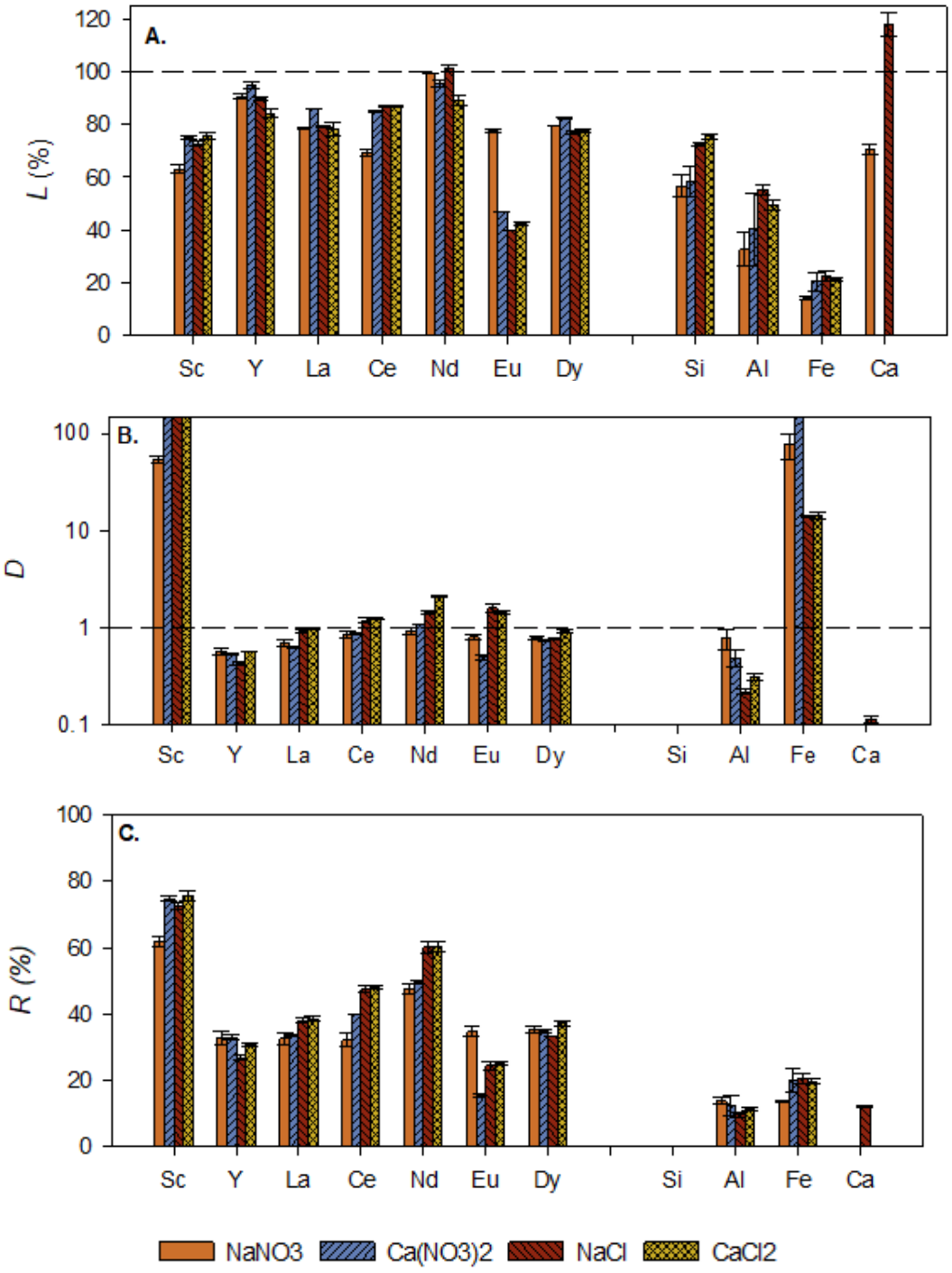

Figure 3.8 Average distribution D (A), average leaching efficiency L (B), and average recovery R (C) after IL extraction process for CFA-F1 with different salts.

*Note: Error bars indicate standard deviation of duplicate samples. In **(A)**, spaces marked with an * indicate zero, meaning that this element (Si) was not found in the IL phase. Columns marked with an † indicate an extremely large value of D.*

No significant differences in L_{bulk} were reported comparing the chloride salts, with the exception of Ca, which had higher L in the presence of NaCl over $CaCl_2$. For the nitrate salts, using $Ca(NO_3)_2$ led to higher L_{bulk} with the exception of Ca, which again had higher L in the presence of NaCl. No differences were observed between the chloride salts for D_{bulk}, aside from a modest increase in D_{Ca}. D_{bulk} was higher for $Ca(NO_3)_2$ over $NaNO_3$, though the impact on D_{Fe} was minimal.

Previous studies found that salt cations do not impact individual element distribution, as salt cations do not form complexes with metal cations.[7] Additional cations can however influence distribution broadly by impacting the solubility of the IL in water as well as the solubility of betaine (and thus also metal-betaine complexes).[7] Following the Hofmeister series, "salting-in" salts increase the solubility of organic molecules in water, while "salting-out" salts decrease their solubility and promote aggregation.[7] In the Hofmeister series, Ca^{2+} has a stronger salting-out effect than Na^+, and chloride has a slightly stronger salting out effect than nitrate.[7] The absence of a consistent trend for either cation in this study indicates that differences in salting-in or -out are likely minor. Such a trend would likely be further obscured by other common cations leached from CFA during IL leaching.

3.4.3.2 Impact of complexing salts on IL extraction (L,D,R) for REEs.

$Ca(NO_3)_2$, $CaCl_2$, and NaCl all increased L_{REEs} relative to $NaNO_3$. D_{REEs} increased slightly in the presence of chloride salts. NaCl had the highest R_{REEs} values.

No consistent trend was observed between anions for L. NaCl achieved higher L_{REEs} relative to $NaNO_3$, while $Ca(NO_3)_2$ was higher relative to $CaCl_2$. $Ca(NO_3)_2$ and NaCl had comparable performances ($L_{REEs,average}$=88.0%, 86.5% respectively). The chloride salts,

both NaCl and $CaCl_2$, demonstrated higher D_{REEs} relative to the nitrate salts. It is hypothesized that the ferric chloride complexes allowed betaine previously complexed with Fe to complex with REEs, causing D_{REEs} increases in the presence of chlorides.

Significant differences were not observed between Ca and Na salts with the same anion (Figure 3.4). As discussed in *3.4.3.1*, the cation does not largely impact elemental partitioning behavior, but anions may form complexes with transition metals.

3.4.3.3 Impact of chloride concentration on IL extraction (L,D,R) for all elements.

NaCl was chosen for additional testing due to its relative increase in D_{REEs} and dramatic decrease in D_{Fe} (as well as the threshold effect observed therein). Higher NaCl concentrations were tested. No further decrease of D_{Fe} was observed as [NaCl] increased from 1.0 to 3.0 M (Figure 3.5). No change in D_{REEs} was observed. Increasing [NaCl] decreased both L_{REEs} and L_{Bulk}. The highest recovery R for both REEs and Fe was observed for 1.0 M NaCl.

Gorrepati et al. determined that Si polymerization increases with increasing ionic strength, and that under acidic conditions, Si nanoparticle formation increased when chloride salts were present.[108] These flocs likely entrain REEs as they leach from the CFA in the strongly acidic CFA-IL-AQ mixture, causing L_{REEs} to decrease.

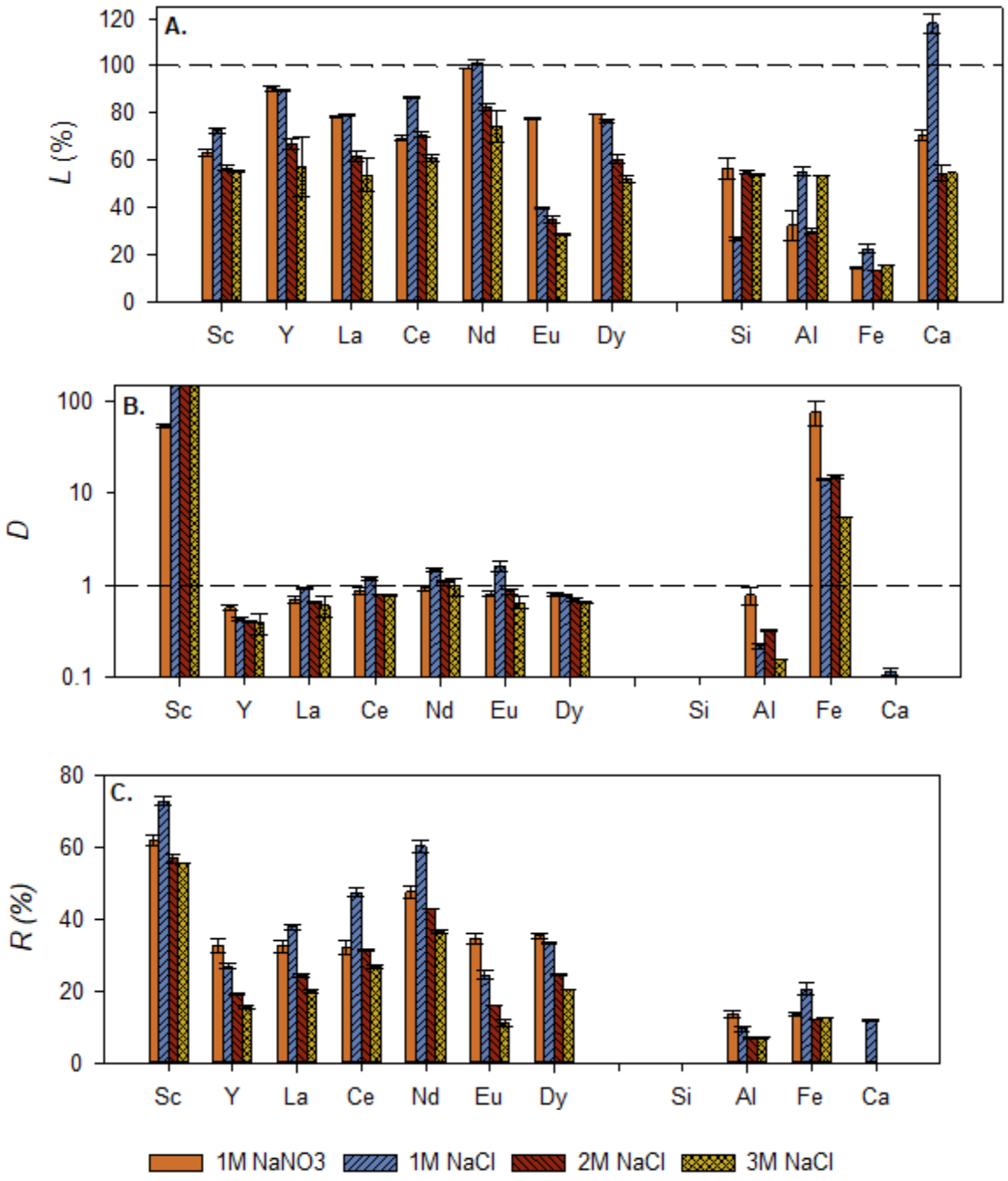

Figure 3.9 Average leaching efficiency L (A), average distribution D (B), and average recovery R (C) after IL extraction process for CFA-F1 with different [NaCl] concentrations.

Notes: Error bars indicate standard deviation of duplicate samples. In ***(A)****, spaces marked with an * indicate zero, meaning that this element (Si) was not found in the IL phase. Columns marked with an † indicate an extremely large value of D.*

3.4.3.4 Summary of complexing salts.

Of the salts investigated, only NaCl successfully decreased D_{Fe}. Despite this 10-fold decrease, R_{Fe} did not decrease. R_{Fe} did decrease at high concentrations of NaCl concentration (≥2 M); however, at these concentrations, R_{REEs} also decreases. Thus, using 1 M NaCl during leaching cannot be employed alone to minimize Fe coextraction into the IL phase.

3.4.4 Ascorbic Acid (AA) Reduction.

Reducing Fe(III) with AA was evaluated to prevent Fe co-extraction. In this study, different concentrations of AA were tested on CFA-F1 in two ways: adding AA to the CFA-IL-AQ mixture directly and adding AA to the IL-AQ mixture after CFA removal.

3.4.4.1 Impact of direct mixing of AA on IL extraction (L,D,R) for all elements.

Adding AA had a dramatic effect on L_{Fe}: at the 100 mM threshold, L_{Fe} doubled (20% to 40%) (Figure 3.6). This increase is likely the result of reductive dissolution in which ferric oxides dissolve in the presence of reductants. AA had minimal impacts on the other bulk elements and a slightly positive relationship with L_{REEs}.

A threshold effect was observed in D for almost all elements at 100 mM AA (Figure 3.6). D_{Fe} experienced a dramatic reduction, dropping from approaching infinity (where ~100% of leached Fe is in the IL phase) to ~0.10 (where ~9% of leached Fe is in the IL phase). D_{REEs} and D_{Ca} increased slightly, while D_{Al} increased after decreasing slightly. Interestingly, D_{REEs} increased past one for several REEs, indicating a shift in preference towards the IL phase over the AQ phase.

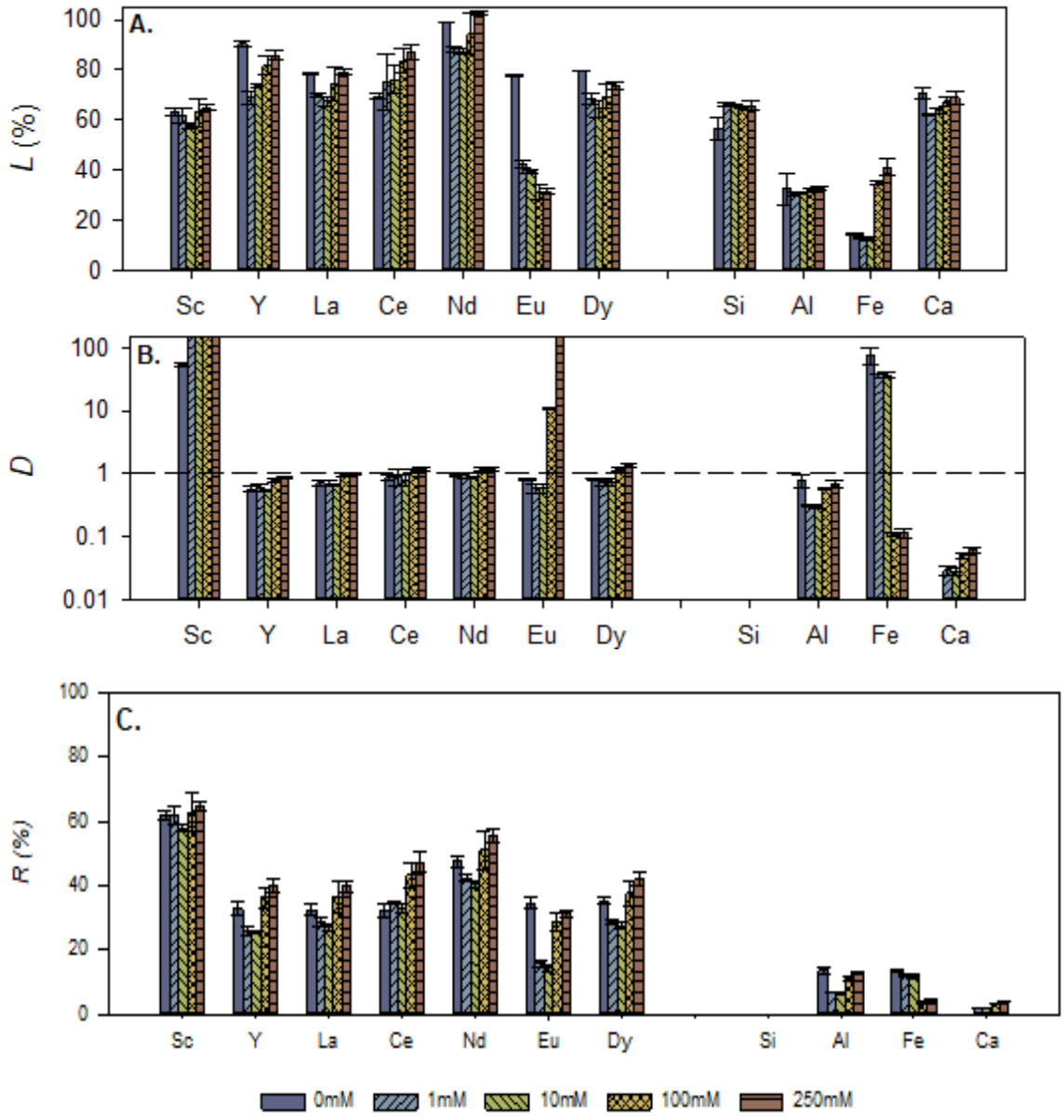

Figure 3.10 Average leaching efficiency L (A), average distribution D (B), and average recovery R (C) after IL extraction process for CFA-F1 with ascorbic acid added directly to the AQ-IL-CFA mixture.

Notes: Error bars indicate standard deviation of duplicate samples. In ***(A)****, spaces marked with an * indicate zero, meaning that this element (Si) was not found in the IL phase. Columns marked with an † indicate an extremely large value of D.*

At high AA conditions (100 mM), R_{Fe} dropped dramatically representing a decrease in extracted Fe in the IL from ~25% of total Fe to 2.3% (Figure 3.6). No significant improvements were observed above the 100 mM threshold. High AA conditions also achieved the highest R_{REEs} values. R_{Al} and R_{Ca} did both slightly increase with ascorbic acid. R_{Si} remained at zero due to its absence in the IL phase.

Previous work evaluated the impact of AA on Fe behavior in other [Hbet][Tf_2N] leaching systems. Onghena et al. studied the use of AA in a [Hbet][Tf_2N]-bauxite residue leaching system and found Fe extraction into the IL phase dropped significantly with the addition of AA, from D_{Fe} = 1 down to 0.02 at AA concentrations ≥ 8 mM.[8] They further determined a molar ratio of 2:1 for Fe:AA was sufficient to reduce Fe coextraction, but chose to reduce Fe(III) with excess AA (15 mM) to ensure Fe remained reduced for the duration of the experiments.[8] Luo et al. found that adding AA to [Hbet][Tf_2N]-waste LCD (liquid crystal display) screens leaching system caused a dramatic decrease in Fe extraction into the IL phase, from D_{Fe} = 59.87 to 8.84.[9] Both studies achieved high extractions (>98%) for the target REEs.

To avoid increased Fe leaching from reductive dissolution, the experiment was repeated such that AA was added after CFA was filtered and removed from the CFA-IL-AQ mixture. Additional concentrations were tested to further assess the threshold of AA.

3.4.4.2 Impact of delayed mixing of AA on IL extraction (L,D,R) for all elements.

Fe and the other bulk elements demonstrated a small increase in *L,* but otherwise showed no relationship between ascorbic acid concentration(Figure 3.7). L_{REEs} also increased, but then showed a slight decrease at higher concentrations of AA.

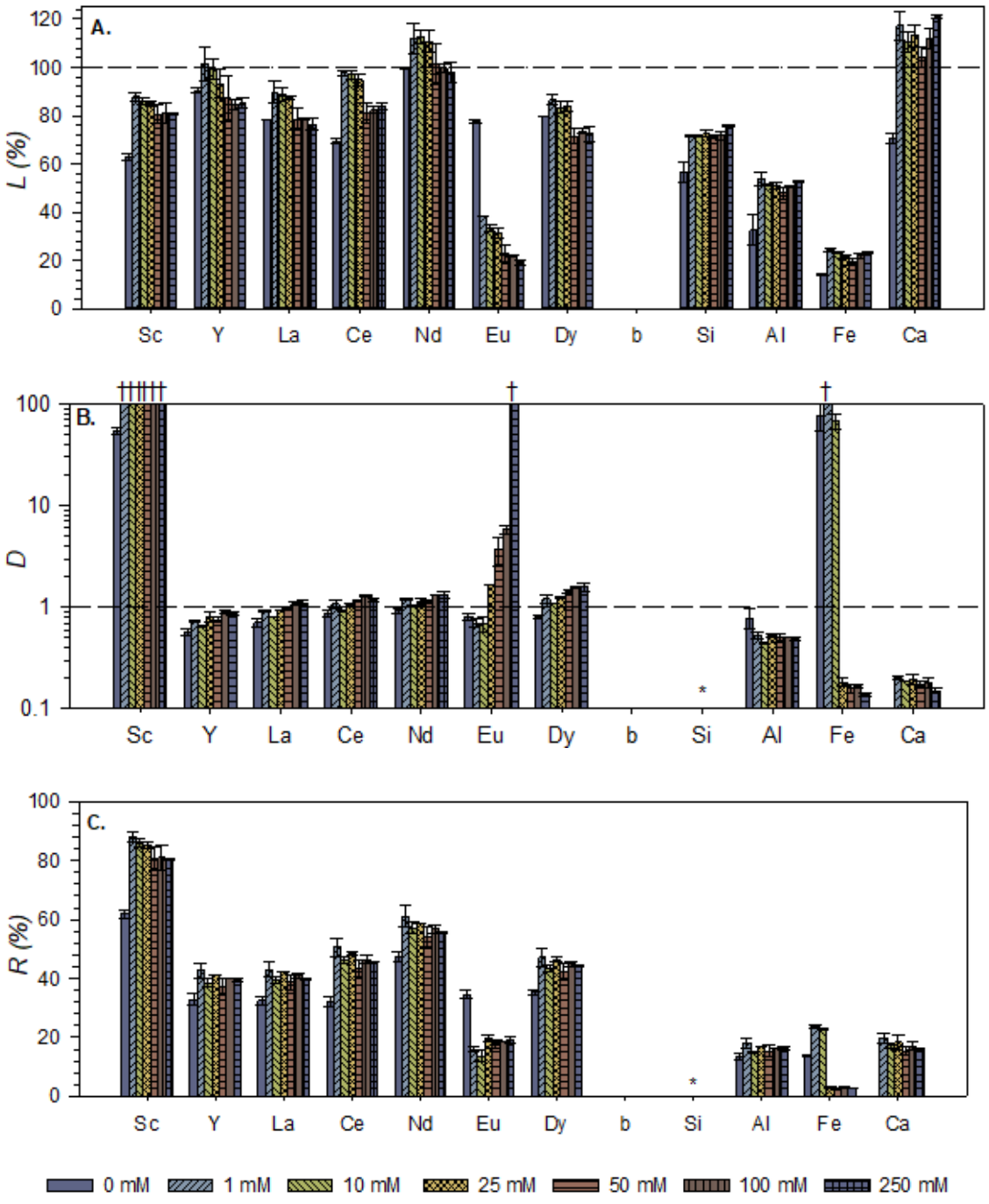

Figure 3.11 Average leaching efficiency L (A), average distribution D (B), and average recovery R (C) after IL extraction process for CFA-F1 with ascorbic acid added to the AQ-IL mixture after the CFA was removed.

*Notes: Error bars indicate standard deviation of duplicate samples. Columns marked with an * indicate zero, meaning that this element (Si) was not found in the IL phase. Columns marked with an † indicate an extremely large value of D.*

A new, lower threshold was observed for *D* compared to the direct AA method. At 25 mM AA, D_{Fe} demonstrated a dramatic decrease (Figure 3.7). D_{REEs} increased slightly, almost linearly with increasing AA, again exceeding one for several REEs. No significant changes in *D* were observed for Al, Ca, and Si, which remained at zero.

This new threshold at 25 mM AA was also reflected in *R*. R_{Fe} dropped dramatically at that concentration. For all other elements, both REEs and bulk, *R* demonstrated a small initial increase with the addition of AA, then a plateau. R_{Si} remained at zero.

Of note is that several additional steps were required to achieve complete leaching: washing with ice-cold DI water and re-stripping. While previous studies have demonstrated that the IL can be completely stripped of all elements using HCl at concentrations ≥ 1.0 M,[68,69] visual observation indicated that some elements remained in the IL phase. Following previous work, the IL phase was washed with DI water twice to reduce the acidity of the IL phase, then stripped again. Of the bulk elements, very small amounts Fe and Al were detected in the washes (≤1% of Fe total and Al total, respectively). More Fe was present at low concentrations of AA (1 and 10 mM), but Al had no relationship with AA. Extremely small quantities of Fe were detected in the stripping phase when AA was in low concentrations, 1 and 10 mM (≤0.3% of Fe total). Si and Ca were not detected at all in any wash or HCl phases. Of the REEs, all were detected in small quantities in the washes (up to 7.5% total of an individual REE), and there appeared to be no correlation with AA concentration. No REEs were detected in the sample without AA.

It is unclear why stripping was incomplete when using AA, or why L_{REEs} decreased at high levels of AA. Loss may be the result of physical loss of AQ phase during filtration.

Alternatively, it may be that some AQ phase is dissolved into the IL phase, as the two liquid phases demonstrate mutual solubility.[68,69] AA may disrupt the IL phase as a polar organic molecule and increase the solubility of the AQ phase in the IL phase. Other work using this IL and AA involved applying AA to liquid Sc- and Fe-rich bauxite leacheate; AA was not directly mixed with the IL.[8]

The ferrozine method was used to confirm Fe speciation (Table 3.3). Without AA, ~99% of the extracted Fe was present as Fe(III). With 100 mM AA, ~95% was present as Fe(II). At the threshold concentration, Fe speciation is mixed between Fe(II) and Fe(III), but ~85% of Fe was found in the AQ phase. Variability of the data was likely due to the rapid degradation of ferrozine and time sensitivity of the ferrozine assay.

Table 3.3 Fe speciation in the AQ and IL phases after AA treatment.

	AQ Phase		**IL Phase**	
AA concentration (mM)	Fe (II)	Fe (III)	Fe (II)	Fe (III)
0	0.3 ± 0.1	0.0 ± 0.0	1.3 ± 0.0	98.7 ± 0.0
25	39.9 ± 55.9	44.3 ± 57.2	9.3 ± 1.7	6.5 ± 0.4
100	79.7 ± 8.2	5.3 ± 7.5	15.0 ± 2.3	1.1 ± 1.5

Notes: AA treatment followed CFA removal. Highlighted cells indicate dominant phases.

3.4.3 Summary on AA addition. Overall, AA added at 25 mM can successfully lower the amount of Fe in the IL phase from 99% of the extracted Fe to ~3%, while simultaneously increasing R_{REEs}. Additional wash/strip cycles may improve REE recovery. The AA addition strategy is effective and should be used in combination with others to reduce Fe co-contamination in the IL phase.

3.5 Conclusions.

Globally, Fe oxide content in CFAs ranges from ~3-26 wt.%, with some Canadian CFAs peaking at ~45%,[150] and Fe is found in both discrete minerals as well as dispersed throughout glassy aluminosilicate phases. As a result, Fe co-extraction is a persistent problem for REE recovery from CFA.

Three Fe mitigation strategies were explored in this study. The first, magnetic separation, sought to reduce the amount of Fe in the CFA starting material, but failed to deplete Fe in CFA due to Fe's distribution throughout the CFA. The second, complexing salt substitution, found that using NaCl instead of $NaNO_3$ reduced D_{Fe} from ~75 to ~14, a five-fold decrease, and increased L_{REEs} and R_{REEs}.. Finally, using AA decreased D_{Fe} even further, to ~0.16, and also increased D_{REEs} slightly. These optimizations accompany other strategies identified in previous work with CFA-[Hbet][Tf_2N] leaching, including alkaline pretreatment and adding supplemental betaine cation.[137] A summary of the best *R* values for REEs, Sc, and Fe from each approach are shown in Table 3.4.

Table 3.4 Summary of Optimal Average R ± Std Dev (%) for CFA-F1.

Elements	Untreated	Alkaline PT[a]	Betaine[b]	NaCl[c]	AA[d]
ΣREEs*	2.0 ± 0.1	35.3 ± 1.8	54.9 ± 0.2	42.7 ± 1.0	47.4 ± 0.3
Sc	7.9 ± 0.5	62.0 ± 1.4	87.0 ± 0.1	72.7 ± 1.1	85.2 ± 1.0
Fe	1.9 ± 0.1	13.7 ± 0.3	16.1 ± 0.2	20.7 ± 1.6	3.3 ± 0.4

*Notes: *ΣREEs includes all REEs except Sc, which is reported separately. Optimal R means high R for REEs and Sc, and low R for Fe. [a]Alkaline pretreatment was performed at 5.0 M NaOH at a 1:10 g/mL solid:liquid ratio. [b]Betaine addition at 10 mg betaine per g AQ phase solution.[137] [c]NaCl at 1.0 M concentration. [d]Ascorbic acid (AA) was added indirectly at 25 mM.*

A final scheme depicts the recommended strategy (Figure 3.8). It includes a number of optimizations, including alkaline pretreatment, adding supplemental betaine, using NaCl instead of $NaNO_3$ in the AQ phase, and finally, removing the CFA and adding AA to the AQ-IL mixture. This process generates an REE-rich acidic solution with very low concentrations of Fe, in contrast to previous work in which Fe presented as a significant co-contaminant.[137]

Recyclable ILs like [Hbet][Tf_2N] present a new approach for extracting REEs from CFA that reduces chemical consumption, waste generation, and energy usage. Future work will determine whether this process can be further optimized to an industrial scale.

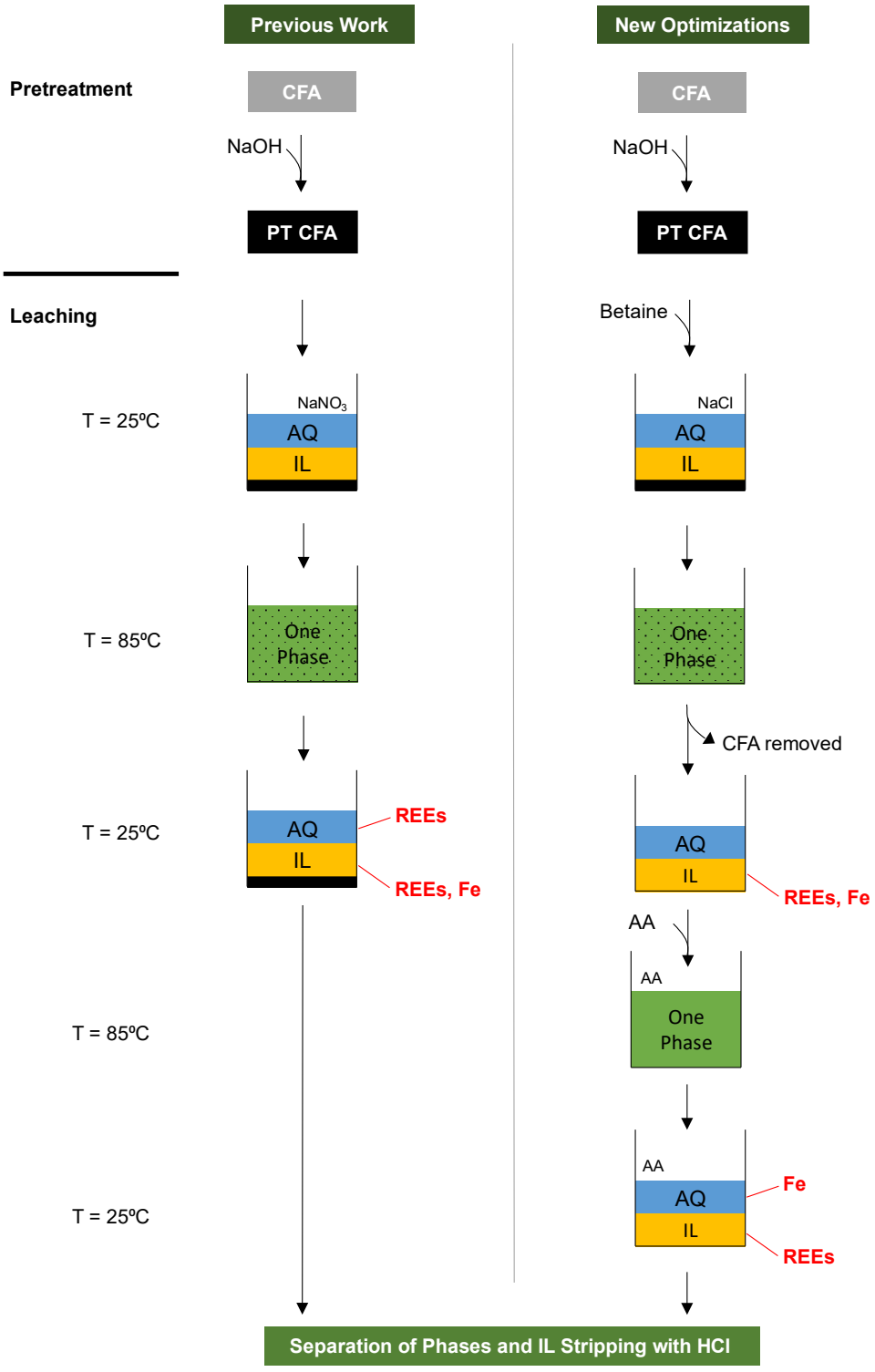

Figure 3.12 Optimized IL extraction scheme.

Notes: Original method shown at left, optimized method shown at right. Pretreatment is only required for Class-F CFAs.

CHAPTER 4. PROCESS EFFICIENCY AND SUSTAINABILITY EVALUATIONS

4.1 Abstract

Previous work found that rare earth elements (REEs), valued for their important roles in manufacturing and green tech, can be recovered from coal fly ash (CFA), a waste product from coal combustion, using an ionic liquid (IL) betainium bis(trifluoromethylsulfonyl)imide ([Hbet][Tf_2N]). This IL has been shown to separate REEs from bulk elements (Si, Al, Ca, and Fe), but little is known about the behavior of other elements. This study investigated 18 additional elements (29 total) and found that in the IL phase, bulk elements were found in low concentrations (<26 wt.%), trace elements were not found (<1.6 mg/kg), and of the actinides, Th was extracted into the IL phase and U was not leached at all. REEs, as previously noted, partition largely between the AQ and IL phases. The study also identified other important optimizations, including pH (no impact observed for pH 2-7), temperature (optimal *L* observed at 85ºC of the studied 45-85ºC range), and duration of leaching (optimal *L* observed at 3 h of the 0.5-12 h range). The process is also compared to several CFA solid extraction methods and CFA leacheate separation methods to place the method in context with existing literature. Finally, a number of process sustainability improvements are recommended, including the use of microwave heating, water and IL recovery strategies, and beneficial uses of the solid residuals.

4.2 Introduction

Recently, coal and coal combustion residuals have been investigated as a potential source of rare earth elements (REEs).[19,25,26,84-86,88-92] REEs, the lanthanides and yttrium and scandium, play important roles in a variety of high-tech applications in fields ranging from electronics, clean energy, aerospace, automotive and defense, and for many of these, there are no adequate replacements. As a result, they are uniquely susceptible to supply chain disruption and have been designated by both the United States and the European Union as "critical materials."[15,16,19] Coal fly ash (CFA), one type of coal combustion residual, has been identified as a resource due to its REE enrichment and the vast quantities produced annually. It is estimated that the US alone produces 130 million metric tons (t) of CFA each year, and of this, 70 million t is landfilled.[2] This, along with decades' worth of coal combustion, fills the approximately 1,000 existing impoundments with approximately 600 million t of CFA since 2000.[2,3] With average REE concentrations of CFA estimated to be 500 mg/kg, annual landfilled CFA contains roughly 41 thousand t REE oxides, valued at ~$1.7 million USD. The U.S. imported 7,340 t REE oxides in 2020.[157]

In addition to valuable REEs, CFA contains many toxins present at trace levels (up to hundreds mg/kg), including arsenic, cadmium, chromium, lead, mercury, selenium, uranium, and thorium.[30,32,33] While their concentrations are low, they become significant at the quantities considered.[34,37] Recent catastrophic spills and groundwater contamination incidents from CFA-holding ponds have prompted governmental regulation and pond closures.[34,37] As the environmental and economic costs of storage increase, there is increased pressure to find alternative uses for CFA.

Recovering REEs from CFAs presents one such alternative use, but extraction methods must address co-extraction of these noxious elements. Most current methods leach indiscriminately or otherwise require complete CFA digestion, consuming large amounts of chemicals in the process.[27,46,78,79] This generates wastes potentially rich in contaminants that must be safely managed as well as necessitating downstream separation methods like liquid membranes, passive columns, and biosorption.[94-96] Furthermore, these methods require highly corrosive solutions and utilize high pressure and high temperature conditions because CFA is composed of durable aluminosilicates. An industrial process should seek to limit energy consumption, reduce chemical use (especially hazardous chemical use), and minimize process complexity.

Chapter 2 describes a recently published proof-of-concept study on REE extraction from CFA utilizing a recyclable ionic liquid.[137] Ionic liquids (ILs) present a number of useful properties for industrial applications, including low flammability, negligible vapor pressure, and high thermal stability. [51,53] The IL under investigation, betainium bis(trifluoromethylsulfonyl)imide ([Hbet][Tf_2N]), features another notable attribute: it demonstrates thermomorphic solubility with water. While slightly hygroscopic, it is nearly immiscible with water at room temperature, but as temperatures increase, its water solubility increases, ultimately forming a single phase above 55ºC.[69,97] This temperature-dependent behavior can be exploited as a built-in extraction mechanism to extract elements into the IL.[6,7,69,97] Extracted elements can be stripped from the IL phase using mildly acidic solutions, making them recyclable and thus limiting chemical consumption and waste generation.[6-8] In particular, [Hbet][Tf_2N] selectively solvates REEs over common transition metals.[5,6,65,68,69] REEs can be extracted from aqueous mixtures or directly from

REE-rich solids, including lamp phosphors, permanent magnets, bauxite residue, liquid crystal display (LCD) screens, and now CFA.[6-9,137] Leaching occurs via a proton-exchange mechanism (Equation 1):[65,68,69]

$$REE_2O_3 + 6\,[Hbet][Tf_2N] \leftrightarrow 2[REE(bet)_3][(Tf_2N)_3] + 3\,H_2O \quad (3)$$

In Chapter 2, [Hbet][Tf_2N] was applied to three representative types of CFA and achieved high leaching efficiencies for REEs (approaching 100%) for all CFAs.[137] Pretreatment with an alkaline solution was required for the more recalcitrant Class-F CFAs, but not for the less resistant, Ca-rich Class-C CFAs.[137] Importantly, alkaline pretreatment did not cause any loss of REEs, unlike the acidic pretreatments investigated.[137] Furthermore, adding additional betainium promoted high REE partitioning into the IL phase over the aqueous (AQ) phase.[137] It was also proved that the IL could be used over multiple leaching-stripping cycles, offering an opportunity to reduce chemical consumption in REE extraction.[137] The process yields a mildly acidic REE-rich solution, with minimal concentrations of bulk elements.[137] While downstream REE separation is still required to achieve single-element concentrates, this work unlocks a new strategy for CFA refinement for REE recovery.[137]

Chapter 2 focused on developing the extraction and separation of seven major REEs (Ce, La, Nd, Sc, Y, Eu, Dy) from major bulk elements (Al, Ca, Fe, Si) for CFAs using the recyclable [Hbet][Tf_2N] IL. Chapter 4 expands the scope of previous work to a much wider range of elements, and to further optimize important variables (i.e., temperature, pH, and time) of the IL leaching/stripping process for better efficiency. Specifically, the objectives were to describe the leaching behavior of other elements in CFA in the IL

leaching/stripping system, and to identify the optimal temperature, pH, and kinetic duration for the IL leaching/stripping system. These variables are crucial not only to obtaining a stronger understanding of the physicochemical reactions at work in the IL leaching/stripping process, but also to optimizing the process toward industrial and economic viability.

4.3 Materials and Methods

4.3.1 Chemicals and Materials.

All chemicals used can be found in Chapter 2 (see *Section 2.3.1*). All chemicals including CFAs were used without further purification.

4.3.2 IL Synthesis.

Synthesis was performed as previously described (see *Chapter 2, Section 2.3.2*).[5,65,137]

4.3.3 CFA Characterization.

One representative CFA was investigated: an unweathered Class-F (CFA-F1) (Table 2.1).[137] CFA-F1 is the NIST SRM 1633c ash, obtained from Sigma Aldrich. Characterization included major oxide and trace element composition analysis, and mineral composition quantification. A full description of the characterization is in Chapter 2 (see *Section 2.3.3*). CFA pH was determined by placing a small quantity of raw or alkaline pretreated CFA in a glass vial with a solution of 1.0 M $NaNO_3$.

4.3.4 CFA Alkaline Pretreatment.

Alkaline pretreatment was performed as described in a previous study.[137] Briefly, CFA was mixed with 5.0 M NaOH in a ratio of 1:10 g/mL and heated with a stir bar at 85°C for five hours. After cooling, the supernatant was removed for elemental analysis by inductively coupled plasma-optical emission spectrometry (ICP-OES) to quantify loss from pretreatment. The CFA was washed with DI water, filtered, and dried at ~80°C prior to leaching and stripping with the IL.

4.3.5 Leaching and Stripping Experiments.

The leaching and stripping process was described in depth previously (Chapter 2).[137]

4.3.5.1 Leaching.

Briefly, CFA, water-saturated IL, and aqueous solution containing 1.0 M $NaNO_3$ were added to a small vial to achieve a liquid-liquid (IL:AQ) mass ratio of 1:1 and solid-liquid ratio of 12.5:1.0 (mg:g). The addition of $NaNO_3$ was to promote IL and AQ phase separation.[6,7,60,68,69] The pH of the $NaNO_3$ solution was adjusted to 3.50 ± 0.05 with HNO_3 and NaOH prior to mixing.[6,7,69] The vial was heated with a stir bar to 85°C for three hours. Then, the vial was cooled to room temperature, then stored at 4°C overnight. After sufficient cooling, the AQ phase was easily separated and prepared for analysis by ICP-OES. The IL phase was transferred to a new vial for stripping. The CFA was washed with DI water, filtered, and dried at ~80°C.

4.3.5.2 Stripping.

Briefly, 1.5 M HCl aqueous solution was added to the new IL-containing vial to achieve a liquid-liquid (IL:HCl) mass ratio of 1:1. Again, the vial was heated in an oil bath with a

stir bar to 85°C for 1.5 hours. Then, the vial was cooled to room temperature, then stored at 4°C overnight. The HCl aqueous phase was then separated and prepared for analysis by ICP-OES.

4.3.6 Quantification of Extraction and Separation.

Elements may be leached from the CFA by the pretreatment (M_{PT}) step, and by the IL/water extraction into the AQ phase (M_{AQ}) and the IL phase (M_{IL}), respectively, where M represents mass. The mass in the IL phase was determined by that measured in the stripping phase. Previous studies have demonstrated that all elements are completely stripped by the stripping phase from the IL using HCl at concentrations ≥ 1.0 M.[68,69]

To quantify the extraction and separation of elements from CFA, leaching efficiency (*L*) and distribution coefficient (*D*) were calculated. *L* represents how much an element is extracted by the procedures compared to its total amount (M_{total}) in the CFA (Equation 2). The total mass of each element in the CFA was determined by total digestion analysis performed in this study or from reported data.

$$L\ (in\ \%) = \frac{M_{PT}\ +\ M_{AQ}\ +.M_{IL}}{M_{Total}} \tag{2}$$

D is the ratio between the element's final mass in the IL phase (M_{IL}) and its mass in the AQ phase (M_{AQ}) (Equation 3):

$$D = \frac{M_{IL}}{M_{AQ}} \tag{3}$$

All leaching and stripping tests were performed in duplicate. *L* and *D* were calculated for elements in each experimental trial and the averages were reported.

4.4 Results and Discussion

4.4.1 Characterization of CFA.

The CFA sample investigated in this chapter was a Class-F, unweathered CFA sample obtained from NIST, and it displayed expected physical and morphological properties as discussed previously (see *Chapter 2, Section 2.4.1*).[104,137] The pH of the raw CFA sample in 1.0 M $NaNO_3$ was 8.20, while the pH of the alkaline-pretreated CFA in the same solution was 9.73.

4.4.2 Broad elemental survey.

To comprehensively study IL leaching on CFA, a total of 29 elements were measured in the alkaline pretreatment, AQ, and HCl stripping phases (Table 4.1). This included 11 REEs (Sc and Y and 9 of the lanthanides; Pm was excluded as it is extraordinarily rare) so as to better understand REE behavior and determine if recovery of other REEs is viable. Only REEs listed on the 1633C NIST certificate were included. Two radioactive actinides commonly found in CFA, U and Th, were also studied as they present risks for disposal as contaminants of concern. Additional potential contaminants of concern investigated include As, Cd, Cr, Pb, and Se. Bulk constituents included Al, Ca, Fe, Si, Mg and Ti, and minor constituents included the aforementioned contaminants of concern as well as Cu, Mn, Ni, V, and Zn.

Table 4.1 Elemental partitioning between pretreatment, leaching, and stripping (IL) phases for IL extraction from CFA-F1.

Element	Total (mg/kg)[a]	PT Phase %	AQ Phase %	IL Phase %	Residual %
REEs					
Sc	37.6 ± 0.6	0.0 ± 0.0	0.0 ± 0.0	68.8 ± 0.9	31.2 ± 0.9
Y[b]	105.2	0.0 ± 0.0	51.6 ± 0.3	27.7 ± 0.1	20.7 ± 0.4
La	87.0 ± 2.6	0.0 ± 0.0	40.7 ± 0.0	31.1 ± 0.1	28.2 ± 0.2
Ce	180	0.0 ± 0.0	38.3 ± 0.3	37.7 ± 0.8	24.0 ± 1.0
Nd	87	0.0 ± 0.0	41.8 ± 0.4	43.7 ± 0.3	14.5 ± 0.1
Sm	19	0.0 ± 0.0	47.5 ± 0.4	45.8 ± 1.0	6.7 ± 0.6
Eu	4.67 ± 0.07	0.0 ± 0.0	12.6 ± 0.7	1.0 ± 0.2	86.4 ± 0.5
Tb	3.12 ± 0.06	N/A	0.0 ± 0.0	0.0 ± 0.0	100.0 ± 0.0
Dy	18.70 ± 0.30	0.0 ± 0.0	30.5 ± 0.0	23.0 ± 0.1	46.6 ± 0.1
Yb	7.7	0.0 ± 0.0	54.2 ± 0.7	0.0 ± 0.0	45.8 ± 0.7
Lu	1.32 ± 0.03	N/A	0.0 ± 0.0	0.0 ± 0.0	100.0 ± 0.0
Actinides					
Th	23.0 ± 0.4	0.0 ± 0.0	0.0 ± 0.0	100.8 ± 5.8	1.6 ± 2.3
U	9.25 ± 0.45	0.0 ± 0.0	0.0 ± 0.0	0.0 ± 0.0	100.0 ± 0.0
Bulk constituents (wt.%)					
Mg	0.50 ± 0.052	0.0 ± 0.0	82.5 ± 1.4	14.8 ± 0.0	2.8 ± 1.3
Al	13.28 ± 0.61	1.7 ± 0.2	35.4 ± 2.5	15.0 ± 0.6	47.9 ± 3.1
Si	21.30 ± 0.57	51.0 ± 9.8	26.1 ± 1.0	0.0 ± 0.0	22.9 ± 1.0
Ca	1.365 ± 0.040	1.2 ± 0.3	94.5 ± 2.7	13.2 ± 0.6	0.0 ± 0.0
Ti	0.724 ± 0.030	0.4 ± 0.1	6.3 ± 0.9	5.0 ± 0.6	88.3 ± 0.3
Fe	10.49 ± 0.39	0.4 ± 0.1	0.0 ± 0.0	26.4 ± 0.3	73.1 ± 0.3
Trace constituents					
V	286.2 ± 7.9	N/A	0.0 ± 0.0	0.0 ± 0.0	100.0 ± 0.0
Cr	258 ± 6	N/A	0.0 ± 0.0	0.0 ± 0.0	100.0 ± 0.0
Mn	240.2 ± 3.4	0.3 ± 0.2	68.5 ± 8	1.6 ± 0.2	29.7 ± 7.8
Ni	132 ± 10	N/A	0.0 ± 0.0	0.0 ± 0.0	100.0 ± 0.0
Cu	173.7 ± 6.4	0.0 ± 0.0	0.0 ± 0.0	0.0 ± 0.0	100.0 ± 0.0
Zn	235 ± 14	61.3 ± 7.2	23.5 ± 1.1	0.6 ± 0.3	14.6 ± 0.7
As	186.2 ± 3.0	N/A	0.0 ± 0.0	0.0 ± 0.0	100.0 ± 0.0
Se	13.9 ± 0.5	N/A	0.0 ± 0.0	0.0 ± 0.0	100.0 ± 0.0
Cd	0.758 ± 0.005	N/A	0.0 ± 0.0	0.0 ± 0.0	100.0 ± 0.0
Pb	95.2 ± 2.5	N/A	0.0 ± 0.0	0.0 ± 0.0	100.0 ± 0.0

Notes: No shading indicates 0-1% partitioning; the light shade indicates 1-10%; the medium shade indicates 10-50%; the medium dark shade indicates 50-80%; and the dark shade indicates 80-100%. N/A indicates data are not available. Extraction efficiencies >100% may be the result of low initial concentration in the solid or potential enrichment in the CFA as the result of alkaline pretreatment.

[a] *Total indicates concentration in untreated CFA as described in the NIST 1633 certificate. All concentrations are reported in mg/kg except bulk constituents which are reported in wt. %.*

[b] *Y concentration was determined by total digestion with HF.*[137]

4.4.2.1 REEs and actinides.

REEs (lanthanides+Sc+Y) and actinides (Th and U) behaved largely similarly. No REEs or actinides were detected in the alkaline pretreatment phase (Table 4.1). This is consistent with previous work and literature, indicating that acidic, not alkaline, solutions must be used to extract REEs from CFA.[79,137] Almost all REEs were detected in both the AQ and IL phases. This is also consistent with previous research that indicated, in the absence of additional betaine, REEs partitioned approximately equally between the AQ and IL phases (D_{REEs} = ~1).[137] Three REEs (Ho, Lu, Tb) were non-detectable in both the IL and AQ phases. This is likely due to their low concentrations in the CFA solid (<5 mg/kg CFA). For actinides, Th was detected in both AQ and IL phases, while U was not detected in either phase.

Generally, detected REEs demonstrated high leaching efficiency values with L_{REEs} ranging from ~70-100% (Table 4.1). Lower L_{REEs} (<60%) was reported for Eu, Dy, and Tb, in which the detection was likely impacted by their very low concentrations in the original CFA. L_{Th} reached nearly 100%.

REEs tended to distribute equally between AQ and IL phases (D_{REEs} = 1).[137] Sc and Th displayed high *D*, indicating that they were strongly extracted into the IL phase via complexation with the carboxylic acid on [Hbet][Tf_2N]'s betaine cation. Carboxylic acids complex strongly with cations with high charge densities, including Fe^{3+}, Sc^{3+}, and Th^{3+} ions (Table 4.1).[7,8,111,113] In contrast, U displayed negligible *D*. This is likely due to the fact that the oxyanion of U(+V) cannot be extracted via complexation with [Hbet][Tf_2N]'s

carboxylic acid group due to charge repulsion and steric hindrance, similarly to the poor extraction of other oxyanions by this IL.[68,69,137]

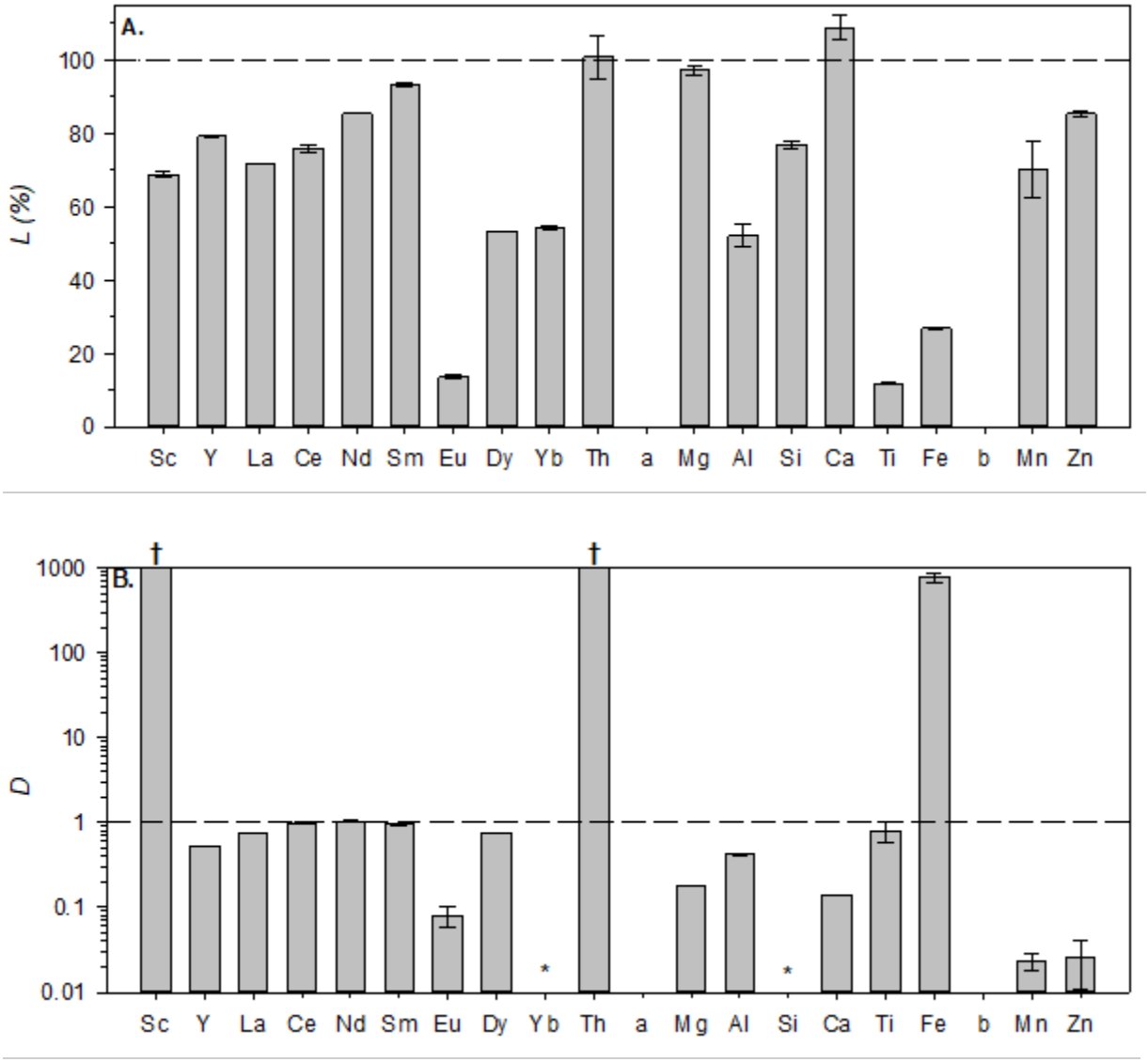

Figure 4.1 Average leaching efficiency L (%) (A) and average distribution D (B) after IL extraction process for CFA-F1 following alkaline pretreatment.

*Notes: Error bars indicate standard deviation of duplicate samples. In **(B)**, columns marked with an * indicate zero elements (Ca and Si) were not found in the IL phase. Columns marked with † indicate that the element was not found in the AQ phase. Extraction efficiencies >100% may be the result of low initial concentration in the solid or potential enrichment in the CFA as the result of alkaline pretreatment.*

4.4.2.2 Bulk elements.

All six bulk elements were detected in at least one phase (pretreatment, AQ, or IL). The behaviors of most bulk elements (Al, Si, Ca, Fe) were described extensively in previous work,[137] and Mg and Ti were two additional bulk elements investigated in this study. All bulk elements except Mg were detected in the pretreatment phase. Under alkaline conditions, Mg may form magnesium silicate hydrate gels, which may explain the lack of Mg in the pretreatment phase.[158] Further, all bulk elements were detected in the AQ phase, with the exception of Fe, which was demonstrated in earlier work to partition strongly in to the IL phase.[137] Finally, almost all bulk elements were detected in the IL phase though in small amounts (5-26% of total analyte) (Table 4.1). Si is known to not be extracted into the IL phase due to steric hindrance of oxyanion for complex formation.[68,69,137]

L_{Bulk} varied from 10-100%. The two alkaline earth metals, Ca and Mg, both displayed nearly 100% leaching (Figure 4.1). Ca is known to leach from CFA under acidic conditions.[137] Izquierdo et al. found that Mg leaching increased with Ca leaching, as carbonate minerals in the CFA were dissolved.[140] High L_{Si} and L_{Al} were largely the result of the alkaline pretreatment (a desilication reaction that degrades the CFA aluminosilicate matrix).[137] Ti is similar to Si structurally in the aluminosilicate matrix but does not follow Si's leaching pattern, and remains virtually immobile regardless of pH.[140] Similarly, Fe is generally poorly soluble, even under acidic conditions,[140] but shows moderate L (Figure 4.1). It is likely that the low quantities of Ti and Fe leached are only accessible in this study due to the alkaline pretreatment-acidic IL sequence. King et al. achieved high REE recovery from CFA using a similar NaOH-dilute acid procedure.[79] Furthermore, leaching

may also be higher than predicted by Izquierdo et al. because of complexation: Fe and Ti complex with betaine, compared to solutions that don't contain chelates.

D_{Bulk} also varied (Figure 4.1). Mg and Ca both showed a preference for the AQ phase ($D = 0.1$). Si was not detected in the IL phase ($D_{Si} = 0$). Al showed a slight preference for the AQ phase, and Fe showed a strong preference for the IL phase. Ti demonstrated D similar to D_{REEs}, likely due to its similar charge density ($D_{REEs,Ti} = 1$).

4.4.2.3 Trace elements.

Of the 12 trace elements investigated, 9 were not detected in the AQ or IL phases, meaning that they remained in the solid and/or leached during alkaline pretreatment: V, Cr, Ni, As, Se, Ag, Cd, Tl, and Pb (Table 4.1). Studies on sequential leaching of CFA indicates that many of these elements are found in recalcitrant phases (silicate-bound or in the insoluble residue) and as a result demonstrate extremely poor leaching.[140,142] Further, divalent elements like Ni, Cd, Ni, and Pb, are poorly extracted in this IL.[68,69] Oxyanions, like those formed by Si, As, Se, and Cr, are poorly extracted, if at all, and are not extracted into the IL phase due to steric hindrance.[68,69]

The remaining three trace elements – the transition metals Mn, Cu, and Zn – were all detected in both the AQ and IL phases. Following this, Mn and Zn both experienced relatively high L (>70%), while Cu showed low leaching (22%) (Table 4.1). However, these three elements have all be demonstrated to leach more from CFA than other transition metals under acidic conditions.[140]

All elements had very low D ($D < 0.03$), which is supported by previous literature indicating that divalent metal ions are poorly extracted in this IL (Figure 4.1).[68,69]

4.4.2.4 Selected elements and IL coextraction.

Leaching and partitioning are complex processes and result from a number of factors beyond steric geometry, including ionic radius, basicity, and electronegativity.[111] The impacts of pH, time, and temperature on these phenomena must be investigated in order to optimize the IL leaching/stripping process. Subsequent analyses only investigated such elements with both (1) detectable concentrations in the AQ or IL phases and (2) listed concentrations in the NIST 1633c certificate materials. Of the REEs and actinides, this included: Sc, Y, La, Ce, Nd, Sm, Eu, Dy, Yb, Th, and U. All bulk elements (Mg, Al, Si, Ca, Ti, and Fe) were included. Finally, three trace elements Mn, Cu, and Zn were included.

Of particular interest are elements co-extract strongly into the IL phase; these will need to be separated in subsequent processing to produce a pure REE product. These elements include Fe (26% of total Fe) and Th (100% of total), and to a lesser extent, Al, Mg, Ca, and Ti (15%, 15%, 13%, 5% of total, respectively) (Table 4.1). Reducing Fe coextraction into the IL phase has been investigated in a related study reported in Chapter 3.

4.4.3 Impact of pH.

Previous studies exploring [Hbet][Tf_2N] behavior found that the pKa of betaine is 1.82, and that for AQ solutions ranging from pH 1.5-10, the equilibrium pH of AQ and IL mixtures is consistently ~1.3, indicating that the IL pH dominates..[111] More alkaline solutions (pH > 10) fully deprotonate the IL, leading to a monophasic mixture ultimately

not useful for extraction experiments.[5,111] More acidic solutions (pH < 1.5) resulted in low extraction efficiencies for REEs from simple feedstock solutions.

CFA can be classified as acidic, mildly alkaline, or strongly alkaline, with pH ranging from ~4 to >12.[159] Overwhelmingly, CFAs are neutral or alkaline in water.[159] CFA pH is the result of both coal origin and power plant boiler type, among other factors.[160] In this study, the pH of the untreated CFA in 1.0 $NaNO_3$ was 8.20; the pH of the alkaline-pretreated CFA in 1.0 $NaNO_3$ was 9.73.

In previous chapters, the AQ phase (1.0 M $NaNO_3$) was adjusted to pH 3.5 with small amounts of HNO_3 and NaOH. In this study, more pH values were tested: pH 2.0, 5.0, and 7.0. Without adjustment, the solution was neutral.

Overall, pH of the AQ phase had negligible effects on both leaching efficiency and distribution (Figure 4.2). Previous work demonstrated that leaching efficiency of all elements was poor for untreated Class-F CFAs, but high for alkaline-pretreated CFAs, indicating that the increase in CFA pH did not negatively impact IL performance.[137] Altogether, this indicates that pH is largely controlled by the IL, as expected. This pH study should be tested for other CFAs, especially acidic CFAs, since only one CFA sample was investigated here. Eliminating pH control would be desirable as it reduces protocol complexity, increasing the likelihood of commercial execution on an industrial scale.

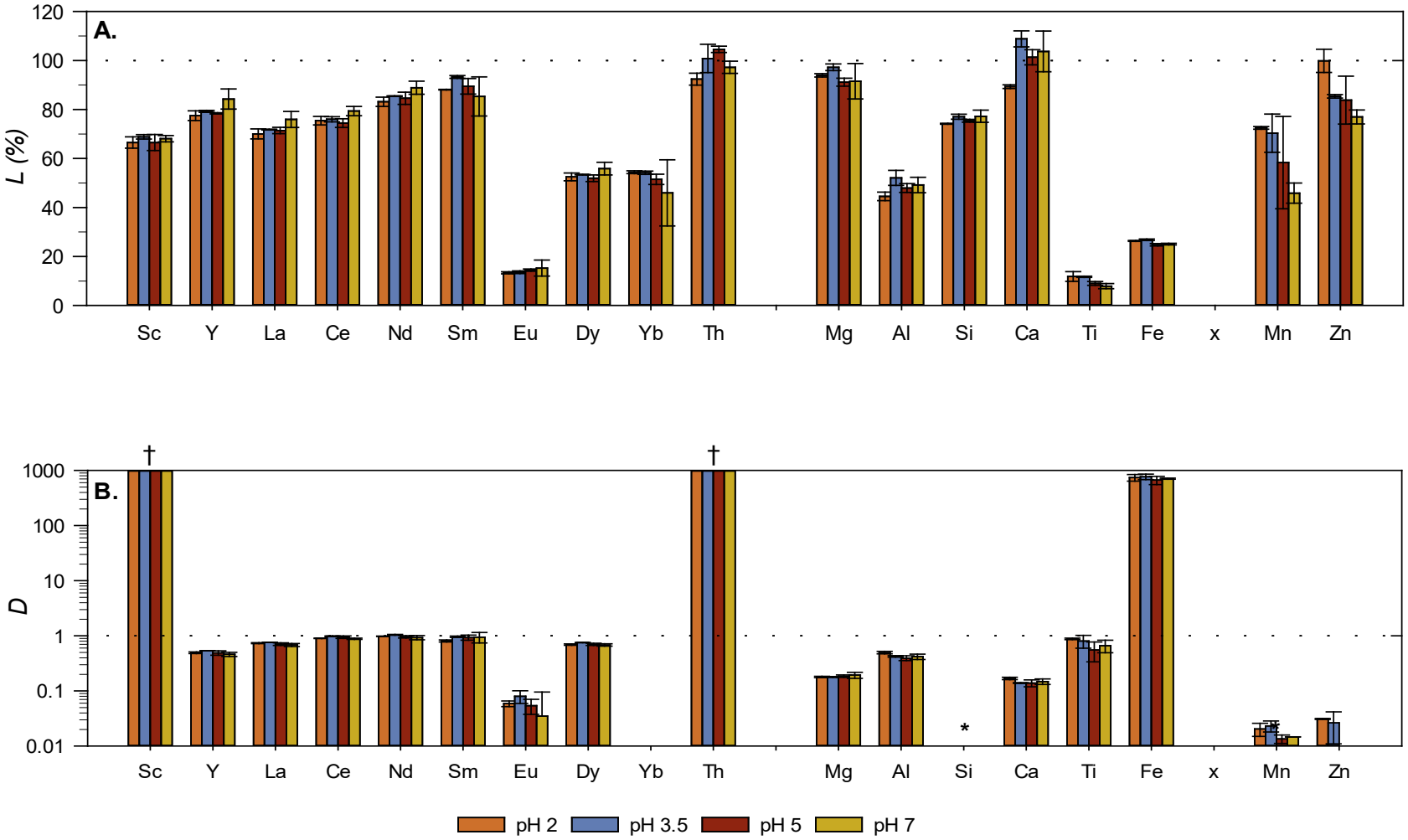

Figure 4.2 Average leaching efficiency L (A) and average distribution D (B) after IL extraction process for CFA-F1 following alkaline pretreatment where IL extraction varied in pH of AQ phase.

*Notes: Error bars indicate standard deviation of duplicate samples. In **(B)**, columns marked with an * indicate zero elements (Ca and Si) were not found in the IL phase. Columns marked with † indicate that the element was not found in the AQ phase: L >100% may be the result of low initial concentration in the solid or potential enrichment in the CFA as the result of alkaline pretreatment.*

4.4.4 Impact of duration and temperature.

Previous studies applying [Hbet][Tf_2N] to other REE-rich wastes (NdFeB magnets and lamp phosphors) examined leaching efficiency for durations of 8-100 h at temperatures ranging from 50 to 90 ºC and found that around 24 h and above 80ºC were required to achieve 100% extraction for REEs.[6,7] Of note is that these early studies on [Hbet][Tf_2N] focused on using the IL dry or with low water content (<10 wt.%) to avoid the loss of ions to the water phase; both studies found that REE extraction improved with increasing water content.[6,7] The NdFeB magnet study and subsequent investigations found optimal extraction conditions when the IL: water ratio was 1:1, which was the basis that this ratio was chosen for the process in this study.[7,8,111] Elevated temperature and increased water content were demonstrated to decrease IL viscosity separately and together. [6,7] Lowered viscosity is hypothesized to increase dissolution rates because solid CFA particles are no longer limited by diffusion across an interface (the IL: water boundary), and access to the complexing functional group – the carboxyl group on the betaine cation – is improved.

Temperature is a critical variable as extraction relies on [Hbet][Tf_2N]'s thermomorphic behavior. In 1:1 mass ratio of the [Hbet][Tf_2N]:H_2O system, the cloud point where phase separation occurs is at 55 ºC. The cloud point can be influenced by the presence of additional ions in the IL or AQ phases.[68,69] Vander Hoogerstraete et al. found that chloride ions increased the cloud point to ~73 ºC at 2.0 M HCl, while betaine decreased the cloud point to 42 °C when the AQ phase contained 25 wt. % betaine.[69] Different ions present different salting-in and salting-out effects following the Hofmeister series.[7,69] The Hofmeister series, first noted in 1888, describes common cations and anions as salting-in

or salting-out based upon their tendency to destabilize or stabilize proteins in aqueous solution, respectively. In this study, $NaNO_3$, a fairly middle-of-the-road salt, was deliberately added to promote separation of IL and AQ phases, but other ions may also be present as CFA leaches, including F^-, Cl^-, CO_3^{2-}, NO_3^-, and SO_4^{2-}, as well as oxyanions of heavy metals.[113] Thus, a higher temperature, 85 ºC, was chosen in earlier work to assure that single phase was achieved during extraction and overcome the salting-out effect but to avoid dangerous high pressure build up in the sealed vials.[137]

Various REE recovery methods from CFA differ considerably in duration. The majority of these methods do not extract REEs directly from CFA solids; rather, they digest the CFA nearly completely to form a leacheate, then extract REEs from the resulting mixture. [1,40-42,45,78,79,94] These methods do successfully extract almost all REEs but require overnight digestion (>12 h) with strong acids (e.g., HF and HNO_3) or by sintering with strong bases (e.g., NaOH and Na_2O_2).[1,40-42,45,78,79,94] All require elevated temperatures (80-100 ºC) for chemical digestions and high temperature (450 ºC) for sintering in a furnace. The few direct leaching protocols, such as those developed by King et al. or Kashiwakura et al., require milder conditions (shorter time (<4 h), milder acids, and lower temperatures (20-70 ºC) – but only achieve middling extraction efficiencies (<50%).[27,79] The duration of three hours was chosen as a mild condition for previous studies to evaluate IL leaching.[137]

Compared to previous studies that employed 3 h duration at 85°C, this study expanded the ranges from 30 min to 12 h in duration and 45-85°C in temperature. Overall, duration from 30 min to 12 h had negligible impacts on both leaching efficiency and distribution for almost all elements (Figure 4.3). That high leaching efficiencies can be achieved in just 30 min was not anticipated given the long durations of other common REE-CFA leaching

processes and presents a significant advantage compared to traditional methods.[1,27,40-42,45,78,79,94] It is likely that, perhaps without alkaline pretreatment, duration would play a larger role, with leaching increasing with longer leaching times. Previous work has found that alkaline pretreatment can significantly increase REE extraction from CFA: NaOH attacks Si-O bonds, attacking the CFA aluminosilicate structure.[79,137] REEs remain behind in the solid CFA or perhaps become entrapped in newly formed sodium aluminum silicate precipitates.[79,137] These precipitates degrade under acidic conditions, including those created by the IL. Thus, alkaline pretreatment makes REEs accessible for following acidic leaching with [Hbet][Tf_2N], such that only short time frames are required.

Temperature impacts both leaching from the CFA solid as well as elemental partitioning between phases. Higher temperatures are required for attacking the durable CFA matrix, as well as achieving one-phase mixing between the IL and AQ phases. With respect to the former, an increase in L_{REEs} was observed at 75°C, with the highest values observed at 85°C (Figure 4.4). 75°C appears to be a threshold for most REEs as well as Th. Such a pattern was not observed with bulk and trace constituents. Most bulk and trace elements (Al, Ca, Fe, Mg, Ti, and Zn) showed negligible impacts from varying temperatures. At 85°C, L_{Mn} showed a dramatic increase and L_{Si} dropped slightly. Izquierdo et al. found that Mn leaching increased with the decreasing pH.[140]

Increased temperatures seemed to increase D_{REEs} slightly (Figure 4.4). Interestingly, most elements (most REEs, Al, Fe, Mg, and Ti) showed a slight decrease in D at 55°C. Sm showed the opposite behavior. A threshold increase was again observed for D at 75°C, with slight improvements in D observed at 85°C.

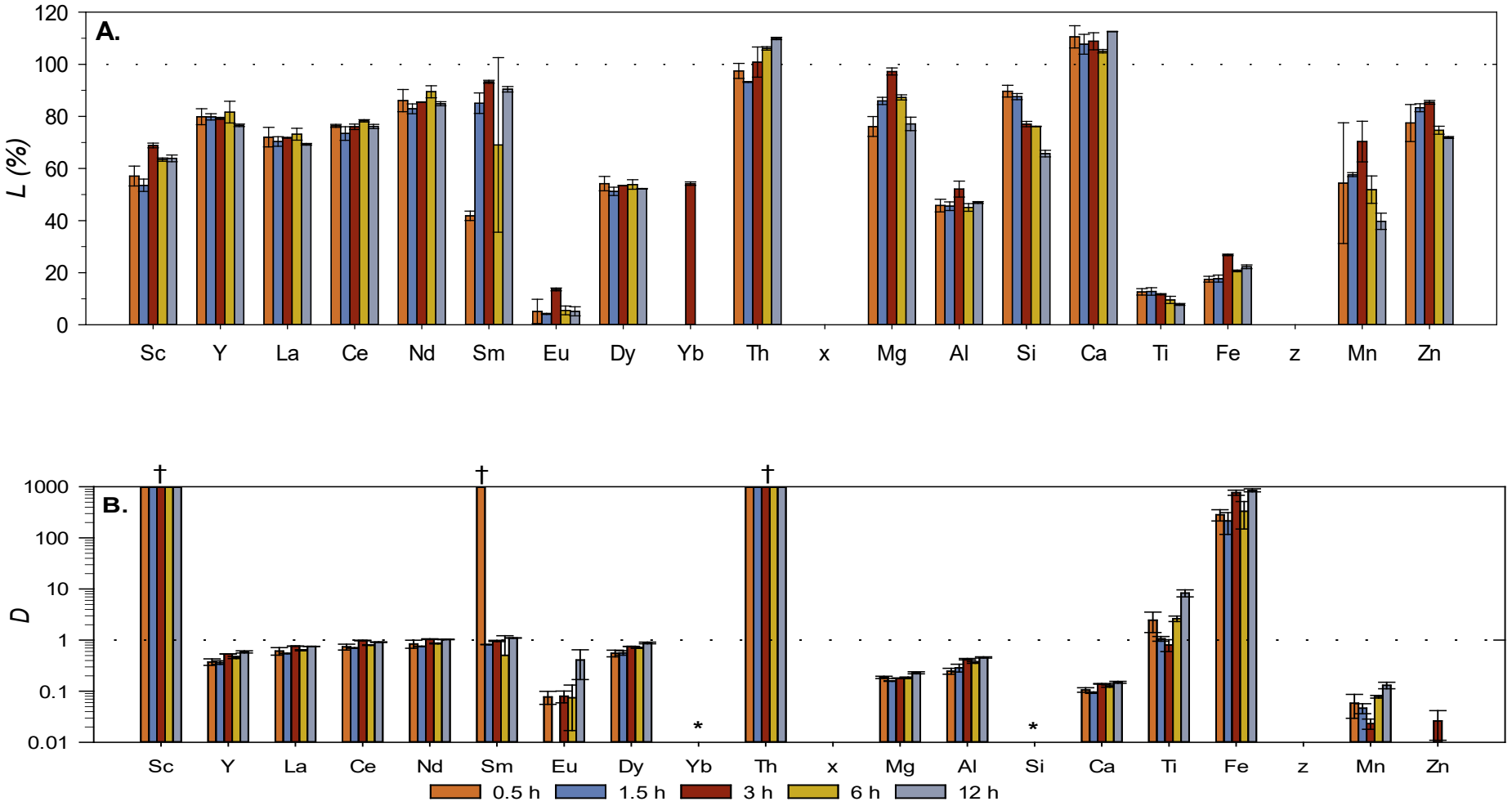

Figure 4.3 Average leaching efficiency L (A) and average distribution D (B) after IL extraction process for CFA-F1 following alkaline pretreatment where IL extraction varied in duration.

*Notes: Error bars indicate standard deviation of duplicate samples. In **(B)**, columns marked with an * indicate zero elements (Ca and Si) were not found in the IL phase. Columns marked with † indicate that the element was not found in the AQ phase. L >100% may be the result of low initial concentration in the solid or potential enrichment in the CFA as the result of alkaline pretreatment.*

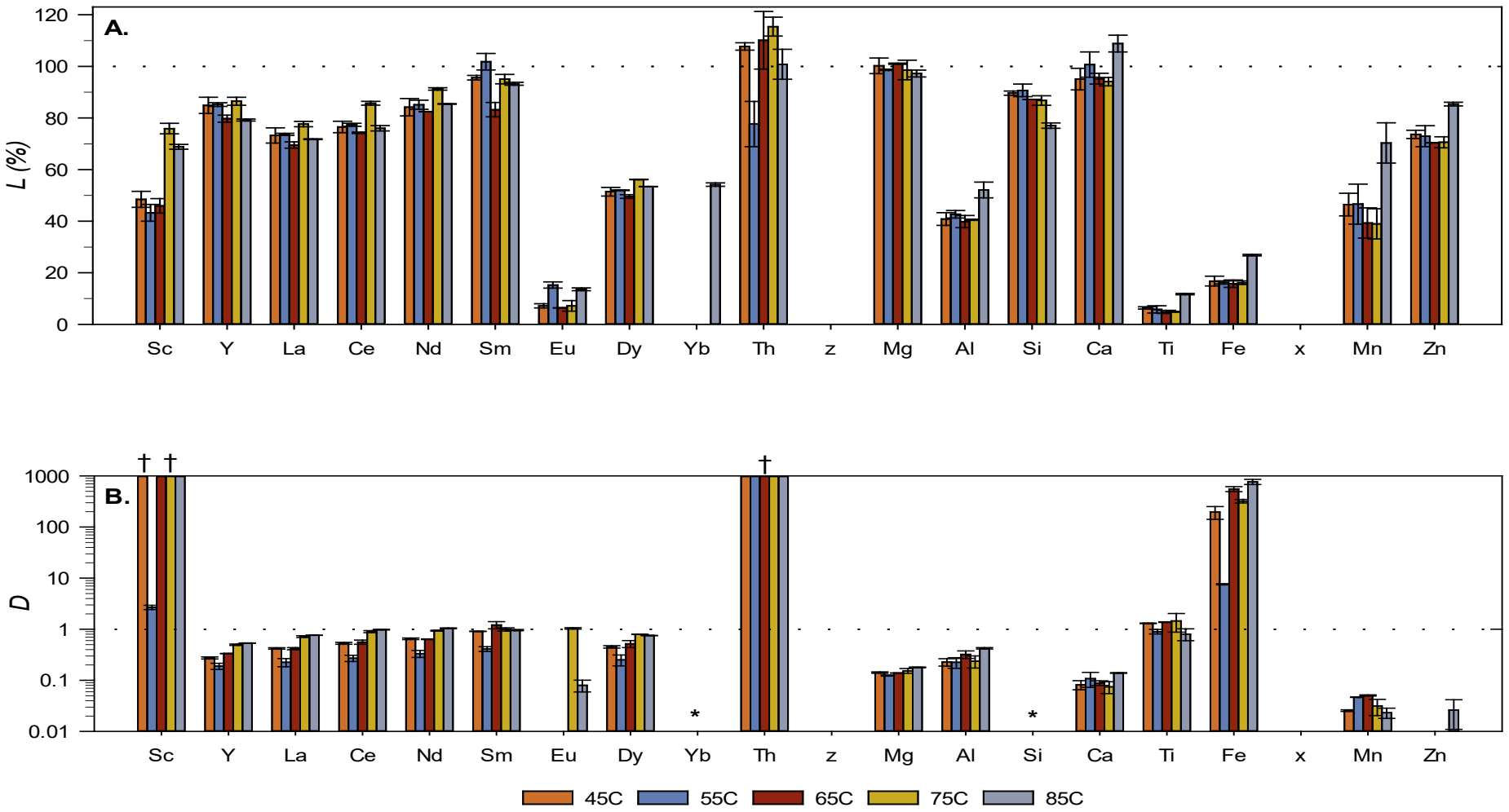

Figure 4.4 Average leaching efficiency L (A) and average distribution D (B) after IL extraction process for CFA-F1 following alkaline pretreatment where IL extraction varied in temperature.

*Notes: Error bars indicate standard deviation of duplicate samples. In **(B)**, columns marked with an * indicate zero elements (Ca and Si) were not found in the IL phase. Columns marked with † indicate that the element was not found in the AQ phase. L >100% may be the result of low initial concentration in the solid or potential enrichment in the CFA as the result of alkaline pretreatment.*

Notably, 45 and 55°C are both near the cloud point of [Hbet][Tf_2N], and it was visually observed during experimentation that the IL-AQ-CFA mixtures did not achieve single-phase between IL and AQ phases. Given the complex mixture of leached cations and anions in the CFA-AQ-IL mixture, it is unclear what the actual cloud point is of the alkaline-pretreated CFA system (and in a mixture containing a black/gray solid like CFA, observing that phenomenon may not be possible with a good degree of accuracy

4.4.5 Process evaluation.

While additional testing must be done before a complete techno-economic assessment is conducted, a general comparison to similar methods is appropriate at this time. Table 4.2 compares the method described in this thesis to other common REE recovery methods

Here, two types of methods are defined: first, extraction methods and separation methods. Extraction methods leach REEs directly from the CFA solid, while separation methods separate REEs from other metals in CFA leachates. Both require intense conditions (high temperature or high pressures, corrosive solutions) either explicitly, to leach out the REEs from the recalcitrant CFA matrix, or implicitly, to generate the CFA leacheate. Generating CFA leacheate often requires nearly complete digestion of the solids either using strong acids (like concentrated HF, HCl, HNO_3, and H_2SO_4) or using alkaline sintering/alkali fusion (high temperature combustion). Though digestion presents high costs in energy consumption and chemical consumption, REE separation often becomes easier, and more techniques become accessible with the elimination of the recalcitrant CFA matrix.

Table 4.2 Process valuation of extracting REEs from CFAs using physicochemical processes.

Feature / Method	This Study 2021[137]	Kashiwakura et al. 2013[27]	Taggart et al. 2016[1]	Banerjee et al. 2021[161]	Smith et. al. 2019[94]	Mondal et al. 2019[162]	Hovey et al. 2021[163]
Key agent	Acidic IL	Dilute acid	Alkali sintering-acid leaching[a]	Dilute acid	Liquid membrane	Impregnated resins	Impregnated resin
Method type	Combo	Extraction	Extraction	Extraction	Separation	Separation	Separation
Application	Solid	Solid	Solid	Solid	Leacheate	Leacheate	Leacheate
Pretreatment required	Mild alkaline[b]	No	No	No	Alkali sintering-acid leaching[c]	Alkali sintering-acid leaching[d]	Acid digestion[e]
Acid consumption	Low	High[f]	High[a]	High[g]	High	High	High
Temperature	75 ºC	80 ºC	450ºC	90 ºC	Ambient	Ambient	Ambient
Pressure	1 atm	1 atm	1 atm	1 atm	1 atm	1 atm	1 atm
Time	3.5 h	2 h	12.5 h[a]	1 h	1 h	18 h	24 h
REE extraction from CFA(s)	High	Low	High	Low	None	None	None
REE – bulk separation	High	None	None	None	High	High	Medium
Final product	REE-rich acidic aq. solution	Impure mixture	Impure mixture	Impure mixture	REE-rich acidic aq. solution	REE-rich acidic aq. solution	REE-rich acidic aq. solution
Additional processing required?	Yes, minor	Yes, major	Yes, major	Yes, major	Yes, minor	Yes, minor	Yes, minor
Recyclable reagents	Yes	No	No	No	No	Yes	Yes

[a] *In alkali sintering, CFA is mixed with solid NaOH and heated for 30 min at 450ºC. After cooling, the solid is mixed with dilute HNO_3 and stirred for 12 h.*[1,94]

[b] *Previous work found that mild alkaline pretreatment was required for Class-F CFAs.*[137]

[c] *Alkali sintering and acid leaching performed following Taggart et al. 2016.*[1]

[d] *Performed in a method similar to Taggart et al. 2016.*[1]

[e] *CFA was leached with concentrated HCl for 22 h. The leacheate was then centrifuged and filtered, and aqueous NaOH was added to increase pH. The leacheate was centrifuged and filtered again.*[163]

[f] *CFA was leached with dilute H_2SO_4.*[27]

[g] *CFA was leached with carboxylic acids (tartaric acid, lactic acid, citric acid, malonic acid, succinic acid).*[161]

4.4.5.1 Comparison with extraction methods.

Extraction methods generally have high REE extraction, but low or no selectivity, generating impure mixtures of REEs and bulk constituents. (Table 4.2). Kashiwakura et al. used dilute H_2SO_4 to leach REEs under similar conditions to the method described here (80°C, 1 atm, 2 h), but only achieved 25-45% REE extraction.[27] Similarly, Banerjee et al. studied various carboxylic acids (90°C, 1 atm, 1 h), and achieved 50-60% extraction.[161] Taggart et al. reported a method using sodium peroxide (Na_2O_2) alkaline sintering, where CFA is mixed with the flux agent and heated to 450°C for 0.5 h. [1] For most CFAs, this achieves high REE extraction (>85%).[1]

In comparison, the [Hbet][Tf_2N]-based method uses the same or lower temperatures, similar pressures, and achieves similar or higher extraction as well as separation. Acid consumption is lower in the IL extraction method as well, conferring another advantage.

4.4.5.2 Comparison with separation methods.

Separation methods have high selectivity, but variable extraction efficiency (Table 4.2). Extraction efficiency depends on both the preceding leacheate generation method and the separation method. Methods are variable in duration, ranging from 1 to 24 h, and temperatures are low (ambient).

Smith et al. investigated two liquid membranes processes relying on di(2-ethylhexyl)phosphoric acid dissolved in kerosene or mineral oil for extraction from CFA leachate.[94] The acid-oil mixture was either configured as a liquid emulsion membrane or as supported liquid emulsion membrane in a resin.[94] Mid-to-high REE extractions were

achieved (50-100%) with 1-h mixing at room temperature.[94] Neither configuration appeared to be recyclable.[94] Somewhat similarly, Mondal et al. used a XAD-7 resin impregnated with TEHDGA (*N,N,N′,N′*-tetrakis-2-ethylhexyldiglycolamide) achieving very high (~100%) extraction efficiencies after 18 h at room temperature.[162] Further, the resin was recycled 10 times and found to maintain performance.[162] Hovey et al. also investigated a resin impregnated with bis(ethylhexyl)amido diethylenetriaminepentaacetic acid (DTPA) and found it to be recyclable over six cycles.[163] This method showed some selectivity for REEs over several bulk elements but achieved variable extractions from CFA leacheate (20-100%).[163]

In comparison to the IL extraction method, these separation methods have similarly high extraction efficiency and separation, and several of them use recyclable reagents. Several take much longer (18-24 h) but require lower temperatures. Critically, however, this assessment neglects these methods' requirement for total digestion of the CFA to be effective, which presents a tremendous disadvantage in energy and chemical consumption.

4.4.6 Process sustainability.

To scale this method to an industrial scale, a number of process improvements must be made to conserve energy, reduce water loss/improve water reuse, recover IL, and use residual CFA solids.

4.4.6.1 Heating methods.

In this study, the CFA-IL-AQ mixture was heated in a traditional oil bath. In several CFA leaching methods, including EPA methods 3051 and 3052 for solid digestion,

programmable microwaves are used to safely achieve specific high pressure and high temperature conditions.[41,42] ILs present a straightforward use case as they absorb microwave radiation very strongly due to their composition: in contrast to aqueous or organic solvent mixtures, they consist entirely of cations and anions.[6,7] Dupont et al. showed that [Hbet][Tf_2N] could be heated to 100°C in under 15 s in a programmable microwave at 100 W (compared to ~25 s for water and >60 s for toluene).[6] Such a strategy could be highly energy-efficient and cost-effective for an industrial scale process.

Further, Dupont et al. determined that heating was not necessarily required for stripping the IL: high REE recovery could be achieved by stripping with HCl at room temperature with intense shaking (1500 rpm) in less than 5 min.

4.4.6.2 Water and IL recovery.

Global water shortages make water minimization and reuse critical to industrial processes. Water is used in both alkaline pretreatment and the IL leaching and stripping process, and while recovery was not specifically investigated in this study, several potential recovery strategies are offered below.

Alkaline pretreatment is a desilication reaction; as a result, water produced from NaOH pretreatment is strongly enriched in Si (10,858 mg/L).[137] Si-enriched solutions can produce a variety of products including zeolites, ceramic powders, precipitated Si, and mesoporous nanosilica.[164-166] In particular, Yan et al. described a method for producing ordered mesoporous nanosilica by treating CFA with concentrated NaOH.[164] If required, other metals including Al and Ca could be removed from solution using common water treatment technologies, including ion exchange (water softener), reverse osmosis, or precipitation.

Such water treatment processes will likely also be sufficient to remove metals from the AQ phase (already REE-poor). The IL should also be recovered from the AQ phase, not only to purify the AQ phase, but to avoid loss of IL. In this study, 1.0 M $NaNO_3$ is used to promote separation of the liquid phases following the Hofmeister series (see Section 4.4.4) and yields IL content in the water phase of 13 wt.%.[7] (Without salt, the water phase contains 14 wt.% of [Hbet][Tf_2N].[7]) While a number of methods can be used to recover the IL from the AQ phase, including adsorbents, electrodialysis or nanofiltration, using a strong salting-out agent like Na_2SO_4 is an inexpensive strategy capable of achieving IL loss in water of <0.15 wt.%.[7] To avoid consumption of Na_2SO_4, an evaporation pond type design could be used, as proposed by Dupont et al.[7]

Previous studies proved the IL could be recycled over multiple cycles, using an aqueous solution (1.5 M HCl) to strip REEs completely from the IL phase.[6,7,9,137] REEs can subsequently be recovered from this acidic solution via electrodeposition, calcination, and/or precipitation. Other studies investigating [Hbet][Tf_2N] use oxalic acid to precipitate REEs directly from the IL phase and achieve similarly high extraction using just a stoichiometric amount of oxalic acid.[6,7] The REE oxalate can be calcined to obtain high purity oxides (>99.9 wt.%).[7] Using oxalic acid or another precipitation agent would reduce water usage without compromising extraction efficiency. Importantly, heating at 70°C for 10 min is required to achieve high stripping efficiency (higher than the conditions described in *4.4.6.1* (room temperature, agitation by shaking)).[6]

4.4.6.3 Beneficial use of residuals.

Following alkaline pretreatment and IL leaching, residual CFA solid remains (Table 4.1). This solid can be filtered from the IL-AQ mixture and potentially applied for reuse. XRD characterization performed previously found that the IL-treated solid is depleted in quartz and amorphous phases but enriched in mullite (Table 2.1).

While determining appropriate beneficial uses is outside the scope of this study, based on the reduced Si content it is likely that the residual is less suitable for concrete or cement applications (one of the most common CFA applications). Comprehensive characterization of the residual solid and an investigation into potential beneficial uses is an important area that merits further research. Managing this solid will close the loop and play an important role in the industrial scalability and sustainability of this process.

4.5 Conclusions

The leaching behavior of 36 elements was investigated in this study. Several REEs (Ce, Dy, La, Nd, Sc, Sm, and Y) achieve high leaching efficiency (>70%) and distribute fairly evenly between AQ and IL phases ($D_{REEs} = 1$). This can be shifted such that $D_{REEs} >> 1$ is achieved by adding additional betaine cation.[137] Sc is of consistently very high recovery ($D_{Sc} \rightarrow \infty$). Of the actinides, U demonstrates poor leaching efficiency and doesn't distribute into the IL phase, while Th achieves high leaching and extracts strongly into the IL phase ($D_{Th} \rightarrow \infty$). Th and Fe are the most significant contaminants in the IL phase. Minor amounts of other bulk constituents (Ti, Mg, Al, and Ca) will also likely need to be removed in subsequent processing. Of the 12 trace elements studied, only three were detected in the AQ and IL phases, indicating very minor leaching and co-contamination. Importantly, co-

contamination is minor compared to other common extraction and separation methods that require total or near total digestion of CFA, thereby leaching all bulk elements in order to extract valuable REEs (Table 4.2).

Of the variables investigated, few impacted REE extraction. The pH of the AQ phase was shown to have negligible effects, though this should be validated for other CFA samples beyond the alkaline-pretreated CFA investigated in this study. Duration also showed negligible effects over the range observed (0.5-12 h). Temperature showed improvements for 75 and 85°C over 45-55°C. Eliminating pH control and shortening leaching duration both contribute to a less complex, easier-to-scale process.

Following these determinations, the [Hbet][Tf_2N] leaching method was compared to other leaching and separation methods described recently in the literature for REE extraction from CFA. Notably, this qualitative analysis shows that most common extraction methods that leach directly from the solid fail to separate REEs from bulk constituents. Separation methods achieve this goal but require total or near total digestion of the CFA, which is chemically and energy intensive.

While [Hbet][Tf_2N] leaching method outperforms other methods in many ways, additional sustainability considerations must be addressed. These goals include to conserve energy, reduce water loss/improve water reuse, recover IL, and use residual CFA solids. This chapter builds off previous work and helps to optimize the process to achieve an industrially viable and economic process.

CHAPTER 5. COMPARISON OF THERMOMORPHIC IONIC LIQUIDS FOR RECOVERY OF RARE EARTH ELEMENTS FROM COAL FLY ASH

5.1 Abstract

Coal fly ash (CFA), generated from burning coal for electricity, is rich in rare earth elements (REEs), elements that play critical roles in a variety of technologies. Extracting REEs from CFA, however, has proven challenging, as most methods consume large amounts of chemicals, create dangerous wastes, and produce impure mixtures of REEs and other bulk elements like Si and Al. Ionic liquids (ILs) have only been recently explored as a sustainable recovery method. One IL, betainium bis(trifluoromethylsulfonyl)imide ([Hbet][Tf_2N]), demonstrated preferential extraction of REEs over bulk elements via a thermomorphic mechanism. In this study, two other thermomorphic ILs, one with a less acidic cation, choline [Chol], and one with a more acidic cation, trimethylammoniumethane hydrogen sulfate ([$N_{111}C_2OSO_3H$]), were compared to [Hbet]. All ILs had the same anion, [Tf_2N]. [Chol][Tf_2N] was broadly unsuccessful at leaching almost all elements from all CFA samples tested, indicating that an additional extractant may be required to achieve high extraction efficiency. [$N_{111}C_2OSO_3H$] was more successful, achieving greater or comparable leaching efficiencies. However, unlike [Hbet][Tf_2N], it did not partition these REEs into the IL phase, but rather into the AQ phase, along with other bulk and trace constituents. Further optimizations should be explored to determine if better selectivity may be induced for [$N_{111}C_2OSO_3H$].

5.2 Introduction

Rare earth elements (REEs) play critical roles in a wide range of industries, from electronics to clean energy to automotive to defense. For many of these applications, there are no substitutes, and most of the world's supply is produced by China. To secure a national supply, the President Joe Biden administration recently issued several executive orders directing federal agencies to investigate potential domestic sources. One potential alternative is coal combustion residuals, specifically coal fly ash (CFA).[19,25,26,84-86,88-92]

REEs are typically found in glass aluminosilicate phases of CFA.[79,93] These phases tend to be very durable and require aggressive methods to extract REEs: strong acids or bases, high temperatures, and/or high pressures.[1,40-42,45,78,79,94] These procedures also digest CFA particles almost completely, generating impure mixtures of REEs and consuming large quantities of chemicals in the process.[1,40-42,45,78,79,94]

Recyclable ionic liquids (ILs) offer another path. ILs consist of an organic cation and anion pair, with much lower freezing points than most common salts.[67,167] Previous work found that REEs could be preferentially extracted from CFA using the IL [Hbet][Tf_2N].[137] The features that make [Hbet][Tf_2N] so attractive include (1) its simple synthesis; (2) its thermomorphic behavior, which can be exploited for extractions from solids and liquid-liquid separations; (3) its ability to be used over multiple cycles, limiting generation of additional wastes; and (4) its ability to selectively solubilize certain metal oxides and not others, directly from solids, limiting the need for further downstream processing. This final highlight is the result of its exchange mechanism, proton exchange (Equation 1):

$$REE_2O_3 + 6\,[Hbet][Tf_2N] \leftrightarrow 2[REE(bet)_3][(Tf_2N)_3] + 3\,H_2O \qquad (4)$$

Upon deprotonation, betaine molecules form zwitterions, which coordinate to the metal cations effectively.[5,65,73] Furthermore, because REEs take the place of a proton in the cationic [Hbet], there is no loss of the cation or anion component of the IL by the exchange reaction (Eq. 1) – a significant advantage of [Hbet][Tf_2N] over other ILs. Cation or anion exchange processes, when occur, ultimately result in the loss of the IL and require additional inputs of these components to remain effective.

There are several ILs that share similar properties to those of [Hbet][Tf_2N]: they are capable of solvating metal ions, display thermomorphic behavior, are simple to synthesize, form biphasic mixtures with water, and rely on proton exchange and form zwitterions when deprotonated. To explore these other thermomorphic ILs for their potential to recover REEs from CFA, two specific ILs with different cations but the same anion, bis(trifluoromethylsulfonyl)imide, were selected for investigation in this study. Compared to [Hbet][Tf_2N], one IL has a more acidic cation (trimethylammoniumethane hydrogen sulfate [Tf_2N], [$N_{111}C_2OSO_3H$][Tf_2N]), and the other is less acidic (choline [Tf_2N], [Chol][Tf_2N]) (Figure 5.1). The ILs' cations play a critical role in the metal complexation process (Eq. 1). The same anion was used in both new ILs due to its efficacy in promoting separation between the IL and water phases and to limit the number of variables in the comparison among the three ILs.

To date, these two ILs have only undergone very limited investigation. [Chol][Tf_2N] has been used for REE extraction from aqueous solutions in conjunction with chelating agents.[168] [$N_{111}C_2OSO_3H$][Tf_2N] has been shown to selectively solvate REEs as ions in aqueous solutions and as well as from REE oxides.[59] A summary of their basic properties can be view below (Table 5.1).

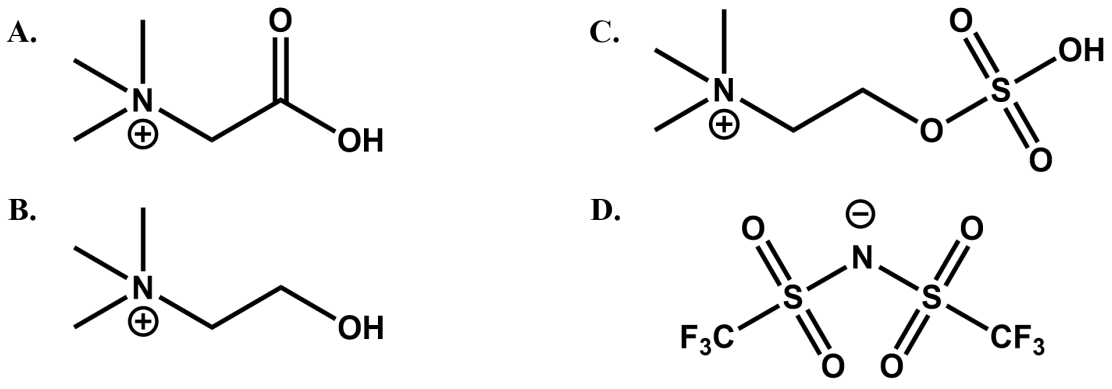

Figure 5.1 (A) betainium cation (B) choline cation (C) $N_{111}C_2OSO_3H$ cation (D) bis(trifluoromethylsulfonyl)imide anion.

Table 5.1 Comparison of acidic IL properties

	[Hbet][Tf_2N]	**[$N_{111}C_2OSO_3H$][Tf_2N]**	**[Chol][Tf_2N]**
Cation / functional group	carboxylic acid	alkyl sulfuric acid	hydroxyl
pKa	2	-3.5	12.5[A]
Charge density	Medium	High	Low
Steric effects	Not bulky	Bulky	Not bulky
Cloud point (ºC)	55	30*[B]	72
Water saturation, RT[C] (wt. %)	13	Miscible without salt	12
Stability (degradation ºC)	200[6]	330[59]	589[169]

[A] *Calculated using ChemDraw Professional Software.*
[B] *Salt must be added in order to achieve biphasic mixture (0.2 M Na_2SO_4 or 1.0 M NaCl).*[59]
[C] *RT indicates room temperature.*

In hydrometallurgy, ILs are a relatively young technology, and applications for complex materials have only recently emerged. The study of the impacts of modification on IL properties has trailed behind these applications, leaving a knowledge gap. Chapter 5 seeks to develop a more comprehensive understanding of the effects of different functional groups on key IL properties and the results will inform future research and applications. The objective of this study was to evaluate the three different ILs ([Hbet][Tf_2N], [Chol][Tf_2N], [$N_{111}C_2OSO_3H$][Tf_2N]) for their efficacy for REE recovery from CFA. Specifically, systematic evaluation was conducted on the leaching behaviors of various

elements in CFA in the IL leaching/stripping system by the three ILs, and the impact of functional group variations on REE recovery from CFA

5.3 Materials and Methods

5.3.1 Chemicals and Characterization.

Most chemicals used can be found in Chapter 2 (see *Section 2.3.1*). Additionally, choline chloride, NaOH, dimethylformamide, and acetone were obtained from Sigma Aldrich. Aqueous bis(trifluoromethylsulfonyl)imide (70-72 wt.%, 99%) was purchased from Iolitec. Chlorosulfonic acid (99%) was purchased from Sigma Aldrich. All chemicals were used without further purification.

5.3.2 CFA Characterization.

Two unweathered CFAs (one Class-C, CFA-C1, and one Class-F, CFA-F1) and one weathered CFA (Class-F, CFA-F2) were comprehensively characterized previously (Table 2.1).[137] Characterization included major oxide and trace element composition and mineral composition quantification. A full description can be found in Chapter 2 (see *Section 2.3.3*).

5.3.3 [Hbet][Tf_2N] Synthesis.

Synthesis was performed as described previously (see *Chapter 2, Section 2.3.2*).[5,65,137]

5.3.4 [Chol][Tf_2N] Synthesis.

[Chol][Tf_2N] synthesis was performed following an existing method.[168] Briefly, choline chloride and lithium bis(trifluoromethylsulfonyl)imide ($LiTf_2N$) were mixed in DI water at room temperature to achieve an equimolar ratio of choline:Tf_2N. After one hour,

the aqueous phase was separated from the IL phase. The IL phase was then washed with small aliquots of cold deionized water to remove chloride impurities. Washing was deemed complete when no chloride impurities were detected using the silver nitrate test. Dry IL was obtained by drying using a vacuum centrifuge at 70°C.

5.3.5 $[N_{111}C_2OSO_3H][Tf_2N]$ Synthesis.

$[N_{111}C_2OSO_3H][Tf_2N]$ synthesis was performed following an existing method.[59] Briefly, choline chloride was dissolved in dimethylformamide in a round-bottom flask with a stir bar in an ice bath for 10 min. While maintaining temperature <5°C, concentrated chlorosulfonic acid was slowly added dropwise into the round-bottom flask while stirring. A concentrated NaOH trap was added to collect produced HCl gas. The mixture was kept cold at 0°C in an ice bath and stirred for 2 h. Afterwards, the mixture was allowed to come to room temperature. Then, the pH was adjusted to pH 10 with concentrated NaOH solution (20 wt.%). The solution was then placed on a rotary evaporator to remove the solvent. A clear mixture with white solids was produced (the zwitterion [N111C2OSO3] and solid NaCl). Solids were removed via filtration on a Buchner funnel with 0.22-μm Whatman filter paper.

In a new round-bottom flask, the zwitterion $[N_{111}C_2OSO_3H]$ was dissolved in DI water. Aqueous bis(trifluoromethylsulfonyl)imide (80 wt. %) was added dropwise at room temperature and stirred for 3 h. The mixture was then subjected to rotary evaporation to remove water.

Acetone was used to wash the residual liquid. A small amount of acetone was added to the round-bottom flask and the mixture was shaken. The mixture was then filtered with

0.22-μm Whatman filter paper to remove solid salts, and the acetone was removed from the solution via rotary evaporation. This process was repeated three times.

The final product, $[N_{111}C_2OSO_3H][Tf_2N]$, was dried via rotary evaporation and was stored dry.

5.3.6 CFA Alkaline Pretreatment.

Alkaline pretreatment was performed as described in a previous study.[137] Briefly, CFA was mixed with 5.0 M NaOH in a ratio of 1:10 g/mL and heated with a stir bar at 85°C for five hours. After cooling, the supernatant was removed for elemental analysis by inductively coupled plasma-optical emission spectrometry (ICP-OES) to quantify loss from pretreatment. The CFA was washed with DI water, filtered, and dried at ~80°C prior to leaching and stripping with the IL.

5.3.7 Leaching and Stripping Experiments.

The leaching and stripping process was described previously (see *Section 2.3.2*).[137]

5.3.7.1 Leaching.

Briefly, CFA, water-saturated IL, and aqueous solution containing 1.0 M $NaNO_3$ were added to a small vial to achieve a liquid-liquid (IL:AQ) mass ratio of 1:1 and solid-liquid ratio of 12.5:1.0 (mg:g). The addition of $NaNO_3$ was to promote IL and AQ phase separation.[6,7,60,68,69] The pH of the $NaNO_3$ solution was adjusted to 3.50 ± 0.05 with HNO_3 and NaOH prior to mixing.[6,7,69] The vial was heated with a stir bar to 85°C for three hours. Then, the vial was cooled to room temperature, then stored at 4°C overnight. After

sufficient cooling, the AQ phase was easily separated and prepared for analysis by ICP-OES. The IL phase was transferred to a new vial for stripping. The CFA was washed with DI water, filtered, and dried at ~80°C.

5.3.7.2 Stripping.

Briefly, 1.5 M HCl aqueous solution was added to the new IL-containing vial to achieve a liquid-liquid (IL:HCl) mass ratio of 1:1. The vial was heated in an oil bath with a stir bar to 85°C for 1.5 hours. Then, the vial was cooled to room temperature, then stored at 4°C overnight. The HCl aqueous phase was then separated and prepared for ICP-OES.

5.3.8 Quantification of Extraction and Separation.

Elements may be leached from the CFA by the pretreatment (M_{PT}) step, and by the IL/water extraction into the AQ phase (M_{AQ}) and the IL phase (M_{IL}), respectively, where M represents mass. The mass in the IL phase was determined by that measured in the stripping phase. Previous studies have demonstrated that all elements are completely stripped by the stripping phase from the IL using HCl at concentrations ≥ 1.0 M.[68,69]

To quantify the extraction and separation of elements from CFA, three parameters were identified: leaching efficiency (*L*), distribution coefficient (*D*), and recovery efficiency (*R*). Leaching efficiency, *L,* shows total extraction of each element into all phases from the starting CFA (M_{total}) (Equation 2).

$$L\ (in\ \%) = \frac{M_{PT}\ +\ M_{AQ}\ +.\ M_{IL}}{M_{Total}} \qquad (2)$$

Distribution coefficient, *D,* reflects an element's preference for the IL phase over the AQ phase as the ratio between the element's mass in the IL phase and its mass in the AQ phase (Equation 3):

$$D = \frac{M_{IL}}{M_{AQ}} \tag{3}$$

Recovery efficiency, *R,* represents the combined effect of leaching efficiency and distribution. When M_{PT} is negligible, *R* can be computed using Equations 2 and 3, generating Equation 5:

$$R\ (\%) = \frac{M_{IL}}{M_{Total}} \cong \frac{L \cdot D}{1 + D} \tag{5}$$

M_{PT} is negligible for all REEs and low for Al, Ca, and Fe for all CFAs.[137] For REEs, high *L*, *D* and *R* are desired. For the bulk and trace elements, low *L*, *D,* and *R* are desired.

All trials were performed in duplicate. All calculations were performed for each element in each trial then averaged.

5.4 Results and Discussion

5.4.1 Characterization of CFA.

The three CFAs investigated in this study displayed all expected physical and morphological properties, which have been discussed in depth in a previous study (see *Chapter 2, Section 2.4.1*).[104,137] Only alkaline pretreated CFA was investigated in this study due to the increased L_{REEs}.[137]

5.4.2 Broad elemental survey of alkaline pretreated CFA using [Chol][Tf_2N].

To comprehensively study leaching on CFA using [Chol][Tf_2N], a total of 26 elements were measured in the alkaline pretreatment, AQ, and HCl stripping phases (Table 5.2, Table 5.3, Table 5.4). This included nine REEs (Sc and Y and seven of the lanthanides; Pm was excluded as it is extraordinarily rare) so as to better understand REE behavior and determine if recovery of other REEs is viable. Only REEs listed on the 1633C NIST certificate were included. Two radioactive actinides commonly found in CFA, U and Th, were also studied as they present risks for disposal as contaminants of concern. Additional potential contaminants of concern investigated include As, Cd, Cr, Pb, and Se. Bulk constituents included Al, Ca, Fe, Si, Mg and Ti, and minor constituents included the aforementioned contaminants of concern as well as Cu, Mn, Ni, V, and Zn.

Table 5.2 Partitioning from CFA-F1 using [Chol][Tf_2N]

Element	Total (mg/kg)[a]	PT Phase %	AQ Phase %	IL Phase %	Residual %
REEs					
Sc	37.6 ± 0.6	0.0 ± 0.0	0.0 ± 0.0	0.0 ± 0.0	100.0 ± 0.0
Y[c]	105.2	0.0 ± 0.0	0.0 ± 0.0	0.0 ± 0.0	100.0 ± 0.0
La	87.0 ± 2.6	0.0 ± 0.0	0.0 ± 0.0	0.0 ± 0.0	100.0 ± 0.0
Ce	180	0.0 ± 0.0	0.0 ± 0.0	0.0 ± 0.0	100.0 ± 0.0
Nd	87	0.0 ± 0.0	0.0 ± 0.0	0.0 ± 0.0	100.0 ± 0.0
Sm	19	0.0 ± 0.0	0.0 ± 0.0	0.0 ± 0.0	100.0 ± 0.0
Eu	4.67 ± 0.07	0.0 ± 0.0	0.0 ± 0.0	0.0 ± 0.0	100.0 ± 0.0
Dy	18.7 ± 0.3	0.0 ± 0.0	0.0 ± 0.0	0.0 ± 0.0	100.0 ± 0.0
Yb	7.7	0.0 ± 0.0	0.0 ± 0.0	0.0 ± 0.0	100.0 ± 0.0
Actinides					
Th	23.0 ± 0.4	0.0 ± 0.0	0.0 ± 0.0	0.0 ± 0.0	100.0 ± 0.0
U	9.25 ± 0.45	0.0 ± 0.0	0.0 ± 0.0	0.0 ± 0.0	100.0 ± 0.0
Bulk constituents (wt.%)					
Mg	0.50 ± 0.052	0.0 ± 0.0	0.0 ± 0.0	0.5 ± 0.7	99.5 ± 0.7
Al	13.28 ± 0.61	1.7 ± 0.2	0.0 ± 0.0	0.3 ± 0.4	98.0 ± 0.4
Si	21.30 ± 0.57	51.0 ± 9.8	0.0 ± 0.0	0.1 ± 0.2	48.9 ± 0.2
Ca	1.37 ± 0.04	1.2 ± 0.3	2.4 ± 0.5	1.9 ± 0.9	94.6 ± 0.4
Ti	0.72 ± 0.03	0.4 ± 0.1	0.0 ± 0.0	0.0 ± 0.0	99.6 ± 0.0
Fe	10.49 ± 0.39	0.4 ± 0.1	0.0 ± 0.0	0.2 ± 0.3	99.3 ± 0.3
Trace constituents					
V	286.2 ± 7.9	N/A	0.0 ± 0.0	0.0 ± 0.0	100.0 ± 0.0
Cr	258 ± 6	N/A	0.0 ± 0.0	0.0 ± 0.0	100.0 ± 0.0
Mn	240.2 ± 3.4	0.3 ± 0.2	0.0 ± 0.0	0.0 ± 0.0	99.7 ± 0.0
Ni	132 ± 10	N/A	0.0 ± 0.0	0.0 ± 0.0	100.0 ± 0.0
Cu	173.7 ± 6.4	0.0 ± 0.0	0.0 ± 0.0	0.0 ± 0.0	100.0 ± 0.0
Zn	235 ± 14	61.3 ± 7.2	0.0 ± 0.0	0.0 ± 0.0	38.7 ± 0.0
As	186.2 ± 3.0	N/A	22.9 ± 3.4	0.0 ± 0.0	77.1 ± 3.4
Se	13.9 ± 0.5	N/A	295.1 ± 69.5	0.0 ± 0.0	0.0 ± 0.0
Cd	0.76 ± 0.01	N/A	0.0 ± 0.0	0.0 ± 0.0	100.0 ± 0.0
Pb	95.2 ± 2.5	N/A	0.0 ± 0.0	0.0 ± 0.0	100.0 ± 0.0

Note 1: No shading indicates 0-1% partitioning; the light shade indicates 1-10%; the medium shade indicates 10-50%; the medium dark shade indicates 50-80%; and the dark shade indicates 80-100%.
Note 2: N/A indicates data are not available.
Note 3: Extraction efficiencies >100% may be the result of low initial concentration in the solid or potential enrichment in the CFA as the result of alkaline pretreatment.

Table 5.3 Partitioning from CFA-F2 using [Chol][Tf_2N]

Element	Total (mg/kg)[a]	PT Phase %	AQ Phase %	IL Phase %	Residual %[b]
REEs					
Sc	39.7	0.0 ± 0.0	0.0 ± 0.0	0.0 ± 0.0	100.0 ± 0.0
Y	91.4	0.0 ± 0.0	0.0 ± 0.0	0.0 ± 0.0	100.0 ± 0.0
La	86.5	0.0 ± 0.0	0.0 ± 0.0	0.0 ± 0.0	100.0 ± 0.0
Ce	169.1	0.0 ± 0.0	0.0 ± 0.0	0.0 ± 0.0	100.0 ± 0.0
Nd	95.5	0.0 ± 0.0	0.0 ± 0.0	0.0 ± 0.0	100.0 ± 0.0
Sm	N/A	N/A	0.0 ± 0.0	0.0 ± 0.0	High[c]
Eu	3.0	0.0 ± 0.0	0.0 ± 0.0	0.0 ± 0.0	100.0 ± 0.0
Dy	14.3	0.0 ± 0.0	0.0 ± 0.0	0.0 ± 0.0	100.0 ± 0.0
Yb	N/A	N/A	0.0 ± 0.0	0.0 ± 0.0	High[c]
Actinides					
Th	N/A	N/A	0.0 ± 0.0	0.0 ± 0.0	High
U	N/A	N/A	0.0 ± 0.0	0.0 ± 0.0	High
Bulk constituents (wt.%)					
Mg	N/A	N/A	0.0 ± 0.0	0.0 ± 0.0	High[c]
Al	16.1	1.2 ± 0.2	0.0 ± 0.0	0.0 ± 0.0	98.8 ± 0.0
Si	24.5	41.3 ± 2.9	0.0 ± 0.0	0.0 ± 0.0	58.7 ± 0.0
Ca	11.4	0.0 ± 0.0	2.6 ± 0.1	0.4 ± 0.5	97.0 ± 0.5
Ti	N/A	N/A	0.0 ± 0.0	0.0 ± 0.0	High[c]
Fe	6.0	0.6 ± 0.1	0.0 ± 0.0	0.0 ± 0.0	99.4 ± 0.0
Trace constituents					
V	N/A	N/A	0.0 ± 0.0	0.0 ± 0.0	High[c]
Cr	N/A	N/A	0.0 ± 0.0	0.0 ± 0.0	High[c]
Mn	N/A	N/A	0.0 ± 0.0	0.0 ± 0.0	High[c]
Ni	N/A	N/A	0.0 ± 0.0	0.0 ± 0.0	High[c]
Cu	N/A	N/A	0.0 ± 0.0	0.0 ± 0.0	High[c]
Zn	N/A	N/A	0.0 ± 0.0	0.0 ± 0.0	High[c]
As	N/A	N/A	Moderate[c]	0.0 ± 0.0	Moderate[c]
Se	N/A	N/A	High[c]	0.0 ± 0.0	Low[c]
Cd	N/A	N/A	0.0 ± 0.0	0.0 ± 0.0	High[c]
Pb	N/A	N/A	0.0 ± 0.0	0.0 ± 0.0	High[c]

[a] *Total determined by total digestion (see Chapter 2, Section 2.3.3).*

[b] *Residual calculated as* $(M_{Total} - M_{PT} - M_{AQ} - M_{IL})/ M_{Total} \times 100 =$ *Residual %*

[c] *As determined compared to concentrations in SRM 2691, a standard Class-C CFA.*

Note 1: No shading indicates 0-1% partitioning; the light shade indicates 1-10%; the medium shade indicates 10-50%; the medium dark shade indicates 50-80%; and the dark shade indicates 80-100%.

Note 2: N/A indicates data are not available.

Table 5.4 Partitioning from CFA-C1 using [Chol][Tf_2N]

Element	Total (mg/kg)[a]	PT Phase %	AQ Phase %	IL Phase %	Residual %[b]
REEs					
Sc	20.6	0.0 ± 0.0	0.0 ± 0.0	0.0 ± 0.0	100.0 ± 0.0
Y	43.7	0.0 ± 0.0	0.0 ± 0.0	0.0 ± 0.0	100.0 ± 0.0
La	53.3	0.0 ± 0.0	0.0 ± 0.0	0.0 ± 0.0	100.0 ± 0.0
Ce	89.8	0.0 ± 0.0	0.0 ± 0.0	0.0 ± 0.0	100.0 ± 0.0
Nd	55.5	0.0 ± 0.0	0.0 ± 0.0	0.0 ± 0.0	100.0 ± 0.0
Sm	N/A	N/A	0.0 ± 0.0	0.0 ± 0.0	High[c]
Eu	2.0	0.0 ± 0.0	0.0 ± 0.0	0.0 ± 0.0	100.0 ± 0.0
Dy	7.3	0.0 ± 0.0	0.0 ± 0.0	0.0 ± 0.0	100.0 ± 0.0
Yb	N/A	N/A	0.0 ± 0.0	0.0 ± 0.0	High[c]
Actinides					
Th	N/A	N/A	0.0 ± 0.0	0.0 ± 0.0	High[c]
U	N/A	N/A	0.0 ± 0.0	0.0 ± 0.0	High[c]
Bulk constituents (wt.%)					
Mg	N/A	N/A	0.0 ± 0.0	Low[c]	High[c]
Al	6.3	7.2 ± 1.0	0.1 ± 0.1	0.3 ± 0.3	92.4 ± 0.2
Si	18.0	6.5 ± 0.7	0.0 ± 0.0	0.0 ± 0.0	93.5 ± 0.0
Ca	18.0	0.0 ± 0.0	2.1 ± 0.3	0.4 ± 0.3	97.5 ± 0.0
Ti	N/A	N/A	0.0 ± 0.0	0.0 ± 0.0	High[c]
Fe	3.6	0.4 ± 0.1	0.0 ± 0.0	0.2 ± 0.1	99.5 ± 0.1
Trace constituents					
V	N/A	N/A	High[c]	0.0 ± 0.0	Low[c]
Cr	N/A	N/A	0.0 ± 0.0	0.0 ± 0.0	High[c]
Mn	N/A	N/A	0.0 ± 0.0	0.0 ± 0.0	High[c]
Ni	N/A	N/A	0.0 ± 0.0	0.0 ± 0.0	High[c]
Cu	N/A	N/A	0.0 ± 0.0	0.0 ± 0.0	High[c]
Zn	N/A	N/A	0.0 ± 0.0	0.0 ± 0.0	High[c]
As	N/A	N/A	Moderate[c]	0.0 ± 0.0	Moderate[c]
Se	N/A	N/A	High[c]	0.0 ± 0.0	Low[c]
Cd	N/A	N/A	0.0 ± 0.0	0.0 ± 0.0	High[c]
Pb	N/A	N/A	0.0 ± 0.0	0.0 ± 0.0	High[c]

[a] *Total determined by total digestion (see Chapter 2, Section 2.3.3).*
[b] *Residual calculated as* $(M_{Total} - M_{PT} - M_{AQ} - M_{IL})/ M_{Total} \times 100 =$ *Residual %*
[c] *As determined compared to concentrations in SRM 2691, a standard Class-C CFA.*
Note 1: No shading indicates 0-1% partitioning; the light shade indicates 1-10%; the medium shade indicates 10-50%; the medium dark shade indicates 50-80%; and the dark shade indicates 80-100%.
Note 2: N/A indicates data are not available.

Of note, some data, including concentrations in pretreatment liquid and total concentration in the solid CFA, are not available for CFA-F2 and CFA-C1. Estimates are provided based on NIST certificate data (SRM 1633c, a standard Class-F CFA and SRM

2691, a standard Class-C CFA, respectively). CFA-F1, the 1633c CFA, is considered the gold standard for the purpose of this study.

5.4.2.1 REEs and actinides.

No REEs or actinides were detected in the AQ or IL phases for CFA-F1, CFA-F2, and CFA-C1 (Table 5.2, Table 5.3, Table 5.4). Previous work determined that REEs are not leached during alkaline pretreatment.[137] This indicates that REEs remain locked in the CFA aluminosilicate glass phases throughout the entire process. Due to their presence in these durable phases, REEs require strong acids for extraction. Class-F CFAs further require alkaline pretreatment for successful extraction.[137] Class-C CFAs tend to be less recalcitrant and do not require alkaline pretreatment.[137]

Previously, high REE extraction was achieved using [Hbet][Tf_2N], an acidic IL (pKa = 2).[137] Additionally, [Hbet][Tf_2N] contains a carboxylic acid group (Figure 5.1), which is known to complex with REEs.[137] In contrast, [Chol][Tf_2N] has only an alcohol group, which has an estimated pKa of 12.5, close to that of water (14.0).

5.4.2.2 Bulk elements.

Overwhelmingly, bulk and trace elements were not detected or were found in very low concentrations in the AQ or IL phases for CFA-F1, CFA-F2, and CFA-C1 (Table 5.2, Table 5.3, Table 5.4). Ca was found in both phases for all CFAs, though notably in higher concentrations in the AQ phase than in the IL phase (~2.4% vs 0.9%). Ca is present in CFA in many modes, both as Ca-minerals like lime, anhydrite, and calcite, and also dispersed in

the glass phase.[140] Regardless of condition, studies have shown Ca to be the most largely released cation, with water-extractable amounts ranging from 7-14%.[48,140]

Other bulk elements (Mg, Al, Si, and Fe) were found in very low concentrations (< ~1 wt. %) in the IL phase for the unweathered CFAs, CFA-F1 and CFA-C1 (Table 5.2, Table 5.3, Table 5.4), and were not detected in the IL for the weathered CFA-F2 sample. Weathered CFA differs in mineralogy from unweathered CFA. As a result of wet storage in ash impoundments, CFA is weathered by contact with water.[106] This hydration has two major effects: (1) new mineral phases develop, including carbonates, and amorphous clays (from glass hydrolysis); and (2) alkaline metals are leached.[106] Accessible elements are thus leached and lost to weathering prior to IL leaching. It is hypothesized that the remaining bulk elements are found in more durable phases, unable to be extricated in the weakly extracting environment presented by [Chol][Tf_2N].

5.4.2.3 Trace elements.

Trace element composition was not available for CFA-F2 and CFA-C1; estimates were determined based on NIST certificate data (SRM 1633c, a standard Class-F CFA and SRM 2691, a standard Class-C CFA, respectively).

Most trace elements were not detected in the AQ or IL phases (Table 5.2, Table 5.3, Table 5.4). As and Se present exceptions: both were found in the AQ phase in moderate and high concentrations, respectively. These concentrations are estimates for CFA-F2 and CFA-C1. As is known to be surface-sorbed to CFA particles as the sparingly soluble oxyanion arsenate.[140] Up to 52% of As is water-extractable, with maximum solubility displayed in the pH 7-11 range.[140] Similarly, Se also condenses on the surface of CFA

particles, sometimes forming Ca compounds (like $CaSeO_3$).[140] Se solubility also peaks at alkaline pH (pH 10-12).[140]

V was also detected in the AQ phase for CFA-C1 and is estimated to be a high proportion of total V. Finally, V may be surface-sorbed, found in glass phases, or found in magnetite mineral phases.[140] Up to 4% of V is water leachable.[140]

5.4.2.4 Summary of [Chol][Tf_2N].

Overall, [Chol][Tf_2N] achieved low extraction rate for almost all elements. No REEs or actinides were extracted, and bulk element extraction was very low (under 1% for almost all elements except Ca, at 2.4% in the AQ phase).

Importantly, most extractions were into the AQ phase (including As, Se, and V), not the IL phase. If REEs could be extracted into the IL phase, co-extraction of actinides, bulk elements, and trace may be minimal. This indicates that the IL may be appropriate as a solvent, where a separate extractant is added to complex with REEs. Onghena et al. achieved high extractions of Nd from aqueous solutions using choline hexafluoroacetylacetone, another choline-based IL, dissolved in [Chol][Tf_2N].[168] Because [Chol][Tf_2N] is not very acidic, it can be used in combination with acidic extractants, unlike [Hbet][Tf_2N].[168]

5.4.3 Broad elemental survey of alkaline pretreated CFA using [$N_{111}C_2OSO_3H$][Tf_2N].

To comprehensively study leaching on CFA using [$N_{111}C_2OSO_3H$][Tf_2N], a total of 26 elements were measured in the alkaline pretreatment, AQ, and HCl stripping phases (Table 5.5, Table 5.6, and Table 5.7). The same elements were used as described in Section 5.4.2.

Table 5.5 Partitioning from CFA-F1 using $[N_{111}C_2OSO_3H][Tf_2N]$.

Element	Total (mg/kg)[a]	PT Phase %	AQ Phase %	IL Phase %	Residual %
REEs					
Sc	37.6 ± 0.6	0.0 ± 0.0	66.5 ± 4.6	21.6 ± 2.5	11.9 ± 7.0
Y[c]	105.2	0.0 ± 0.0	99.1 ± 10.0	6.3 ± 0.9	1.1 ± 1.6
La	87.0 ± 2.6	0.0 ± 0.0	45.9 ± 3.5	4.0 ± 0.5	50.1 ± 4.0
Ce	180	0.0 ± 0.0	63.4 ± 5.3	3.5 ± 0.8	33.1 ± 6.0
Nd	87	0.0 ± 0.0	97.9 ± 8.8	7.4 ± 0.8	0.8 ± 1.1
Sm	19	0.0 ± 0.0	102.7 ± 9.8	10.2 ± 0.9	0.0 ± 0.0
Eu	4.67 ± 0.07	0.0 ± 0.0	62.4 ± 5.3	0.0 ± 0.0	37.6 ± 5.3
Dy	18.7 ± 0.3	0.0 ± 0.0	81.8 ± 5.3	7.0 ± 0.8	11.1 ± 6.1
Yb	7.7	0.0 ± 0.0	107.3 ± 4.5	4.3 ± 1.2	0.0 ± 0.0
Actinides					
Th	23.0 ± 0.4	0.0 ± 0.0	102.3 ± 5.3	46.2 ± 3.1	0.0 ± 0.0
U	9.25 ± 0.45	0.0 ± 0.0	0.0 ± 0.0	0.0 ± 0.0	100.0 ± 0.0
Bulk constituents (wt.%)					
Mg	0.50 ± 0.052	0.0 ± 0.0	79.8 ± 8.6	3.4 ± 0.4	16.8 ± 9.0
Al	13.28 ± 0.61	1.7 ± 0.2	43.6 ± 5.7	1.1 ± 0.1	53.5 ± 5.8
Si	21.30 ± 0.57	51.0 ± 9.8	29.2 ± 1.1	0.0 ± 0.0	19.9 ± 1.1
Ca	1.37 ± 0.04	1.2 ± 0.3	93.4 ± 11.2	5.0 ± 0.3	0.5 ± 11.6
Ti	0.72 ± 0.03	0.4 ± 0.1	14.4 ± 0.4	1.0 ± 0.0	84.2 ± 0.4
Fe	10.49 ± 0.39	0.4 ± 0.1	14.1 ± 0.9	6.9 ± 0.5	78.6 ± 1.4
Trace constituents					
V	286.2 ± 7.9	N/A	2.8 ± 0.4	0.0 ± 0.0	97.2 ± 0.4
Cr	258 ± 6	N/A	0.0 ± 0.0	0.0 ± 0.0	100.0 ± 0.0
Mn	240.2 ± 3.4	0.3 ± 0.2	72.3 ± 5.2	3.7 ± 0.3	23.7 ± 5.5
Ni	132 ± 10	N/A	36.6 ± 11.1	0.0 ± 0.0	63.4 ± 11.1
Cu	173.7 ± 6.4	0.0 ± 0.0	135.8 ± 33.0	11.7 ± 2.4	0.0 ± 0.0
Zn	235 ± 14	61.3 ± 7.2	27.8 ± 0.2	0.0 ± 0.0	11.0 ± 0.2
As	186.2 ± 3.0	N/A	19.6 ± 3.8	0.0 ± 0.0	80.4 ± 3.8
Se	13.9 ± 0.5	N/A	134.0 ± 0.0	0.0 ± 0.0	0.0 ± 0.0
Cd	0.76 ± 0.01	N/A	0.0 ± 0.0	0.0 ± 0.0	100.0 ± 0.0
Pb	95.2 ± 2.5	N/A	0.0 ± 0.0	0.0 ± 0.0	100.0 ± 0.0

Note: No shading indicates 0-1% partitioning; the light shade indicates 1-10%; the medium shade indicates 10-50%; the medium dark shade indicates 50-80%; and the dark shade indicates 80-100%.

Table 5.6 Partitioning from CFA-F2 using $[N_{111}C_2OSO_3H][Tf_2N]$.

Element	Total (mg/kg)[a]	PT Phase %	AQ Phase %	IL Phase %	Residual %
REEs					
Sc	39.7	0.0 ± 0.0	73 ± 3.3	18.6 ± 1.6	8.5 ± 1.7
Y[c]	91.4	0.0 ± 0.0	101.1 ± 8.9	5.9 ± 0.4	0.0 ± 0.0
La	86.5	0.0 ± 0.0	47.3 ± 1.2	3.6 ± 0.4	49.1 ± 0.8
Ce	169.1	0.0 ± 0.0	60.3 ± 2.2	2.3 ± 0.1	37.4 ± 2.1
Nd	95.5	0.0 ± 0.0	78.4 ± 3.1	5.0 ± 0.5	16.7 ± 2.6
Sm	N/A	N/A	High[c]	Low[c]	Low[c]
Eu	3.0	0.0 ± 0.0	66.0 ± 0.2	0.0 ± 0.0	34.0 ± 0.2
Dy	14.3	0.0 ± 0.0	88.7 ± 2.8	7.1 ± 0.5	4.1 ± 3.4
Yb	N/A	N/A	High[c]	2.9 ± 0	Low[c]
Actinides					
Th	N/A	N/A	High[c]	Moderate[c]	Low[c]
U	N/A	N/A	0.0 ± 0.0	0.0 ± 0.0	High[c]
Bulk constituents (wt.%)					
Mg	N/A	N/A	Moderate[c]	Low[c]	Moderate[c]
Al	16.1	1.2 ± 0.2	31.7 ± 1.2	0.7 ± 0.1	66.4 ± 1.1
Si	24.5	41.3 ± 2.9	23.4 ± 0.8	0.0 ± 0.0	35.3 ± 0.8
Ca	11.4	0.0 ± 0.0	65.5 ± 4.7	3.2 ± 0.0	31.3 ± 4.7
Ti	N/A	N/A	Moderate[c]	Low[c]	Moderate[c]
Fe	6.0	0.6 ± 0.1	18.9 ± 0.4	6.6 ± 0.4	73.9 ± 0
Trace constituents					
V	N/A	N/A	Low[c]	Low[c]	High[c]
Cr	N/A	N/A	0.0 ± 0.0	0.0 ± 0.0	High[c]
Mn	N/A	N/A	Moderate[c]	Low[c]	Moderate[c]
Ni	N/A	N/A	Moderate[c]	0.0 ± 0.0	Moderate[c]
Cu	N/A	N/A	High[c]	Low[c]	Low[c]
Zn	N/A	N/A	Moderate[c]	Low[c]	Moderate[c]
As	N/A	N/A	Low[c]	0.0 ± 0.0	High[c]
Se	N/A	N/A	0.0 ± 0.0	0.0 ± 0.0	High[c]
Cd	N/A	N/A	0.0 ± 0.0	High[c]	Low[c]
Pb	N/A	N/A	Moderate[c]	0.0 ± 0.0	Moderate[c]

[a] *Total determined by total digestion (see Chapter 2, Section 2.3.3).*

[b] *Residual calculated as* $(M_{Total} - M_{PT} - M_{AQ} - M_{IL})/ M_{Total} \times 100 =$ *Residual %*

[c] *As determined compared to concentrations in SRM 2691, a standard Class-C CFA.*

Note 1: No shading indicates 0-1% partitioning; the light shade indicates 1-10%; the medium shade indicates 10-50%; the medium dark shade indicates 50-80%; and the dark shade indicates 80-100%. Note 2: N/A indicates data are not available.

Table 5.7 Partitioning from CFA-C1 using $[N_{111}C_2OSO_3H][Tf_2N]$.

Element	Total (mg/kg)[a]	PT Phase %	AQ Phase %	IL Phase %	Residual %[b]
REEs					
Sc	20.6	0.0 ± 0.0	51.8 ± 4.5	46.2 ± 1.0	15.2 ± 5.9
Y	43.7	0.0 ± 0.0	40.8 ± 3	8.5 ± 0.5	50.6 ± 3.5
La	53.3	0.0 ± 0.0	9.9 ± 0.5	7.6 ± 0.4	86.7 ± 1.0
Ce	89.8	0.0 ± 0.0	10.3 ± 0.4	4.4 ± 0.3	88.7 ± 0.9
Nd	55.5	0.0 ± 0.0	15.0 ± 0.5	3.3 ± 0.3	80.6 ± 0.8
Sm	N/A	N/A	Moderate[c]	Low[c]	Moderate[c]
Eu	2.0	0.0 ± 0.0	0.0 ± 0.0	0.0 ± 0.0	100.0 ± 0.0
Dy	7.3	0.0 ± 0.0	22.1 ± 0.1	3.5 ± 0.2	70.3 ± 0.3
Yb	N/A	N/A	Moderate[c]	Low[c]	Moderate[c]
Actinides					
Th	N/A	N/A	Moderate[c]	Moderate[c]	Low[c]
U	N/A	N/A	0.0 ± 0.0	0.0 ± 0.0	High[c]
Bulk constituents (wt.%)					
Mg	N/A	N/A	Moderate[c]	Low[c]	Moderate[c]
Al	6.3	7.2 ± 1.0	84.9 ± 2	5.6 ± 0.8	2.4 ± 2.8
Si	18.0	6.5 ± 0.7	8.2 ± 0.8	0.0 ± 0.0	85.2 ± 0.8
Ca	18.0	0.0 ± 0.0	9.1 ± 0.3	1.1 ± 0.4	89.8 ± 0.1
Ti	N/A	N/A	Low[c]	0.0 ± 0.0	High[c]
Fe	3.6	0.4 ± 0.1	35.5 ± 0.5	16.3 ± 1.5	47.8 ± 2.0
Trace constituents					
V	N/A	N/A	Moderate[c]	0.0 ± 0.0	Moderate[c]
Cr	N/A	N/A	0.0 ± 0.0	0.0 ± 0.0	High[c]
Mn	N/A	N/A	Moderate[c]	Low[c]	Moderate[c]
Ni	N/A	N/A	Moderate[c]	0.0 ± 0.0	Moderate[c]
Cu	N/A	N/A	Moderate[c]	Low[c]	Moderate[c]
Zn	N/A	N/A	Moderate[c]	0.0 ± 0.0	Moderate[c]
As	N/A	N/A	High[c]	0.0 ± 0.0	Low[c]
Se	N/A	N/A	High[c]	0.0 ± 0.0	Low[c]
Cd	N/A	N/A	0.0 ± 0.0	0.0 ± 0.0	High[c]
Pb	N/A	N/A	0.0 ± 0.0	0.0 ± 0.0	High[c]

Note 1: No shading indicates 0-1% partitioning; the light shade indicates 1-10%; the medium shade indicates 10-50%; the medium dark shade indicates 50-80%; and the dark shade indicates 80-100%. Note 2: N/A indicates data are not available.

[a] *Total determined by total digestion (see Chapter 2, Section 2.3.3).*

[b] *Residual calculated as* $(M_{Total} - M_{PT} - M_{AQ} - M_{IL})/ M_{Total} \times 100 =$ *Residual %*

[c] *As determined compared to concentrations in SRM 2691, a standard Class-C CFA.*

5.4.3.1 REEs and actinides.

For the Class-F CFAs, most REEs (Y, Nd, Sm, Dy, and Yb) partitioned strongly into the AQ phase (Table 5.5 and Table 5.6). The others (La, Ce, Eu) partitioned moderately between the AQ phase (45-73%) and the residual phase (34-49%). For all CFAs, Sc partitioned mostly between the AQ and IL phases, with less than 15% remaining in the residual phase. In contrast, in the Class-C CFAs, REEs largely remained in the residual phase (with the exception of Sc and Y) (Table 5.7).

For all CFAs, Th partitioned high into the AQ phase, and moderately into the IL phase, and U remained completely in the residual phase (Table 5.5, Table 5.6, and Table 5.7).

Class-C CFAs are understood to be less recalcitrant than Class-F CFAs, so it is surprising to observe lower relative REE leaching (Table 5.7). This may be the result of the higher Ca content in Class-C CFAs. Both Si and Ca leaching from CFA in sequential alkaline-acidic treatments is not well understood mechanistically. During alkaline pretreatment, Ca minerals are dissolved, forming Ca-silicates that may capture REEs.[79] Additionally, under acidic conditions, dissolved Si forms orthosilicic acid (SiO_4^-) which may self-polymerize to form gels or may precipitate as secondary silicates.[79,108] It is hypothesized that, under the strongly acidic leaching conditions using $[N_{111}C_2OSO_3H][Tf_2N]$, Ca and Si precipitates form and preclude access to REEs. To confirm this, the residual CFA solid should be further characterized (XRD and SEM-EDS).

5.4.3.2 Bulk elements.

For all CFAs, bulk elements partitioned mostly between the AQ and residual phases, with low concentrations (<7%) observed in the IL phase (Table 5.5, Table 5.6, and Table 5.7).

For Class-F CFAs, Mg showed a moderate preference for the AQ phase (Table 5.5, and Table 5.6). Al and Fe both showed slight preferences for the residual phase over the AQ phase. Si partitioned similarly between the AQ and residual phases. Ca showed a strong preference for the AQ phase for CFA-F1, and only a slight preference in CFA-F2. In contrast, Ti showed a strong preference for the residual phase for CFA-F1, and only a slight preference in CFA-F2. Having more complete composition data for CFA-F2 will illuminate the strength of these trends in Class-F CFAs. Differences between the two CFAs are likely due to the impacts on mineralogy from weathering.

For the Class-C CFA, Mg and Fe showed similar, equitable partitioning between the AQ and residual phases (Table 5.7). Al was strongly extracted into the AQ phase, while Si and Ca remained strongly in the residual. This supports the previous hypothesis that under the acidic conditions presented by $[N_{111}C_2OSO_3H][Tf_2N]$, Si and Ca form precipitates, thus increasing the Si and Ca content in the residual phase. Finally, similar to the Class-F CFAs, Ti was found mostly in the residual phase.

5.4.3.3 Trace elements.

Trace element composition was not available for CFA-F2 and CFA-C1; estimates were determined based on NIST certificate data (SRM 1633c, a standard Class-F CFA and SRM 2691, a standard Class-C CFA, respectively).

Generally, partitioning behavior was similar between the unweathered and weathered Class-F CFAs (Table 5.5 and Table 5.6). Few elements were found in the IL phase. V, Cr, and As partitioned predominantly into the residual phase. Mn, Ni, and Zn all partitioned moderately between the AQ and residual phases. Cu showed a preference for the AQ phase.

Differences were observed between Se, Cd and Pb (Table 5.5 and Table 5.6). In the unweathered CFA, CFA-F1, Se was found in the AQ phase only, while it was found in the residual only in the weathered CFA, CFA-F2. As previously described, Se can be found on CFA particle surfaces, occasionally as Ca compounds like $CaSeO_3$. More Ca remains in the residual phase in CFA-F2 compared to CFA-F1; it may be the result of the formation of insoluble selenates like $CaSeO_3$.[140]

Cd and Pb were found solely in the residual phase in CFA-F1 (Table 5.5). In contrast, in CFA-F2 , Cd was found strongly partitioned into the IL phase and Pb was divided between AQ and residual phases (Table 5.6). Cd is associated with CFA surface and leaches more strongly at acidic pH (up to 10% at pH 1), while Pb can be associated with CFA surface or found in the glassy matrix and is poorly soluble at low pH.[140] Differences between the CFAs are likely due to the impacts on mineralogy from weathering.

Similar to the Class-F CFAs, very few elements were found in the IL phase for the Class-C CFA (Table 5.7). More elements were found in moderate concentrations in the AQ phase relative to the residual, including V, Mn, Ni, Cu, and Zn. As and Se were found in higher concentrations in the AQ phase than the residual, a trend also observed for leaching CFA-C1 with [Chol][Tf_2N]. Cr, Cd, and Pb were found only in the residual phase, similar to CFA-F1, indicating that these elements may only be accessible for weathered CFA.

5.4.3.4 Summary of [$N_{111}C_2OSO_3H$][Tf_2N].

Compared to [Chol][Tf_2N], [$N_{111}C_2OSO_3H$][Tf_2N] leached more elements from all CFAs. This can be attributed to its strong acidity and the alkyl sulfuric acid group's affinity for metal cations.[59] Previous research on alkyl sulfuric ILs found that [$N_{111}C_2OSO_3H$][Tf_2N] could efficiently dissolve a number of metal oxides, including CaO, CuO, NiO, La_2O_3, Nd_2O_3, Co_3O_4 and Fe_2O_3.[59] Notably, however, similar to the choline-based IL, few elements showed a preference for the IL phase. Comparison of [$N_{111}C_2OSO_3H$][Tf_2N] and [Hbet][Tf_2N].

5.4.3.5 Leaching efficiency (L%) comparison.

Leaching performance varied by CFA type. For CFA-F1, L_{REEs} , including $L_{Sc,}$ was all higher with [$N_{111}C_2OSO_3H$] (Figure 5.2). L_{Bulk} and L_{Trace} were about the same for most elements. Cu was higher with [$N_{111}C_2OSO_3H$], and Mg and Fe were higher with [Hbet][Tf_2N]. [$N_{111}C_2OSO_3H$][Tf_2N] is known to be more acidic and capable of dissolving solid metal oxides.[59] As this IL attacked the CFA, perhaps more aggressively than [Hbet][Tf_2N], more REEs were leached.

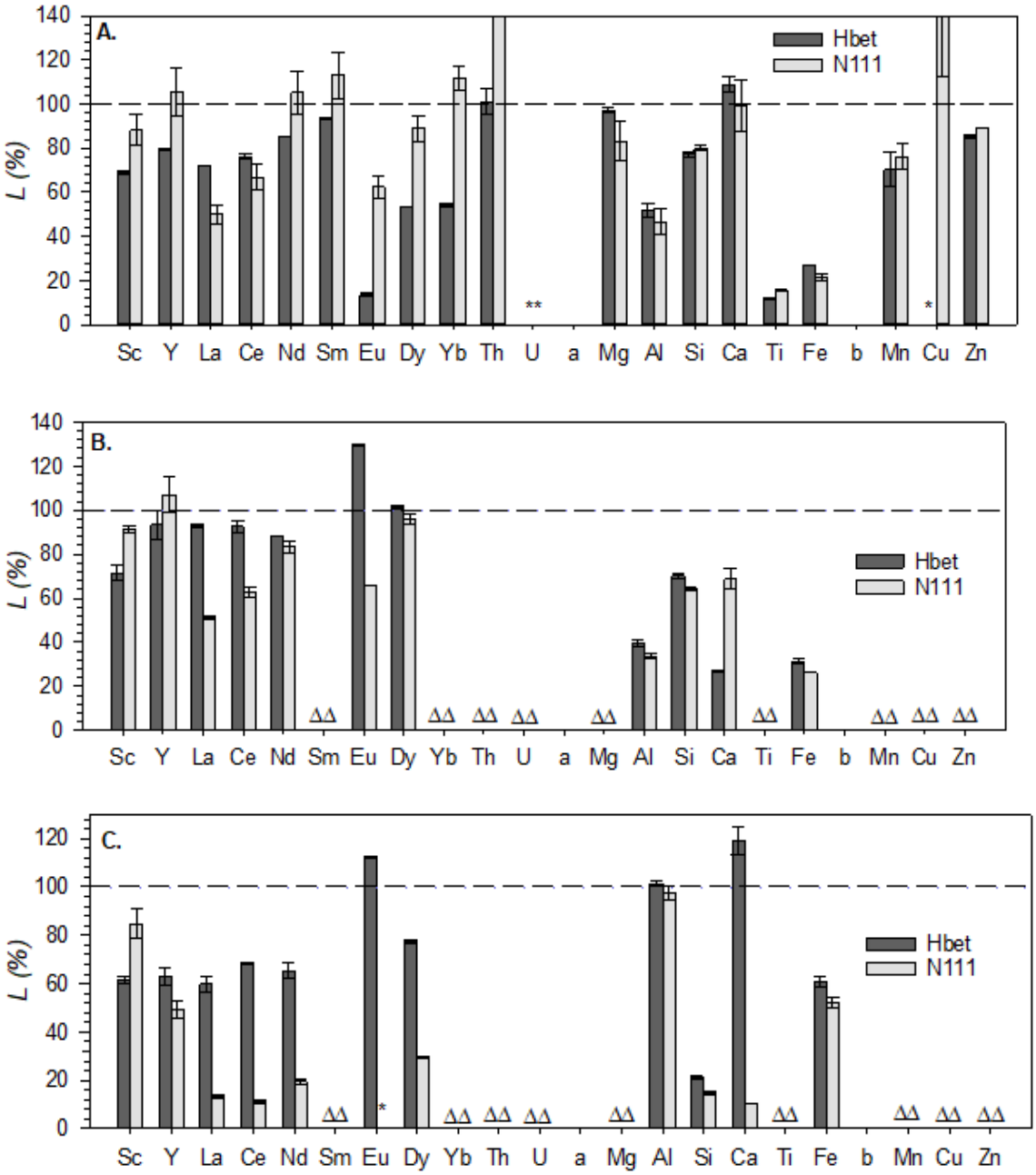

Figure 5.2 Average leaching efficiency L for CFA-F1 (A), CFA-F2 (B), and CFA-C1 (C) after IL extraction.

Notes: *[Hbet][Tf_2N] is labeled Hbet) and [$N_{111}C_2OSO_3H$][Tf_2N] is labeled N111. All CFAs underwent alkaline pretreatment prior to IL leaching. Error bars indicate standard deviation of duplicate samples. Columns marked with a * indicate zero. Columns marked with a Δ indicate the data is not available. Extraction efficiencies >100% may be the result of low initial concentration in the solid or potential enrichment in the CFA as the result of alkaline pretreatment.*

For CFA-F2, [$N_{111}C_2OSO_3H$] had a mixed effect on L_{REEs}, though L_{Sc} remained high (Figure 5.2). It is unclear why L_{REEs} by [$N_{111}C_2OSO_3H$] would decrease for CFA-F2, compared to CFA-F1. L with [Hbet][Tf_2N] remained higher for bulk elements Al, Si, and Fe, though not significantly higher. L_{Ca} was higher with [$N_{111}C_2OSO_3H$]. There are only slight differences between L for bulk elements, with the exception of L_{Ca} ; if more Ca is leached (and not remaining in the residual solid), it is not likely the Ca precipitates formed may act as a sink for REEs. Further research should explore the behavior of other elements to discern whether they are related to the drop of L_{REEs} by [$N_{111}C_2OSO_3H$] in CFA-F2.

For CFA-C1, L was higher with [Hbet][Tf_2N] for almost all elements, with the exception of L_{Sc} (Figure 5.2). The decrease in L_{Ca} by [$N_{111}C_2OSO_3H$] versus by [Hbet][Tf_2N] is particular notable and further supports the hypothesis that Ca-silicates form when the Class-C CFA leaches under the stronger acidic conditions presented by [$N_{111}C_2OSO_3H$][Tf_2N], thus increasing the Si and Ca content in the residual phase (and decreasing L_{Ca} and L_{Si}).

5.4.3.6 Distribution (D) comparison.

For almost all elements evaluated in the three CFAs, distribution, D, was much higher for [Hbet][Tf_2N] than [$N_{111}C_2OSO_3H$][Tf_2N] (Figure 5.3). Only three exceptions where D was higher for the alkyl sulfuric acid IL were observed: for CFA-F1, Mn and Cu, and for CFA-F2, Ca. Mn (atomic number 25) and Cu (atomic number 29) are similarly sized transition metals that are commonly present as divalent cations (though Mn can exist as 2+, 3+, 4+, 6+, and 7+, and Cu can exist as 1+ or 2+). As such, their charge density is fairly low. [Hbet][Tf_2N] complexes strongly with metal cations with high charge density[68,69] and

thus would be expected to extract Mn and Cu poorly. $[N_{111}C_2OSO_3H][Tf_2N]$ is known to be more acidic and capable of dissolving solid metal oxides.[59] The third exception where D is higher for $[N_{111}C_2OSO_3H][Tf_2N]$, Ca in the weathered CFA, CFA-F2, stands out because it is the opposite for the unweathered CFA samples (CFA-F1 and CFA-C1). Importantly, D_{Ca} is still low (D_{Ca} = 0.05, and Ca in the IL phase is only 3.2%). It is likely that Ca is present as different minerals in weathered CFA compared to unweathered CFAs. Previous work has found that exposure to water leaches soluble alkali metals, including Ca, during weathering.[106] It is hypothesized that the combination of physical damage to the CFA particles as well as the dissolution of Ca during alkaline pretreatment exposes additional surfaces for acidic IL leaching, leading to high leaching efficiency for REEs.[137]

As discussed previously, there are many elements that had zero partitioning into the IL phase for $[N_{111}C_2OSO_3H][Tf_2N]$ (D = 0, Table 5.5, Table 5.6, and Table 5.7). For CFA-F1, these include Eu, U, Si, V, Cr, Mn, Ni, Zn, As, Se, Cd, and Pb. For CFA-F2, these include Eu, U, Cr, Ni, As, Se, and Pb. For CFA-C1, this includes Eu, U, Si, Ti, V, Cr, Ni, Zn, As, Se, Cd, and Pb. Some of these, like Si and U, form oxyanions, which are bulky and tend to poorly extract into $[Hbet][Tf_2N]$.[68,69] Steric hindrance may also be relevant for $[N_{111}C_2OSO_3H][Tf_2N]$. Others are divalent cations with low charge density, which are poorly extracted by $[Hbet][Tf_2N]$[68,69] and may also be poorly extracted by $[N_{111}C_2OSO_3H][Tf_2N]$.

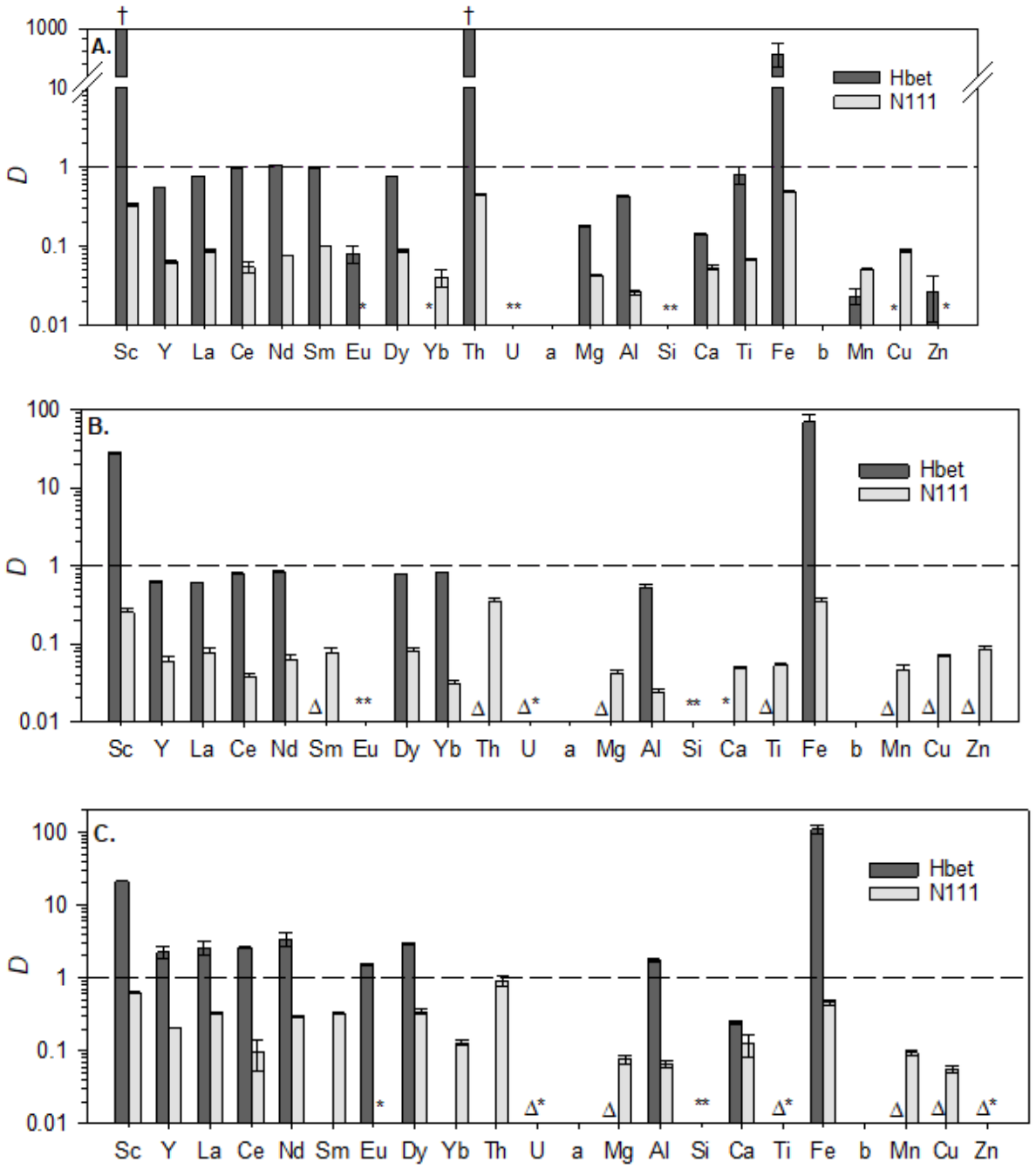

Figure 5.3 Average distribution D for CFA-F1 (A), CFA-F2 (B), and CFA-C1 (C) after IL extraction

*Notes: [Hbet][Tf_2N] is labeled Hbet and [$N_{111}C_2OSO_3H$][Tf_2N] is labeled N111. All CFAs underwent alkaline pretreatment prior to IL leaching. Error bars indicate standard deviation of duplicates. Columns marked with a * indicate D = 0 (i.e., element was not found in the IL phase). Columns marked with a † indicate that the element was not detected in the AQ phase (D →∞). Columns marked with a Δ indicate the data are not available.*

5.4.3.7 Recovery (R %) comparison.

To achieve high recovery efficiency, *R*, elements must have reasonably high *D* and *L* values. Because $[N_{111}C_2OSO_3H][Tf_2N]$ uniformly poorly extracted elements into the IL phase (low *D)*, [Hbet][Tf_2N] consistently outperforms for all elements for all CFAs (Figure 5.4).

However, $[N_{111}C_2OSO_3H][Tf_2N]$ may still prove suitable for REE recovery from CFA, especially given the high L_{REEs} values it achieved for CFA-F1 (higher than [Hbet][Tf_2N]). Rather, a different model using this IL may be required, where REEs are recovered from the AQ phase, and bulk and trace elements are induced to partition into the IL phase. Dupont et al. designed one such [Hbet][Tf_2N] leaching system where Fe partitioned into the IL phase and REEs partitioned into the AQ phase.[7] The critical factor is to achieve separation between the desired and unwanted elements. With increasingly complex systems, as with CFA leaching, with dozens of elements present in varying concentrations, achieving such separations becomes more challenging.

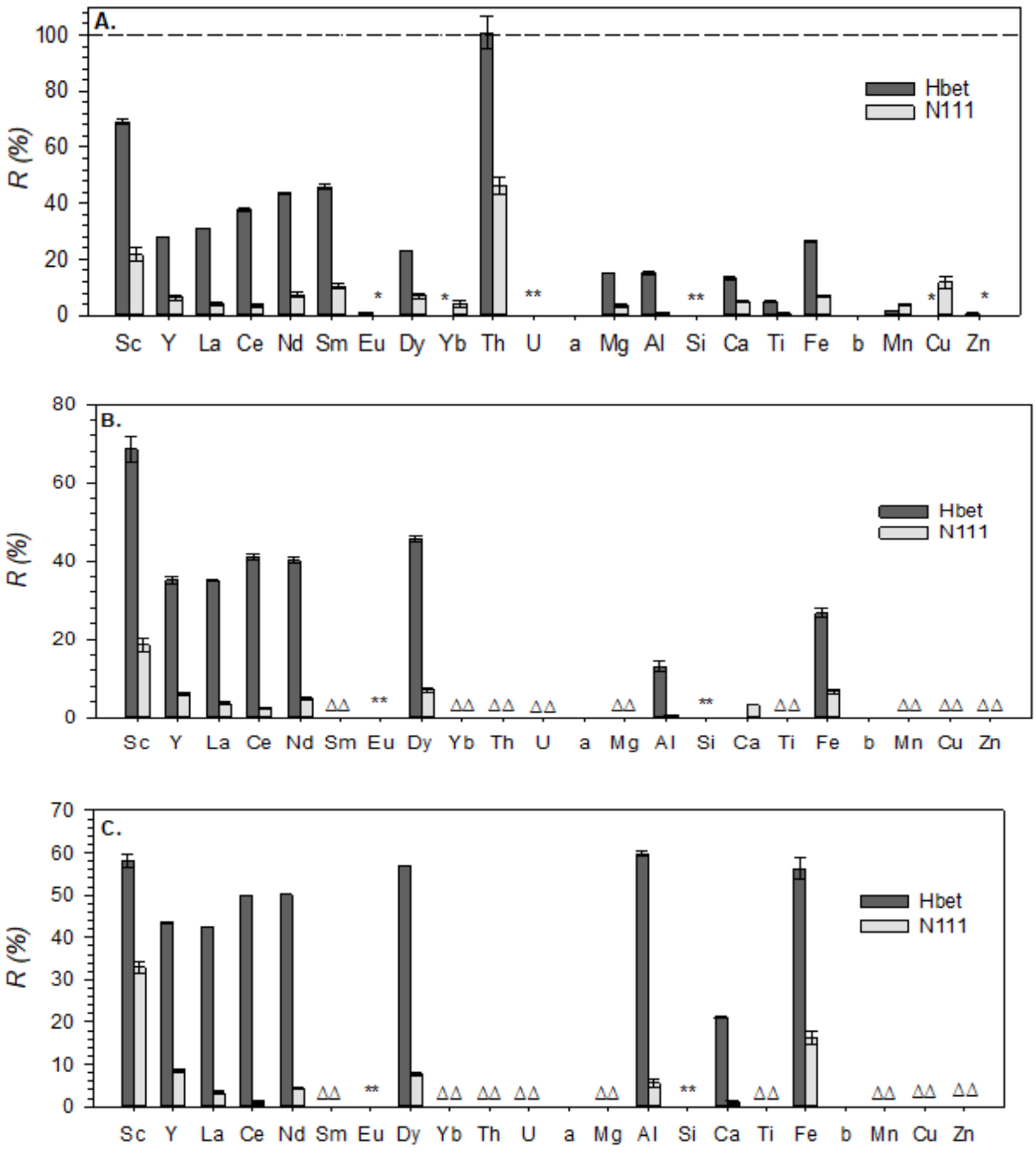

Figure 5.4 Average recovery R for CFA-F1 (A), CFA-F2 (B), and CFA-C1 (C) after IL extraction

*Notes: [Hbet][Tf_2N] is labeled Hbet and [$N_{111}C_2OSO_3H$][Tf_2N] is labeled N111. All CFAs underwent alkaline pretreatment prior to IL leaching. Error bars indicate standard deviation of duplicates. Columns marked with a * indicate R = 0 (i.e., element was not found in the IL phase). Columns marked with a † indicate that the element was not detected in the AQ phase (D →∞). Columns marked with a Δ indicate the data is not available.*

5.5 Conclusions

In this study, two ILs, [Chol][Tf_2N] and [$N_{111}C_2OSO_3H$][Tf_2N], were applied to three representative CFAs: an unweathered Class-F CFA, a weathered Class-F CFA, and an unweathered Class-C CFA. These ILs were chosen to serve as comparisons to [Hbet][Tf_2N], an IL demonstrated to successfully preferentially extract REEs from CFA.[137] All three ILs share the same anion, but differ by the cation functional group. While [Hbet][Tf_2N] has a carboxylic acid functional group on its cation, [Chol][Tf_2N] has a simple alcohol and [$N_{111}C_2OSO_3H$] has an alkyl sulfuric acid functional group. [Chol][Tf_2N] was broadly unsuccessful at leaching most elements from all CFAs, indicating that an additional extractant may be required to achieve high extraction efficiency. Acidic ligands, potentially with carboxylic acid function groups that complex favorably with REEs, should be the subject of future research. [$N_{111}C_2OSO_3H$] was more successful, achieving greater leaching efficiency for CFA-F1 and comparable leaching efficiency for CFA-F2 than [Hbet][Tf_2N] for most REEs. However, it did not partition these REEs into the IL phase, but rather the AQ phase. Other bulk and trace metals also partitioned into this AQ phase. Unfortunately, this establishes [$N_{111}C_2OSO_3H$][Tf_2N] as a less selective IL relative to [Hbet][Tf_2N]. Further optimizations may be explored in future work to determine if better selectivity may be induced.

CHAPTER 6. CONCLUSIONS AND FUTURE PERSPECTIVES

6.1 Conclusions

6.1.1 Conclusions related to [Hbet][Tf_2N]

Extracting REEs from CFA, a waste material produced in vast supplies throughout the world, requires a green and industrially viable solution that reduces chemical and energy consumption and reduces the overall processing required for production of REE oxides and metals by separating REEs from bulk and trace elements.

This dissertation focuses on developing a new valorization process based on the ionic liquid (IL) betainium bis(trifluoromethylsulfonyl)imide ([Hbet][Tf_2N]) for preferential extraction of REEs from different CFAs. Efficient extraction relies on [Hbet][Tf_2N]'s thermomorphic behavior with water: upon heating, water and the IL form a single liquid phase, and REEs are leached from CFA via a proton-exchange mechanism. Upon cooling, the water and IL separate, and leached elements partition between the IL and aqueous (AQ) two phases. REEs were preferentially extracted over bulk elements from CFAs into the IL phase then recovered in a subsequent mild acid stripping step, regenerating the IL. Alkaline pretreatment significantly improved REE leaching efficiency from recalcitrant Class-F CFAs, and additional betaine improved REEs and bulk elements' separation. Weathered CFA showed slightly higher REE leaching efficiency than unweathered CFA, and Class-C CFA demonstrated higher leaching efficiency but less selective partitioning than Class-F CFAs. Significantly, this method consistently exhibits a particularly high extraction efficiency for scandium across different CFAs.

The IL extraction process yields a mildly acidic REE-rich solution contaminated with Fe. The second study in this thesis investigates three strategies for limiting Fe coextraction into the IL phase: magnetic separation, complexing salts, and ascorbic acid reduction. Magnetic separation, intended to reduce the amount of Fe in the initial CFA, failed to deplete Fe in CFA and ultimately increased the amount of Fe in the IL phase. When NaCl was used instead of NaNO3 as an alternative salt, the overall recovery (R_{Fe}) of iron did not decrease but the distribution (D_{Fe}) of iron between the IL and AQ phases decreased from ~75 to ~14, a five-fold decrease, and the leaching efficiency (L_{REEs}) and recovery (R_{REEs}) of REEs both increased. Finally, using ascorbic acid decreased D_{Fe} even further, to ~0.16, indicating a preference for the AQ phase over the IL phase and causing R_{Fe} to also drop. These optimizations should be used together in conjunction with other strategies identified in previous work with CFA-[Hbet][Tf_2N] leaching, including alkaline pretreatment and adding supplemental betaine cation, to generate an REE-rich acidic solution with very low concentrations of Fe.

The third part of this dissertation expands upon the CFA leaching behavior with [Hbet][Tf_2N]. This IL has been shown to separate REEs from bulk elements (Si, Al, Ca, and Fe), but little is known about the behavior of other elements. Eighteen additional elements were studied (29 total) and found that in the IL phase, bulk elements were found in low concentrations (<26 wt.%), trace elements were not found (<1.6 mg/kg), and of the actinides, Th was extracted into the IL phase and U was not leached at all. REEs, as previously noted, partition largely between the AQ and IL phases. The study also identified other important optimizations, including pH (no impact observed for pH 2-7), temperature (optimal L observed at 85ºC of the studied 45-85ºC range), and duration of leaching

(optimal *L* observed at 3 h of the 0.5-12 h range). The process is also compared to several published CFA solid extraction methods and CFA leacheate separation methods to place the recovery method developed by this dissertation in context with existing literature. Finally, a number of process sustainability improvements are recommended, including the use of microwave heating, water and IL recovery strategies, and beneficial uses of the residual solids.

6.1.2 Conclusions related to other ILs

Two other ILs were studied along with [Hbet][Tf_2N] to investigate the effect of IL's cation functional group modifications. The two ILs possess the same anion [Tf_2N], but one with a less acidic cation having an alcohol functional group, choline [Chol], and one with a more acidic cation having an alkyl sulfonic acid functional group, trimethylammoniumethane hydrogen sulfate ([$N_{111}C_2OSO_3H$]), in comparison with [Hbet]. [Chol][Tf_2N] was broadly unsuccessful at leaching almost all elements from all CFA samples tested, indicating that an additional extractant may be required to achieve high extraction efficiency. [$N_{111}C_2OSO_3H$][Tf_2N] was more successful, achieving greater or comparable leaching efficiencies; however, unlike [Hbet][Tf_2N], it did not partition the REEs into the IL phase, but rather into the AQ phase, along with other bulk and trace constituents. Further optimizations should be explored to determine if better selectivity may be induced for [$N_{111}C_2OSO_3H$].

6.2 Future Perspectives

Based on the current conclusions from this dissertation, future work to advance the understanding of REE recovery from CFA using ILs may include the following:

1. While CFA broadly shares similarities in composition, mineralogy, and morphology, heterogeneity is the rule rather than the exception. Variability in CFA depends on parent coal and combustion conditions, including grinding mill efficiency, combustion environment, boiler configuration, and the rate of particle cooling. Further work should validate the IL extraction process for other CFA samples from various regions, as well as more samples of weathered CFA from storage ponds. This evaluation should include partitioning behaviour for all elements, but most importantly the most critical REEs and potentially dangerous trace contaminants.

2. To scale up an extraction process, all wastes must be characterized and accounted for, with the goal of limited waste production and sequestration of potentially dangerous contaminants. This may include reuse and recycling, as well as optimizing processes to generate specific products. From the perspective of utility companies tasked with managing CFA as solid waste, this extraction process must include some use for the residual solid aside from landfilling. Future work should consider potential applications for the residual solid, and carefully monitor the legacy of any contaminants.

3. Care should be taken specially to conserve the active agent, the IL. [Hbet][Tf_2N] was determined to be recyclable over three leaching/stripping cycles, but this number is likely higher and should be investigated. Disposal of the IL or waters containing the IL should rely on best practices and address any toxicity concerns. IL toxicity is largely dependent on the structure (cation family, chain length, and anion moiety). The ILs evaluated in this study were determined to be relatively

nontoxic, as betaine is a biomolecule and another IL containing Tf_2N has been determined to be "practically harmless" based on its EC50 value.[135,136] Any IL intended for use at scales in which aquatic or terrestrial environments may be impacted by a spill or other adverse event should be evaluated comprehensively for (eco)toxicity and biodegradability.

4. Given the tuneability of ILs, there are a near infinite number of potential ILs, with various cations and anions with varying-length alkyl chains and functional groups. This thesis focused on acidic ILs that (1) showed a potential for REE extraction, (2) have low viscosity, (3) rely on a proton exchange mechanism, and (4) demonstrate thermomorphic behaviour with water as a convenient exploitable extraction system. It may be that other acidic ILs, likely other carboxylic acid containing ILs, or phosphonium-based ILs, may also be successful at extracting REEs from CFA.

5. Prior to this study, [Hbet][Tf_2N] had been shown to extract REEs from acidic aqueous solutions and directly from several REE-rich wastes, including NdFeB magnets, lamp phosphors, LCD screens, and bauxite residue leacheate (a liquid). Other REE-rich materials should be investigated, including ores, acid mine drainage fluids and sludges, municipal waste incineration ashes, industrial and municipal wastewater sludges, and produced waters from oil and gas exploration sites. Post-consumer products like electronics may also be suitable. Ideally, the IL leaching and stripping process would be agnostic to the influent material and would successfully extract REEs regardless of source. However, it is much more likely that such a system would require optimizations specific to each waste.

6. Finally, this study investigated several basic optimizations – pH, temperature, leaching duration, AQ phase salt, to name a few – for the standard CFA (the Class-F NIST CFA). These variables should be evaluated for other CFAs as well as any other wastes. Other variables that should be investigated include solid to liquid ratio (meaning solid CFA:IL ratio or solid CFA:IL-AQ mixture ratio) as well as liquid to liquid ratio (IL:AQ). In this study, only solid-liquid ratio was investigated (50mg CFA: 4 g IL-AQ mixture) and one liquid to liquid ratio (1:1 water-saturated IL: AQ phase ratio by mass) was employed. These ratios will be critical in limiting the production of wastes and conserving the IL.

REFERENCES

REFERENCES

1. Taggart, R. K.; Hower, J. C.; Dwyer, G. S.; Hsu-Kim, H., Trends in the rare earth element content of U.S.-based coal combustion fly ashes. *Environ. Sci. Technol.* **2016,** *50* (11), 5919-5926.

2. *Coal Combustion Product (CCP) production & use survey report*; American Coal Ash Association: 2016.

3. Agency, U. S. E. P. Coal Ash Basics. https://www.epa.gov/coalash/coal-ash-basics.

4. Jork, C.; Kristen, C.; Pieraccini, D.; Stark, A.; Chiappe, C.; Beste, Y. A.; Arlt, W., Tailor-made ionic liquids. *The Journal of Chemical Thermodynamics* **2005,** *37* (6), 537-558.

5. Nockemann, P.; Thijs, B.; Pittois, S.; Thoen, J.; Glorieux, C.; Van Hecke, K.; Meervelt, L. V.; Kirchner, B.; Binnemans, K., Task-specific ionic liquid for solubilizing metal oxides. *J. Mater. Chem. B* **2006,** *110*, 90978-20992.

6. Dupont, D.; Binnemans, K., Rare-earth recycling using a functionalized ionic liquid for the selective dissolution and revalorization of Y2O3:Eu3+ from lamp phosphor waste. *Green Chem.* **2015,** *17* (2), 856-868.

7. Dupont, D.; Binnemans, K., Recycling of rare earths from NdFeB magnets using a combined leaching/extraction system based on the acidity and thermomorphism of the ionic liquid [Hbet][Tf2N]. *Green Chem.* **2015,** *17* (4), 2150-2163.

8. Onghena, B.; Borra, C. R.; Van Gerven, T.; Binnemans, K., Recovery of scandium from sulfation-roasted leachates of bauxite residue by solvent extraction with the ionic liquid betainium bis(trifluoromethylsulfonyl)imide. *Sep. Purif. Technol.* **2017,** *176*, 208-219.

9. Luo, D.; Zhu, N.; Li, Y.; Cui, J.; Wu, P.; Wang, J., Simultaneous leaching and extraction of indium from waste LCDs with acidic ionic liquids. *Hydrometallurgy* **2019,** *189*, 105146.

10. Zhu, W.; Ritchie, M., China Stokes Rare Earths Concerns With Possible Export Controls. *Bloomberg News* 6/4/2019, 2019.

11. Haxel, G. B.; Hedrick, J. B.; Orris, G. J., Fact Sheet 087-02: Rare Earth Elements-Critical Resources for High Technology. United States Geological Survey 2002.

12. Gambogi, J., Annual Mineral Commodity Summaries: Rare Earths. United States Geological Survey: 2016.

13. Rare earth elements: a review of production, processing, and recyling, and associated environmental issues. Cincinnati, OH, 2012; Vol. EPA/600/R-12/572.

14. Eggert, R. G.; Carpenter, A. S.; Freiman, S. W.; Graedel, T. E.; Meyer, D. A.; McNulty, T. P.; Moudgil, B. M.; Poulton, M. M.; Surges., L. J., Minerals, critical minerals and the US economy. 2008.

15. Group, R. M. S., Critical raw materials for the EU. European Commission Enterprise and Industry: 2010.

16. Long, K. R., The Future of Rare Earth Elements- Will These High-tech Industry Elements Continue in Short Supply? U.S. Department of the Interior: 2011.

17. Stringer, D., Trump's Quest to Quit China's Rare Earths Hits Outback Australia. *Bloomberg News* 8/7/2019, 2019.

18. Dlouhy, J. A., Trump Enlists Pentagon on Rare-Earth Magnets Amid Chinese Threat. *Bloomberg News* 7/22/2019, 2019.

19. Dutta, T.; Kim, K. H.; Uchimiya, M.; Kwon, E. E.; Jeon, B. H.; Deep, A.; Yun, S. T., Global demand for rare earth resources and strategies for green mining. *Environ. Res.* **2016,** *150*, 182-90.

20. Grasso, V. B., Rare Earth Elements in National Defense: Background, Oversight Issues, and Options for Congress. Congressional Research Service: 2013.

21. Report on Critical Raw Materials for the EU. European Commission: 2014.

22. Nassar, N. T.; Du, X.; Graedel, T. E., Criticality of the rare earth elements. *J. Ind. Ecol.* **2015,** *19*, 1044-1054.

23. Mudd, G. M., The sustainability of mining in Australia- key production trends and their environmental implications for the future. Department of Civil Engineering, Monash University, and Mineral Policy Institute: Girrawheen, Australia, 2009.

24. Dai, S.; Zhao, L.; Hower, J. C.; Johnston, M. N.; Song, W.; Wang, P.; Zhang, S., Petrology, mineralogy, and chemistry of size-fractioned fly ash from the Jungar power plant, inner Mongolia, China, with emphasis on the distribution of rare earth elements. *Energy Fuels* **2014,** *28* (2), 1502-1514.

25. Franus, W.; Wiatros-Motyka, M. M.; Wdowin, M., Coal fly ash as a resource for rare earth elements. *Environ. Sci. Pollut. Res.* **2015,** *22* (12), 9464-74.

26. Seredin, V. V.; Dai, S.; Sun, Y.; Chekryzhov, I. Y., Coal deposits as promising sources of rare metals for alternative power and energy-efficient technologies. *Appl. Geochem.* **2013,** *31*, 1-11.

27. Kashiwakura, S.; Kumagai, Y.; Kubo, H.; Wagatsuma, K., Dissolution of rare earth elements from coal fly ash particles in a dilute H2SO4 solvent. *Open J. Phys. Chem* **2013,** *03* (02), 69-75.

28. Mardon, S. M.; Hower, J. C., Impact of coal properties on coal combustion by-product quality: examples from a Kentucky power plant. *Int. J. Coal Geol.* **2004,** *59* (3-4), 153-169.

29. Kutchko, B.; Kim, A., Fly ash characterization by SEM–EDS. *Fuel* **2006,** *85* (17-18), 2537-2544.

30. Dai, S.; Zhao, L.; Peng, S.; Chou, C.-L.; Wang, X.; Zhang, Y.; Li, D.; Sun, Y., Abundances and distribution of minerals and elements in high-alumina coal fly ash from the Jungar Power Plant, Inner Mongolia, China. *Int. J. Coal Geol.* **2010,** *81* (4), 320-332.

31. Zhang, F.-S.; Yamasaki, S.; Kimura, K., Waste ashes for use in agricultural production- II. Contents of minor and trace metals. *Sci. Total Environ.* **2002,** *286*, 111-118.

32. Praharaj, T.; Powell, M. A.; Hart, B. R.; Tripathy, S., Leachability of elements from sub-bituminous coal fly ash from India. *Environ. Int.* **2002,** *27*, 609-615.

33. Jegadeesan, G.; Al-Abed, S. R.; Pinto, P., Influence of trace metal distribution on its leachability from coal fly ash. *Fuel* **2008,** *87* (10-11), 1887-1893.

34. Fact Sheet: 2015 Final Rule on Coal Combustion Residuals Generated by Electric Utilities. United State Environmental Protection Agency Office of Resource Conservation and Recovery: 2015.

35. Shoichet, C. E., Spill spews tons of coal ash into North Carolina river. *CNN* 2014.

36. Gang, D. W., 5 years after coal-ash spill, little has changed. *USA Today* 2013.

37. Chapman, D., Georgia Power to close ash lagoons sooner, could cost $2 billion. *The Atlanta Journal-Constitution* August 13, 2016, 2016.

38. EPA Seeks Input on Proposals to Establish a Clear and Stable Regulatory Framework for Coal Combustion Residuals and Reduce More Pollutants Under Effluent Limitation Guidelines. In *News Releases from Headquarters*, Environmental Protection Agency- Land and Emergency Management (OLEM): 2019.

39. What are Coal Combustion Products? https://www.acaa-usa.org/What-are-CCPs.

40. Agency, U. S. E. P., Method 3050b Acid digestion of solids. **1996**, 1-12.

41. Agency, U. S. E. P., Method 3051: Microwave assisted acid digestion of sediments, sludges, soils, and oils. **1994**, 1-14.

42. Method 3052 Total Digestion of solids. United States Environmental Protection Agency: 1996; pp 1-20.

43. Joseph E. Taggart, J., Analytical methods for chemical analysis of geologic and other materials, U.S. Geological Survey. *United States Geological Survey* **2002**.

44. Briggs, P. H.; Meier, A. L., The determination of forty-two elements in geological materials by inductively coupled plasma- mass spectrometry. *United States Geological Survey* **2002,** *I*, 1-14.

45. Meier, A. L.; Slowik, T., Rare earth elements by inductively coupled plasma-mass spectrometry. *United States Geological Survey* **2002,** *K*, 1-8.

46. Dai, S.; Wang, X.; Zhou, Y.; Hower, J. C.; Li, D.; Chen, W.; Zhu, X.; Zou, J., Chemical and mineralogical compositions of silicic, mafic, and alkali tonsteins in the late Permian coals from the Songzao Coalfield, Chongqing, Southwest China. *Chem. Geol* **2011,** *282* (1-2), 29-44.

47. Hasegawa, H.; Rahman, I. M. M.; Egawa, Y.; Sawai, H.; Begum, Z. A.; Maki, T.; Mizutani, S., Recovery of the rare metals from various waste ashes with the aid of temperature and ultrasound irradiation using chelants. *Water, Air, Soil Pollut.* **2014,** *225* (9).

48. Kim, A. G.; Kazonich, G.; Dahlberg, M., Relative solubility of cations in Class F fly ash. *Environ. Sci. Technol.* **2003,** *37*, 4507-4511.

49. Tan, Q.; Li, J., Recycling metals from wastes: a novel application of mechanochemistry. *Environ. Sci. Technol.* **2015,** *49* (10), 5849-61.

50. Hower, J. C., Petrographic examination of coal-combustion fly ash. *Int. J. Coal Geol.* **2012,** *92*, 90-97.

51. Tian, G.-c.; Li, J.; Hua, Y.-x., Application of ionic liquids in hydrometallurgy of nonferrous metals. *Trans. Nonferrous Met. Soc.* **2010,** *20* (3), 513-520.

52. Wellens, S.; Thijs, B.; Binnemans, K., An environmentally friendlier approach to hydrometallurgy: highly selective separation of cobalt from nickel by solvent extraction with undiluted phosphonium ionic liquids. *Green Chem.* **2012,** *14* (6), 1657.

53. Nakashima, K.; Kubota, F.; Maruyama, T.; Goto, M., Ionic liquids as a novel solvent for lanthanide extraction. *Anal. Sci.* **2003,** *19*, 1097-1098.

54. Grabda, M.; Oleszek, S.; Panigrahi, M.; Kozak, D.; Eckert, F.; Shibata, E.; Nakamura, T., Theoretical selection of most effective ionic liquids for liquid–liquid extraction of NdF3. *Comput. Theor. Chem.* **2015,** *1061*, 72-79.

55. Wellens, S.; Brooks, N. R.; Thijs, B.; Meervelt, L. V.; Binnemans, K., Carbene formation upon reactive dissolution of metal oxides in imidazolium ionic liquids. *Dalton Trans.* **2014,** *43* (9), 3443-52.

56. Abbott, A. P.; Boothby, D.; Capper, G.; Davies, D. L.; Rasheed, R. K., Deep eutectic solvents formed between choline chloride and carboxylic acids. *J. Am. Chem. Soc.* **2004,** *126*, 9142-9147.

57. Abbott, A. P.; Capper, G.; Davies, D. L.; McKenzie, K. J.; Obi, S. U., Solubility of metal oxides in deep eutectic solvents based on choline chloride. *J. Chem. Eng. Data* **2006,** *51*, 1280-1282.

58. Abbott, A. P.; Capper, G.; Davies, D. L.; Rasheed, R. K.; Shikotra, P., Selective extraction of metals from mixed oxide matrixes using choline-based ionic liquids. *Inorg. Chem.* **2005,** *44*, 6497-6499.

59. Dupont, D.; Renders, E.; Binnemans, K., Alkylsulfuric acid ionic liquids: a promising class of strongly acidic room-temperature ionic liquids. *Chem. Commun.* **2016,** *52* (25), 4640-3.

60. Rout, A.; Binnemans, K., Separation of rare earths from transition metals by liquid-liquid extraction from a molten salt hydrate to an ionic liquid phase. *Dalton Trans.* **2014,** *43* (8), 3186-95.

61. Freiderich, J. W.; Stankovich, J. J.; Luo, H.; Dai, S.; Moyer, B. A., Dissolution of the rare-earth mineral bastnaesite by acidic amide ionic liquid for recovery of critical materials. *Eur. J. Inorg. Chem.* **2015,** *2015* (26), 4354-4361.

62. Sun, X.; Peng, B.; Ji, Y.; Chen, J.; Li, D., The solid–liquid extraction of yttrium from rare earths by solvent (ionic liquid) impreganated resin coupled with complexing method. *Sep. Purif. Technol.* **2008,** *63* (1), 61-68.

63. Sun, X.; Waters, K. E., Development of industrial extractants into functional ionic liquids for environmentally friendly rare earth separation. *ACS Sustainable Chemistry & Engineering* **2014,** *2* (7), 1910-1917.

64. Yang, F.; Kubota, F.; Baba, Y.; Kamiya, N.; Goto, M., Selective extraction and recovery of rare earth metals from phosphor powders in waste fluorescent lamps using an ionic liquid system. *J. Hazard. Mater.* **2013,** *254-255*, 79-88.

65. Nockemann, P.; Thijs, B.; Parac-Vogt, T. N.; Hecke, K. V.; Meervelt, L. V.; Tinant, B.; Hartenbach, I.; Schleid, T.; Ngan, V. T.; Nguyen, M. T.; Binnemans, K., Carboxyl-functionalized task-specific ionic liquids for solubilizing metal oxides. *Inorg. Chem.* **2008,** *47*, 9987-9999.

66. Dinarès, I.; Garcia de Miguel, C.; Ibáñez, A.; Mesquida, N.; Alcalde, E., Imidazolium ionic liquids: A simple anion exchange protocol. *Green Chem.* **2009,** *11* (10), 1507.

67. Abbott, A. P.; Frisch, G.; Hartley, J.; Ryder, K. S., Processing of metals and metal oxides using ionic liquids. *Green Chem.* **2011,** *13* (3), 471.

68. Vander Hoogerstraete, T.; Onghena, B.; Binnemans, K., Homogeneous liquid-liquid extraction of metal ions with a functionalized ionic liquid. *J. Phys. Chem. Lett.* **2013,** *4* (10), 1659-63.

69. Vander Hoogerstraete, T.; Onghena, B.; Binnemans, K., Homogeneous liquid-liquid extraction of rare earths with the betaine-betainium bis(trifluoromethylsulfonyl)imide ionic liquid system. *Int. J. Mol. Sci.* **2013,** *14* (11), 21353-77.

70. Grabda, M.; Panigrahi, M.; Oleszek, S.; Kozak, D.; Eckert, F.; Shibata, E.; Nakamura, T., COSMO-RS screening for efficient ionic liquid extraction solvents for NdCl3 and DyCl3. *Fluid Ph. Equilibria* **2014,** *383*, 134-143.

71. Wellens, S. Ionic liquid technology in metal refining: dissolution of metal oxides and separation by solvent extraction. Katholieke Universiteit Leuven, Belgium, 2014.

72. Wellens, S.; Vander Hoogerstraete, T.; Möller, C.; Thijs, B.; Luyten, J.; Binnemans, K., Dissolution of metal oxides in an acid-saturated ionic liquid solution and investigation of the back-extraction behaviour to the aqueous phase. *Hydrometallurgy* **2014,** *144-145*, 27-33.

73. Dupont, D.; Raiguel, S.; Binnemans, K., Sulfonic acid functionalized ionic liquids for dissolution of metal oxides and solvent extraction of metal ions. *Chem. Commun.* **2015,** *51* (43), 9006-9.

74. Hou, H.; Xu, J.; Wang, Y.; Chen, J., Solvent extraction performance of Pr (III) from chloride acidic solution with 2-ethylhexyl phosphoric acid-2-ethylhexyl ester (EHEHPA) by using membrane dispersion micro-extractor. *Hydrometallurgy* **2015,** *156*, 116-123.

75. Zhong, Y.; Feng, X.; Chen, W.; Wang, X.; Huang, K. W.; Gnanou, Y.; Lai, Z., Using UCST ionic liquid as a draw solute in forward osmosis to treat high-salinity water. *Environ. Sci. Technol.* **2016,** *50* (2), 1039-45.

76. Rozelle, P. L.; Khadilkar, A. B.; Pulati, N.; Soundarrajan, N.; Klima, M. S.; Mosser, M. M.; Miller, C. E.; Pisupati, S. V., A study on removal of rare earth elements from U.S. coal byproducts by ion exchange. *Metallurgical and Materials Transactions E* **2016,** *3* (1), 6-17.

77. Painter, P.; Pulati, N.; Cetiner, R.; Sobkowiak, M.; Mitchell, G.; Mathews, J., Dissolution and dispersion of coal in ionic liquids. *Energy Fuels* **2010,** *24* (3), 1848-1853.

78. Taggart, R. K.; Hower, J. C.; Hsu-Kim, H., Effects of roasting additives and leaching parameters on the extraction of rare earth elements from coal fly ash. *Int. J. Coal Geol.* **2018,** *196*, 106-114.

79. King, J. F.; Taggart, R. K.; Smith, R. C.; Hower, J. C.; Hsu-Kim, H., Aqueous acid and alkaline extraction of rare earth elements from coal combustion ash. *Int. J. Coal Geol.* **2018,** *195*, 75-83.

80. Amde, M.; Liu, J. F.; Pang, L., Environmental application, fate, effects, and concerns of ionic liquids: a review. *Environ. Sci. Technol.* **2015,** *49* (21), 12611-27.

81. MacDonald, A., U.S. Faces Uphill Climb to Rival China's Rare-Earth Magnet Industry *The Wall Street Journal* 2021.

82. United States, E. O. o. t. P. J. B., E.O. 14017: Executive Order on America's Supply Chains February 24, 2021: 2021.

83. Duke Energy, North Carolina regulators and environmentalists reach agreement to permanently close all remaining ash basins in North Carolina Duke Energy: 2020.

84. Smith Stegen, K., Heavy rare earths, permanent magnets, and renewable energies: An imminent crisis. *Energy Policy* **2015,** *79*, 1-8.

85. Ayora, C.; Macías, F.; Torres, E.; Lozano, A.; Carrero, S.; Nieto, J.-M.; Pérez-López, R.; Fernández-Martínez, A.; Castillo-Michel, H., Recovery of rare earth elements and yttrium from passive-remediation systems of acid mine drainage. *Environ. Sci. Technol.* **2016,** *50* (15), 8255-8262.

86. Stewart, B. W.; Capo, R. C.; Hedin, B. C.; Hedin, R. S., Rare earth element resources in coal mine drainage and treatment precipitates in the Appalachian Basin, USA. *Int. J. Coal Geol.* **2017,** *169*, 28-39.

87. Smith, Y. R.; Kumar, P.; McLennan, J. D., On the extraction of rare earth elements from geothermal brines. *Resources* **2017,** *6* (3), 39.

88. Roth, E.; Bank, T.; Howard, B.; Granite, E., Rare earth elements in Alberta oil sand process streams. *Energy Fuels* **2017,** *31* (5), 4714-4720.

89. Peterson, R.; Heinrichs, M.; Argumedo, D.; Taha, R.; Winecki, S.; Johnson, K.; Lane, A.; Riordan, D. *Recovery of Rare Earth Elements from Coal and Coal Byproducts via a Closed Loop Leaching Process: Final Report*; United States, 2017.

90. Jin, H.; Park, D. M.; Gupta, M.; Brewer, A. W.; Ho, L.; Singer, S. L.; Bourcier, W. L.; Woods, S.; Reed, D. W.; Lammers, L. N.; Sutherland, J. W.; Jiao, Y., Techno-economic assessment for integrating biosorption into rare earth recovery process. *ACS Sustain. Chem. Eng.* **2017,** *5* (11), 10148-10155.

91. Lin, R.; Stuckman, M.; Howard, B. H.; Bank, T. L.; Roth, E. A.; Macala, M. K.; Lopano, C.; Soong, Y.; Granite, E. J., Application of sequential extraction and hydrothermal treatment for characterization and enrichment of rare earth elements from coal fly ash. *Fuel* **2018,** *232*, 124-133.

92. Kose Mutlu, B.; Cantoni, B.; Turolla, A.; Antonelli, M.; Hsu-Kim, H.; Wiesner, M. R., Application of nanofiltration for rare earth elements recovery from coal fly ash leachate: performance and cost evaluation. *Chem. Eng. J.* **2018,** *349*, 309-317.

93. Liu, P.; Huang, R.; Tang, Y., Comprehensive understandings of rare earth element (REE) speciation in coal fly ashes and implication for REE extractability. *Environ. Sci. Technol.* **2019,** *53* (9), 5369-5377.

94. Smith, R. C.; Taggart, R. K.; Hower, J. C.; Wiesner, M. R.; Hsu-Kim, H., Selective recovery of rare earth elements from coal fly ash leachates using liquid membrane processes. *Environ. Sci. Technol.* **2019,** *53* (8), 4490-4499.

95. Sarswat, P. K.; Leake, M.; Allen, L.; Free, M. L.; Hu, X.; Kim, D.; Noble, A.; Luttrell, G. H., Efficient recovery of rare earth elements from coal based resources: a bioleaching approach. *Mater. Today Chem.* **2020,** *16*, 100246.

96. Park, D.; Middleton, A.; Smith, R.; Deblonde, G.; Laudal, D.; Theaker, N.; Hsu-Kim, H.; Jiao, Y., A biosorption-based approach for selective extraction of rare earth elements from coal byproducts. *Sep. Purif. Technol.* **2020,** *241*, 116726.

97. Vander Hoogerstraete, T.; Jamar, S.; Wellens, S.; Binnemans, K., Determination of halide impurities in ionic liquids by total reflection X-ray fluorescence spectrometry. *Anal. Chem* **2014,** *86* (8), 3931-8.

98. Hower, J.; Groppo, J.; Joshi, P.; Dai, S.; Moecher, D.; Johnston, M. N., Location of cerium in coal-combustion fly ashes: Implications for recovery of lanthanides. *Coal Comb. Gasific. Prod.* **2013,** *5*, 73-78.

99. Huang, C.; Wang, Y.; Huang, B.; Dong, Y.; Sun, X., The recovery of rare earth elements from coal combustion products by ionic liquids. *Miner. Eng.* **2019,** *130*, 142-147.

100. Wirth, X.; Benkeser, D.; Yeboah, N. N. N.; Shearer, C.; Kurtis, K.; Burns, S., Evaluation of Alternative Fly Ashes as Supplementary Cementitious Materials. *ACI Mater. J.* **2019,** *116*.

101. Eze, C. P.; Nyale, S. M.; Akinyeye, R. O.; Gitari, W. M.; Akinyemi, S. A.; Fatoba, O. O.; Petrik, L. F., Chemical, mineralogical and morphological changes in weathered coal fly ash: A case study of a brine impacted wet ash dump. *J. Environ. Manage* **2013,** *129*, 479-492.

102. Yeheyis, M.; Shang, J.; Yanful, E., Chemical and Mineralogical Transformations of Coal Fly Ash after Landfilling. *Proc. of World of Coal Ash Conference (WOCA)* **2009**, 1-13.

103. Yeboah, N. N. N.; Shearer, C. R.; Burns, S. E.; Kurtis, K. E., Characterization of biomass and high carbon content coal ash for productive reuse applications. *Fuel* **2014,** *116*, 438-447.

104. McCarthy, G. J.; Solem, J. K.; Manz, O. E.; Hassett, D. J., Use of a database of chemical, mineralogical and physical properties of North American fly ash to study the nature of fly ash and its utilization as a mineral admixture in concrete. *MRS Proceedings* **1989,** *178* (3).

105. International, A., ASTM C618-19: Standard Specification for Coal Fly Ash and Raw or Calcined Natural Pozzolan for Use in Concrete. West Conshohocken, PA, 2019.

106. Wirth, X.; Glatstein, D. A.; Burns, S. E., Mineral phases and carbon content in weathered fly ashes. *Fuel* **2019,** *236*, 1567-1576.

107. Catalfamo, P.; Di Pasquale, S.; Corigliano, F.; Mavilia, L., Influence of the calcium content on the coal fly ash features in some innovative applications. *Resour Conserv Recycl* **1997,** *20* (2), 119-125.

108. Gorrepati, E. A.; Wongthahan, P.; Raha, S.; Fogler, H. S., Silica precipitation in acidic solutions: mechanism, pH effect, and salt effect. *Langmuir* **2010,** *26* (13), 10467-10474.

109. Puligilla, S.; Mondal, P., Co-existence of aluminosilicate and calcium silicate gel characterized through selective dissolution and FTIR spectral subtraction. *Cem. Concr. Res.* **2015,** *70*, 39-49.

110. Khater, H. M., Effect of Calcium on Geopolymerization of Aluminosilicate Wastes. *J. Mater. Civ.* **2012,** *24* (1), 92-101.

111. Onghena, B.; Binnemans, K., Recovery of scandium(III) from aqueous solutions by solvent extraction with the functionalized ionic liquid betainium bis(trifluoromethylsulfonyl)imide. *Ind. Eng. Chem. Res.* **2015,** *54* (6), 1887-1898.

112. Sthoer, A.; Hladílková, J.; Lund, M.; Tyrode, E., Molecular insight into carboxylic acid–alkali metal cations interactions: reversed affinities and ion-pair formation revealed by non-linear optics and simulations. *Physical Chemistry Chemical Physics* **2019,** *21* (21), 11329-11344.

113. Matusiewicz, H.; Natusch, D. F. S., Ion chromatographic determination of soluble anions present in coal fly ash leachates. *Int J Environ An Ch* **1980,** *8* (3), 227-233.

114. Doucet, F. J.; van der Merwe, E. M.; Nyet, N.; Prinsloo, L. C., Extraction of Aluminum and other Strategic Metals from Coal Fly Ash using a Novel Process and a Low-cost Recoverable Agent. *Proc. of World of Coal Ash Conference (WOCA)* **2015**, 1-10.

115. Zgureva, D.; Boycheva, S., Synthetic zeolitic ion-exchangers from coal ash for decontamination of nuclear wastewaters. *BgNS Transactions* **2015,** *20*, 132-136.

116. Hartmann, A.; Petrov, V.; Buhl, J.-C.; Rubner, K.; Lindemann, M.; Prinz, C.; Zimathies, A., Zeolite Synthesis under Insertion of Silica Rich Filtration Residues from Industrial Wastewater Reconditioning. *Adv. Chem. Engineer. Sci.* **2014,** *4* (2), 15.

117. Dian Pahlevi, N.; Binglin, G.; Sasaki, K., Immobilization of selenate in cancrinite using a hydrothermal method. *Ceram. Int* **2018,** *44*, 8635-8642.

118. Gollakota, A. R. K.; Volli, V.; Shu, C.-M., Progressive utilisation prospects of coal fly ash: a review. *Sci. Total Environ.* **2019,** *672*, 951-989.

119. Zeng, L.; Li, Z., Solubility and modeling of sodium aluminosilicate in NaOH–NaAl(OH)4 solutions and its application to desilication. *Ind. Eng. Chem. Res.* **2012,** *51* (46), 15193-15206.

120. Golbad, S.; Khoshnoud, P.; Abu-Zahra, N., Hydrothermal synthesis of hydroxy sodalite from fly ash for the removal of lead ions from water. *Int. J. Environ. Sci. Technol.* **2017,** *14* (1), 135-142.

121. Felsche, J.; Luger, S.; Baerlocher, C., Crystal structures of the hydro-sodalite Na6[AlSiO4]6 8H2O and of the anhydrous sodalite Na6[AlSiO4]6. *Zeolites* **1986,** *6* (5), 367-372.

122. Li, H.; Hui, J.; Wang, C.; Bao, W.; Sun, Z., Extraction of alumina from coal fly ash by mixed-alkaline hydrothermal method. *Hydrometallurgy* **2014,** *147-148*, 183-187.

123. Zeng, L.; Li, Z., Solubility and Modeling of Sodium Aluminosilicate in NaOH–NaAl(OH)4 Solutions and Its Application to Desilication. *Industrial & Engineering Chemistry Research* **2012,** *51* (46), 15193-15206.

124. Crundwell, F. K., On the Mechanism of the Dissolution of Quartz and Silica in Aqueous Solutions. *ACS Omega* **2017,** *2* (3), 1116-1127.

125. DOUGLAS, R. W.; EL-SHAMY, T. M. M., Reactions of Glasses with Aqueous Solutions. *J. Am. Ceram. Soc.* **1967,** *50* (1), 1-8.

126. Maraghechi, H.; Rajabipour, F.; Pantano, C. G.; Burgos, W. D., Effect of calcium on dissolution and precipitation reactions of amorphous silica at high alkalinity. *Cem. Concr. Res.* **2016,** *87*, 1-13.

127. Molchanov, V. S.; Prikhidko, N. E., Corrosion of silicate glasses by alkaline solutions. *Bulletin of the Academy of Sciences of the USSR, Division of chemical science* **1957,** *6* (10), 1179-1184.

128. Hartman, R. L.; Fogler, H. S., Reaction Kinetics and Mechanisms of Zeolite Dissolution in Hydrochloric Acid. *Industrial & Engineering Chemistry Research* **2005,** *44* (20), 7738-7745.

129. Wang, T.; Wang, J.; Tang, Y.; Shi, H.; Ladwig, K., Leaching characteristics of arsenic and selenium from coal fly ash: role of calcium. *Energy Fuels* **2009,** *23* (6), 2959-2966.

130. Chen, J. J.; Thomas, J. J.; Taylor, H. F. W.; Jennings, H. M., Solubility and structure of calcium silicate hydrate. *Cem. Concr. Res.* **2004,** *34* (9), 1499-1519.

131. Weng, Z. H.; Jowitt, S. M.; Mudd, G. M.; Haque, N., Assessing rare earth element mineral deposit types and links to environmental impacts. *Appl. Earth Sci.* **2013,** *122* (2), 83-96.

132. Gao, Z.; Zhou, Q., Contamination from rare earth ore strip mining and its impacts on resources and eco-environment. *Chin J Ecol* **2011,** *30* (12), 2915-2922.

133. Huang, X.; Deng, H.; Zheng, C.; Cao, G., Hydrogeochemical signatures and evolution of groundwater impacted by the Bayan Obo tailing pond in northwest China. *Sci. Total Environ.* **2016,** *543*, 357-372.

134. Huang, X.; Zhang, G.; Pan, A.; Chen, F.; Zheng, C., Protecting the environment and public health from rare earth mining. *Earths Future* **2016,** *4* (11), 532-535.

135. *PubChem Compound Summary for CID 11545, Betaine hydrochloride.*; National Center for Biotechnology Information: 2020.

136. Costa, S. P. F.; Pinto, P. C. A. G.; Lapa, R. A. S.; Saraiva, M. L. M. F. S., Toxicity assessment of ionic liquids with Vibrio fischeri: An alternative fully automated methodology. *J. Hazard. Mater.* **2015,** *284*, 136-142.

137. Stoy, L.; Diaz, V.; Huang, C.-H., Preferential Recovery of Rare-Earth Elements from Coal Fly Ash Using a Recyclable Ionic Liquid. *Environ. Sci. Technol.* **2021**.

138. Rao Ch, J.; Venkatesan, K. A.; Nagarajan, K.; Srinivasan, T. G., Dissolution of uranium oxides and electrochemical behavior of U(VI) in task specific ionic liquid. *Radiochim. Acta* **2008,** *96* (7), 403.

139. Sasaki, K.; Suzuki, T.; Mori, T.; Arai, T.; Takao, K.; Ikeda, Y., Selective liquid–liquid extraction of uranyl species using task-specific ionic liquid, betainium bis(trifluoromethylsulfonyl)imide. *Chem. Lett.* **2014,** *43* (6), 775-777.

140. Izquierdo, M.; Querol, X., Leaching behaviour of elements from coal combustion fly ash: An overview. *Int. J. Coal Geol.* **2012,** *94*, 54-66.

141. Warren, C. J.; Dudas, M. J., Leaching behaviour of selected trace elements in chemically weathered alkaline fly ash. *Sci. Total Environ.* **1988,** *76*, 229-246.

142. Norris, P.; Chen, C.-W.; Pan, W.-P., A technique for sequential leaching of coal and fly ash resulting in good recovery of trace elements. *Anal. Chim. Acta* **2010,** *663* (1), 39-42.

143. Jones, K. B.; Ruppert, L. F.; Swanson, S. M., Leaching of elements from bottom ash, economizer fly ash, and fly ash from two coal-fired power plants. *Int. J. Coal Geol.* **2012,** *94*, 337-348.

144. Vassilev, S. V.; Vassileva, C. G., Methods for Characterization of Composition of Fly Ashes from Coal-Fired Power Stations: A Critical Overview. *Energy Fuels* **2005,** *19*, 1084-1098.

145. Meawad, A. S.; Bojinova, D. Y.; Pelovski, Y. G., An overview of metals recovery from thermal power plant solid wastes. *Waste Management* **2010,** *30* (12), 2548-2559.

146. Prakash, S.; Mohanty, J. K.; Das, B.; Venugopal, R., Characterisation and removal of iron from fly ash of talcher area, Orissa, India. *Miner. Eng.* **2001,** *14* (1), 123-126.

147. Lin, R.; Howard, B. H.; Roth, E. A.; Bank, T. L.; Granite, E. J.; Soong, Y., Enrichment of rare earth elements from coal and coal by-products by physical separations. *Fuel* **2017,** *200*, 506-520.

148. van Riessen, A.; Chen-Tan, N., Beneficiation of Collie fly ash for synthesis of geopolymer: Part 1 – Beneficiation. *Fuel* **2013,** *106*, 569-575.

149. Honaker, R.; Groppo, J.; Zhang, W., Ash Benficiation for REE recovery. In *2015 World of Coal Ash*, Nashville, TN, 2015.

150. Bhatt, A.; Priyadarshini, S.; Acharath Mohanakrishnan, A.; Abri, A.; Sattler, M.; Techapaphawit, S., Physical, chemical, and geotechnical properties of coal fly ash: A global review. *Case Studies in Construction Materials* **2019,** *11*, e00263.

151. Hower, J. C.; Rathbone, R. F.; Robertson, J. D.; Peterson, G.; Trimble, A. S., Petrology, mineralogy, and chemistry of magnetically-separated sized fly ash. *Fuel* **1999,** *78* (2), 197-203.

152. Vassilev, S. V.; Vassileva, C. G.; Karayigit, A. I.; Bulut, Y.; Alastuey, A.; Querol, X., Phase-mineral and chemical composition of fractions separated from composite fly ashes at the Soma power station, Turkey. *International Journal of Coal Geology* **2005,** *61* (1), 65-85.

153. Coles, D. G.; Ragaini, R. C.; Ondov, J. M., Chemical studies of stack fly ash from a coal-fired power plant. *Environ. Sci. Technol.* **1979,** *13* (4), 455-459.

154. Valeev, D.; Kunilova, I.; Alpatov, A.; Varnavskaya, A.; Ju, D., Magnetite and Carbon Extraction from Coal Fly Ash Using Magnetic Separation and Flotation Methods. *Minerals* **2019,** *9* (5), 320.

155. Akinyemi, S. A.; Gitari, W. M.; Thobakgale, R.; Petrik, L. F.; Nyakuma, B. B.; Hower, J. C.; Ward, C. R.; Oliveira, M. L. S.; Silva, L. F. O., Geochemical fractionation of hazardous elements in fresh and drilled weathered South African coal fly ashes. *Environ. Geochem. Health* **2020,** *42* (9), 2771-2788.

156. Wise, S. A.; Watters, R. L. *Certificate of Analysis: Standard Reference Material® 1633c Trace Elements in Coal Fly Ash*; National Institute of Standards & Technology: 2011.

157. Gambogi, J., 2021 Mineral Commodity Summaries: REEs United States Geological Survey: 2021.

158. Brew, D. R. M.; Glasser, F. P., Synthesis and characterisation of magnesium silicate hydrate gels. *Cem. Concr. Res.* **2005,** *35* (1), 85-98.

159. Roy, W.; Berger, P., Geochemical Controls of Coal Fly Ash Leachate pH. *Coal Combustion and Gasification Products* **2011,** *3*, 63-66.

160. Chu, T.-Y. J.; Kim, B. R.; Ruane, R. J., Behavior in Coal Ash Particles in Water: Trace Metal Leaching and Ash Settling. Development, O. o. R. a., Ed. U.S. Environmental Protection Agency: Research Triangle Park, NC 27711, 1980.

161. Banerjee, R.; Mohanty, A.; Chakravarty, S.; Chakladar, S.; Biswas, P., A single-step process to leach out rare earth elements from coal ash using organic carboxylic acids. *Hydrometallurgy* **2021,** *201*, 105575.

162. Mondal, S.; Ghar, A.; Satpati, A. K.; Sinharoy, P.; Singh, D. K.; Sharma, J. N.; Sreenivas, T.; Kain, V., Recovery of rare earth elements from coal fly ash using TEHDGA impregnated resin. *Hydrometallurgy* **2019,** *185*, 93-101.

163. Hovey, J. L.; Dardona, M.; Allen, M. J.; Dittrich, T. M., Sorption of rare-earth elements onto a ligand-associated media for pH-dependent extraction and recovery of critical materials. *Sep. Purif. Technol.* **2021,** *258*, 118061.

164. Yan, F.; Jiang, J.; Tian, S.; Liu, Z.; Shi, J.; Li, K.; Chen, X.; Xu, Y., A Green and Facile Synthesis of Ordered Mesoporous Nanosilica Using Coal Fly Ash. *ACS Sustainable Chemistry & Engineering* **2016,** *4* (9), 4654-4661.

165. Meier, M.; Sonnick, S.; Asylbekov, E.; Rädle, M.; Nirschl, H., Multi-scale characterization of precipitated silica. *Powder Technol.* **2019,** *354*, 45-51.

166. Ghosh, N. N.; Pramanik, P., Synthesis of nano-sized ceramic powders using precipitated silica in aqueous sol-gel method. *Nanostruct. Mater.* **1997,** *8* (8), 1041-1045.

167. Abbott, A. P.; Capper, G.; Davies, D. L.; Shikotra, P., Processing metal oxides using ionic liquids. *Mineral Processing and Extractive Metallurgy* **2013,** *115* (1), 15-18.

168. Onghena, B.; Jacobs, J.; Meervelt, L.; Binnemans, K., Homogeneous liquid-liquid extraction of neodymium(III) by choline hexafluoroacetylacetonate in the ionic liquid choline bis(trifluoromethylsulfonyl)imide. *Dalton transactions (Cambridge, England : 2003)* **2014,** *43*.

169. Huang, Y.; Chen, Z.; Crosthwaite, J. M.; N.V.K. Aki, S.; Brennecke, J. F., Thermal stability of ionic liquids in nitrogen and air environments. *The Journal of Chemical Thermodynamics* **2021,** *161*, 106560.